Non-Covalent and Macromolecular Approaches to Study Protein Binding, Drug Delivery and Artificial Blood

Devanshi Singh

PhD Thesis

Dr L. J. Twyman

September 2018

Declaration

I hereby declare that the research discussed has not been submitted, either entirely or partly, for this or any other degree. All the work presented in this thesis is the original work of the author, except where other sources have been acknowledged by references. This work was carried out at the University of Sheffield between October 2013 and September 2017.

Signature: .....

Devanshi Singh

Date: .....

Acknowledgments-Part 1

My journey as a student at The University of Sheffield started with the MSc Polymers for Advanced Technologies course. It was the afternoon when Dr Twyman was assigning Project supervisors to our batch that he understood what I really wanted to work on, finding a cure for cancer! My research work with dendrimers was the highest marked that year, and since then, there's been no turning back. Dr Twyman has been a father figure to me and my inspiration that I won't ever be able to explain or express. He taught me to be patient yet determined, honest and to never back down! He showed me many times in simple ways that life is not about what we've achieved but what difference have we made by being where we are today. There were times when I have found it difficult to hold on to my beliefs as a human and not to crumble, his simple yet logical approach has always encouraged me and helped me move forward. If I am one of the best, it is only because, he is the best! Although, he'll never admit that. Thank you so much, Dr Twyman, for being my Supervisor, my father figure and indeed my inspiration. It might take me a while, but I'll for sure make you proud one day!

Next, my beloved Twyman group. With this group, I have laughed, argued, fought and at times been emotional too. It's all been possible because this group has been together as a family and I hope the family continues to remain strong! Hamza, you've been my brother guiding, scolding, and protecting me whenever necessary. Alaa, thank you for all the good times we've had together in the past four years, they'll never be forgotten. Greg, thank you for being one of the closest friends, times together will be cherished. Fatema, Jawad, Samira, Bunian, Ibrahim and Talal, thank you for being supportive and understanding, they all have been great, and I wish nothing but the best for them.

My research wouldn't be complete if it wasn't for Meng, Kanika, Juliette, Giles and Dylan. Thank you for being super awesome 'Masters' of Science and Chemistry.

My heartfelt gratitude goes out to the Department of Chemistry, especially Dr Crook to begin with, as if not for him in giving me the opportunity to study masters in Sheffield, I'd have never been where I am today. Heather, you've been an excellent support system, thank you for all the boo-boo fixes that you did in the lab to get me through my PhD. This thankfulness is extended towards Richard, Melanie and Keith for their constant backing and technical support. I would also like to thank the IT office, Chemistry stores, Accounts office and the PG office for all the help and assistance they've provided me throughout. Last but not the least, thank you The University of Sheffield, where I found a sense of belonging and the fact that race, colour, religion, or gender doesn't define you rather your work and outlook towards this world does!

Acknowledgments-Part 2

We never truly realise importance of our parents, family, and friends until we are miles away from them and that sudden realisation kicks in that no matter where you are, hearts are always connected and beating together!

Mummy and Daddy, I worship you! I am waiting on the day that you are close to me, here. Mummy, no one knows better than you what goes on inside me. You can literally see through me, even miles apart. I am your girl, you've raised me with your strength and courage that today reflects in me. Because of you, I began this wonderful journey, living my dream, witnessing it, fulfilling it! And the best part is, I feel you doing the same with me, every single moment! I've said it before and I'll say it again, you are my strength! Words will never be enough! Daddy, how could I have possibly done this without you? Your cool calm attitude wins over, every time! And that's what I have going on too! Thank you so much for believing in me and supporting me every step of the way! Best dad, ever! My dearest brother, Appu, couldn't ask for anything better than you by my side, remember when you explained me how good polymer science is, when the admission results came out for DU? Every time, even in the slightest doubtfulness, I remember that day and it gives me the will to go on! Heena Bhabhi, thank you for coming into my life as my much-needed sister. You are cool, superb, and pretty and yes, I've got you booked already for my special day! Vagmi, my little Goddess Lakshmi, I love you to bits and can't wait to spoil you with all my love and care! I promise to protect you with my life! Casper, my little baby, miss you and love you so much! My Snowy, you are so adorable! Dearest Romy and Elle, thank you for being there and keeping my brother and sister-in-law on their toes, all the time! Goofy, my bff, always with me!

My Godparents, Mamma and CP Mamaji, thank you for giving me all the love and care, I miss you two a lot and wish we could be together! Shalu and Anjoo didi, thank you for being super cool sisters with super cool kids! All my love to you! Avinash, distance might have drifted us apart, but we are never truly away, our childhood spent together, is one of the best things that has ever happened, thank you so much! My dearest Hemant Mama, your love, courage, and belief in me has made me good, thank you for ever and ever! My SP Mamaji, you are precious to me because you made me your precious daughter, thank you so much for all the love you've always given me!

Finally, the lot that cannot be patient anymore!

Panos, you are one of the best things that has happened to me! It is incredible how almost every time you get to know if something is up with me! You are a blessing! Souls connected! You are my bestie, my brother, my everything, and no day goes by when I don't thank God for sending you to me! Listen to me, thank you for giving me a perfect family in Greece! Also, thank you for bringing Anthi into my life, she's super lucky to have you and I am super lucky to have her!

Dena, my big sister, you are my stronghold! I fall back in you, confide in you! You stood by me through troubled times and moments when I needed someone I can rely on, thank you so much! I can't thank God enough for you!

Kuljit, we started out as student-mentor and look where we are today! My family away from home part 2! Your love and care have given me so much, I don't think I'll be able to make up for it! My loving sister, thank you for loving me so much!

Erik, thank you so much for being such a good friend, you've given me strength and support even without realising it! Breakfasts and coffees are real fun with you! Meng, my little artificial blood brother, thank you for always helping me and making me laugh like crazy!

Christos, Florentios, and Azra, no picture is complete without you guys! Orpita, there are times when I wish we two could go away from everything like we did and just enjoy life, thank you for being one of a kind! Hope, wish we could relive the moments we did back then, thank you for being a wonderful friend! Kanika, the apple of my eye, little sis! special mention! Big shout out!

This bit is for someone I met towards the end of my PhD and I didn't realise how incomplete my life was before he came in to it! Dylan, you are everything I want and more! I never knew someone could love me so much, pamper me and stand by me! There have been times when I have doubted myself, but you never did and always made me believe in the best, yes, we are in this together! Your love completes me, and I can't wait to start our life together! You've given me my second mummy and daddy, a family I always longed for, couldn't ask for more! I love you so much!

I've got myself a little happy perfect world! Thank you, God!

Mummy & Daddy,

A little gift just to say...

You mean the world to me!

My beloved Softy,

Not a day goes by when I don't think about you. I never really knew that you were living inside me, as a part of my soul, I wish I could have you with me today right beside me, so please let this do for now.

It's not the best, but a start towards becoming the best...

This is for you...

Abstract

To begin with, macromolecules consisting of poly(amido)amine dendrimers (PAMAM), polyglycidol, hyperbranched poly(amido)amine (HYPAM) were synthesized and characterized extensively. Porphyrins were also synthesized, characterized and modified in line with respective studies. Hereafter, surface modified TRIS PAMAM dendrimers and its analogs (hyperbranched polymers, hyperbranched PAMAMs) as potential drug delivery systems were studied with the use of model drugs (Ibuprofen and Porphyrin). Analogs of the model drugs were used to investigate the role of secondary interactions for high drug loading(s). UV-Vis Spectroscopy was utilized for studying and determining the maximum loading of the macromolecules under investigation. Further ahead, non-covalent approaches to improve dendrimer-protein binding were used by introducing amino acid chains as targeting groups on the dendrimer surface. Surface modified carboxylate PAMAM dendrimers were studied for their ability to bind with zinc metallated porphyrin. UV-Vis and Fluorescence Spectroscopy were used for protein binding studies. Lastly, Surface Crosslinked Micelles were synthesized and utilized as artificial blood mimics with an attempt to increase the half-life of encapsulated iron porphyrin acting as the heme mimic with the help of UV-Vis Spectroscopy.

Contents

Chapter 1

Polymer Therapeutics-An Overview

Table of Contents

Abbreviations

10-HCPT – 10-hydroxycamptothecin

A549 – Adenocarcinomic human alveolar basal epithelial cells

$AgNO_3$ – Silver nitrate

AP 5346 – N-(2-Hydroxypropyl) methacrylamide copolymer platinate

BACPT – 7-butyl 10-aminocamptothecin

C26 – Murine colon adenocarcinoma

CDP – cyclodextrin based polymer

CMC – Critical Micelle Concentration

CPT – Camptothecin

CTAB – Cetyl trimethylammonium bromide

DACH – diamino cyclohexane

DDS – Drug Delivery Systems

DNA – Deoxyribonucleic acid

DOX – Doxorubicin

DTD – Drug targeting and delivery

EDA – Ethylene diamine

EPR – Enhanced permeability retention

G4-PGLSA – Generation 4-poly (glycerol succinic acid)

GNR – Gold nanorod

$HAuCl_4$ – Chloroauric acid

HBP(s) – Hyperbranched polymers

HeLa cells – Cervical cancer cells derived from cancer patient 'Henrietta Lacks'

HIV – Human immunodeficiency virus

HPMA – N-(2-Hydroxypropyl) methacrylamide

HT-29 – Human colon cancer cells

IC_{50} – Half maximal inhibitory concentration

IT-101 – Insert Therapeutics

LLC – Lewis lung carcinoma

$NaBH_4$ – Sodium borohydride

NIR – Near infra-red radiation

NSAIDS – Non-steroidal anti-inflammatory drugs

NT – Neurotensin

P(MAA-g-EG) – Poly (methacrylic-g-ethylene glycol)

PAMAM – Poly (amidoamine)

PDT – Photodynamic therapy

PEG – Poly (ethylene glycol)

PEG-CPT – Poly (ethylene glycol)-camptothecin conjugate

PEG-cys-PAMAM – Poly (ethylene glycol) modified Poly (amidoamine) dendrimers

PEG-SN38/ EZN-2208 – Poly (ethylene glycol)-camptothecin derivative

PEI – Poly (ethylenimine)

PEI-(Cys)x(Ac) – Poly (ethylenimine)-N'-methacryloyl-cystamine conjugate

PEI-(Cys)x(MAc) – Poly (ethylenimine)-N'-scryloyl-cystamine conjugate

PEI-Cys – Poly (ethylenimine)-cystamine conjugates

PG(s) – Polyglycerols

PGA-PRZ – Poly (γ-glutamic acid)-phloridzin bio-conjugate

pH – power of hydrogen

PLA – Poly (lactic acid)

PLA-*b*-PMPC – Copolymers of poly (lactic acid) and poly (2-methacryloyloxyethyl phosphorylcholine)

PLGA – Poly (lactic-co-glycolic acid)

pNT- Pseudo-neurotensin

PPI – Poly (propyleneimine)

PpIX – Protoporphyrin IX

PPO – Polypropylene oxide

PRZ – Phloridzin

PSMA – Prostate-specific membrane antigen

Pt – Platinum

Pt(IV) - *cis,cis,trans*-diamminedichloridodiscuccinatoplatinum(IV)

PT(s) – Polymer therapeutics

PTT – Photothermal therapy

PVA – Polyvinyl alcohol

QAC(s) – Quaternary ammonium compounds

RAFT – Reversible addition fragmentation chain transfer polymerisation

RNA – Ribonucleic acid

ROMBP – Ring opening multi-branching polymerization

RPMI – Roswell park memorial culture medium

SGLT1 – Sodium glucose cotransporter

siRNA – Small interfering ribonucleic acid

SPR – Surface plasmon resonance

tate – Octreotate

TNP-470 – (O-(chloracetyl-carbomoyl) fumagillol))

TNT – Titania nanotube arrays

γ-PGA – Poly (γ-glutamic acid)

List of Figures

1.1 Polymer therapeutics

Every year, millions of lives are lost to Cancer, HIV (human immunodeficiency virus) and similar life-threatening diseases. With advancements in medical science towards better and speedy cures for such diseases, many hurdles remain in place, blocking effective treatments. These blockades range from effectively delivering the drug to the target site due to the incapability of the drug to distribute itself when administered. Beside these limiting factors, side effects of improper drug administration are also present; bio-toxicity and bioavailability etc. all play major roles in determining proper working of the drug. All these factors have caused great concern in the medical and science field in recent years. Because of these heightened concerns, science has invested a great deal of its research in developing novel Drug Delivery Systems (DDS) [1]. This field of science, particularly in Polymer Science, is known as Polymer Therapeutics [2]. As the name states, Polymer Therapeutics is a class of polymers that act as therapeutic drugs for the treatment of diseases such as Breast cancer, Alzheimer's etc. These therapeutic drugs range from linearly branched polymers to bulky star polymers and micelles. They can be classified into conjugated polymers, hyperbranched polymers (HBPs), micelles, polymersomes, dendrimers and star polymers, polyvalent and multivalent polymers, to name a few (Figure 1.1). Polymers that have clinically succeeded or are at clinical development stage as potential polymer therapeutics are discussed in this short overview.

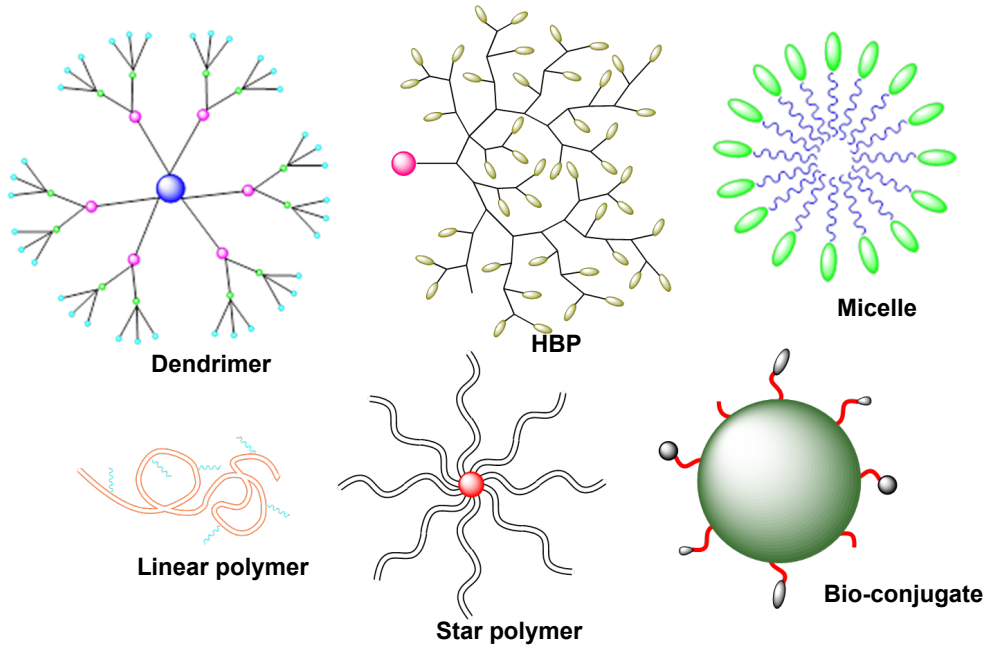

Figure1.1. Graphical representation of known polymer therapeutics: Dendrimer, HBP (hyperbranched polymer), micelle, linear polymer, star polymer and bio-conjugates.

1.1.1 Types of Polymer Therapeutics

Polymer therapeutics can be described as a group of polymers and macromolecules capable of acting as therapeutic agents, storing drugs within their structural moieties and transporting them to the target site. They usually consist of conjugates such as polymer-drug or polymeric drugs, polymer-protein and polymer micelles. Polymers have been an integral part of millions of lives in the past years however their usefulness as biomedical agents and applicants have come to light in the last 30 years [3]. Before being investigated as novel drug delivery systems; polymers were well known for temporal or spatial control of drug delivery which led to the invention of bio-adhesive polymers responsible for the adhesion of an epithelial cell layer to a delivery system [4]. Another outstanding discovery was that of 'smart' polymeric hydrogel systems capable of delivering bioactive agents on response to specific stimuli [4]. In terms of macromolecules, dendrimers and hyperbranched polymers are common examples of PTs. Polymer therapeutics were or are customarily designed for treatment of cancer however; many other diseases such as diabetes, hepatitis B & C, multiple sclerosis has attracted attention as well. Besides acting as DDS, certain PTs hold the capacity of functioning as 'implanted reservoir systems'.

For a polymer to function as a PT, properties for maintaining an all-round therapeutic effect need to be met. Surface properties such as hydrophilicity, lubricity, and smoothness (hydrolytic degradation and swelling) [5] are important. But, if the polymer or polymeric material needs to be applied for a long term use especially in case of dental and orthopaedic applications, the polymer should be capable of repelling water and degrading at a very slow rate to avoid weakening its toughness and strength. These ideal surface properties can be effectively achieved by chemical, physical and biological means. And once the ideal properties required are accomplished; the addition or adhesion of drugs or proteins on to the polymer surface or within the cavities of the polymer becomes possible paving way for polymer therapeutics that could transport through organs and cells [6]. It is imperative to mention that while molecular weight, adhesion and solubility need to be considered as important bulk properties for determining the release mechanisms of the drug(s); structural properties such as micro-morphology and pore size play an important role defining the entry and exit of the drug [7, 8].

1.1.1.1 Linear polymers

Linear polymers consist of simple chains having least and smallest branches if at all. Their ability to form random coils in good solvents while exhibiting multi-functionality (induced in the backbone of the chain) constructed the initial phase of Polymer Therapeutics. However, over the past decades they have become a difficult class of conjugates, reason being their poor drug loading capacity when compared with other types of polymer architectures such as hyperbranched polymers. Even though, they are not a popular class of polymer therapeutics, research to make them apt and valuable has been conducted ever since.

Larson et al studied the importance of linear poly (ethylene glycol) PEG-drug conjugates. Although, PEG is biocompatible, easily synthesized with specific molecular weights; it suffers the drawback of being non-biodegradable and possessing low drug loading capacity [9]. Its non-biodegradability leads to its accumulation inside cells and tissues over time causing toxicity and side effects. However, in this study on conjugation with the camptothecin (CPT) derivative SN38 using glycine as the linker, the PEG-SN38 showed a drug loading of 3.7wt%. This was higher when compared to its earlier analogue PEG-CPT conjugate with a loading of only 1.7wt% [10]. Besides the high payload, good aqueous solubility, enhanced bio-degradability and longer blood circulation half-life was observed as well. This new conjugate is known as EZN-2208 and has progressed to phase II clinical trials for the treatment of metastatic breast cancer (Figure 1.2).

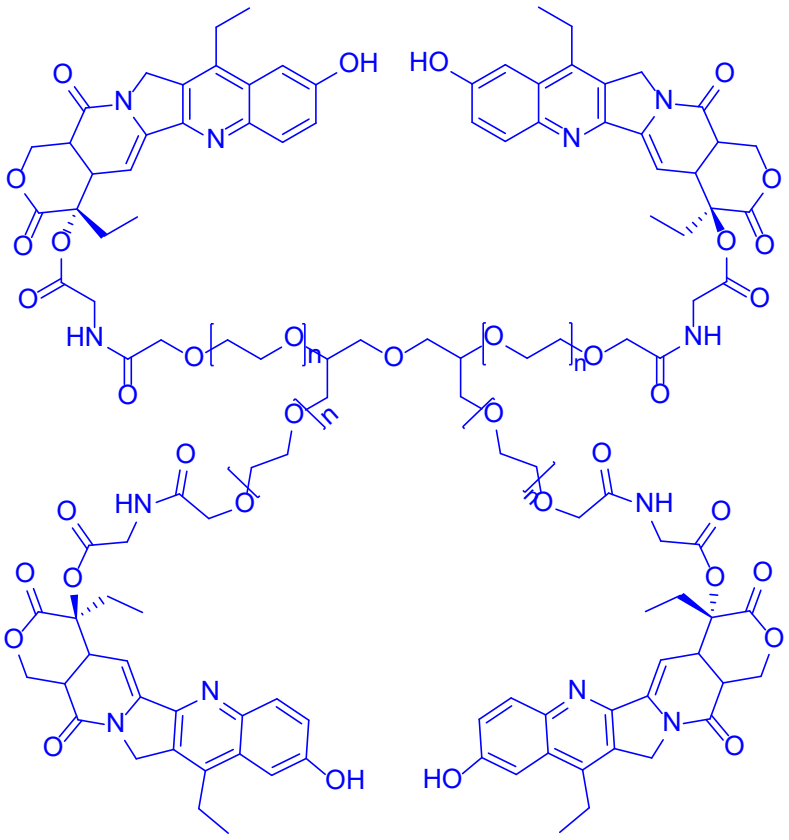

Figure 1.2. Chemical structure of PEG-SN38 conjugate EZN-2208.

The importance of linear polymers is highlighted as they are utilized in gene-delivery systems. Responsive gene-delivery systems are preferred especially if they can deliver the nucleic acids safely inside the cells. This is possible by using bio-reducible linear polyethylenimine (PEI) [11]. The polymer has disulphide bonds that reduce the toxicity as charge density falls on cleaving under reducing conditions inside the cell. The polymer could remain stable in extracellular environments and undergo rapid degradation within cells successfully inducing in vitro DNA or small interfering RNA (siRNA) transfection (Figure 1.3) [12].

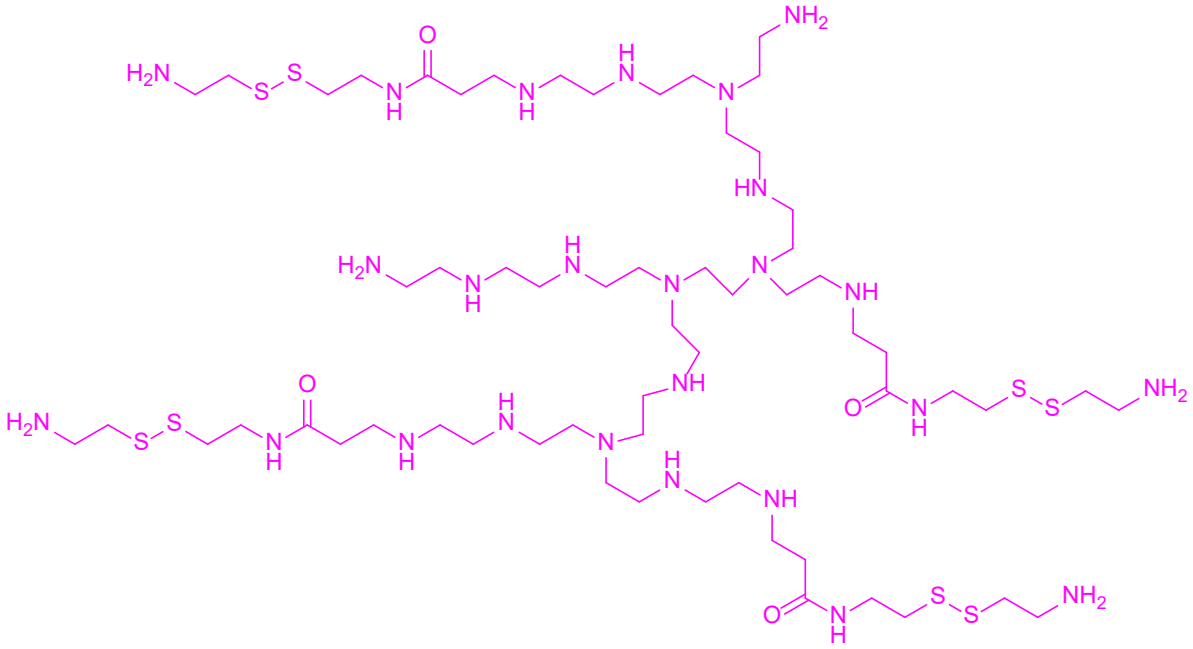

PEI-(Cys)x(Ac) (Poly (ethylenimine)-N'-scryloyl-cystamine conjugate)

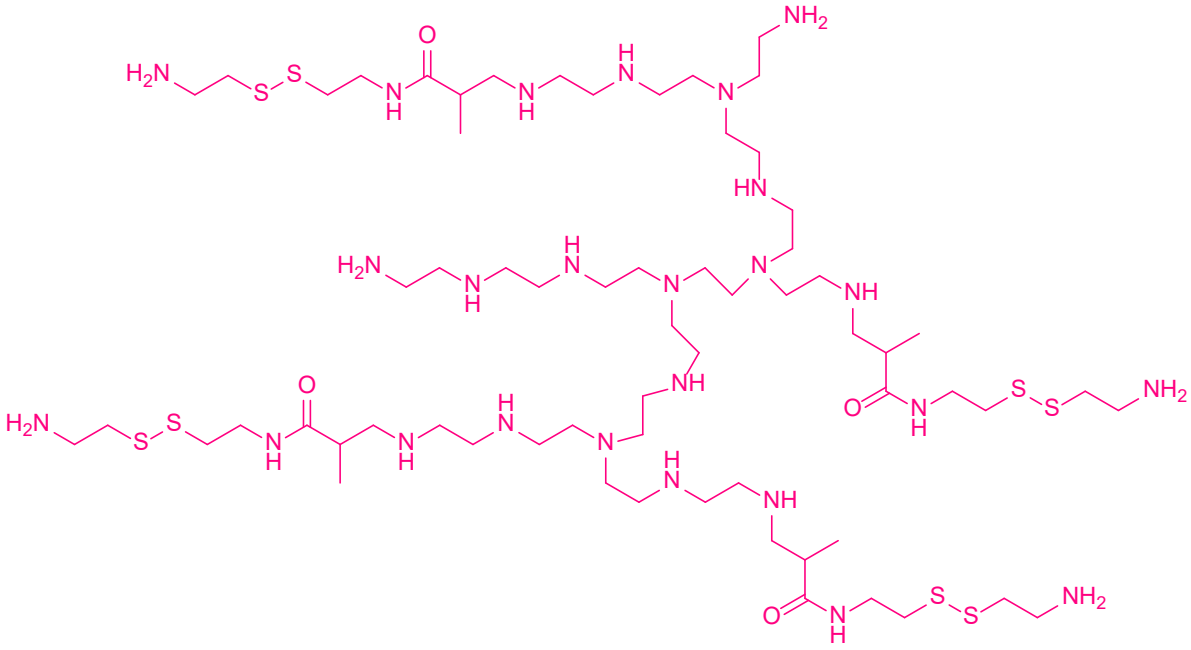

PEI-(Cys)x(MAc) (Poly (ethylenimine)-N'-methacryloyl-cystamine conjugate)

Figure 1.3. Chemical structure of branched PEI derivatives with reductively cleavable cystamine (PEI-Cys) periphery for safe and efficient in-vitro gene transfer.

Linear polymer conjugates are known for improving the half-life and intracellular targeting of drugs however limited drug payload capacity holds them back from being one of the selected therapeutic agents. Hereafter this overview discusses the progress research has made with architecturally different polymers to overcome these limitations.

1.1.1.2 Drug-Polymer Conjugate

Cellular internalization and cell specificity improvement requires the drug to be delivered at the target site however certain delivery systems have the tendency to control the distribution of the drug and its release at the target site over time [13]. Nanoparticles as a result are the preferred linkers between polymers and drug as they can be labile towards certain digestive enzymes and acidic conditions rendering them well versed for cancer treatment [14]. Such polymer systems are known as Drug-Polymer Conjugates (Figure 1.4).

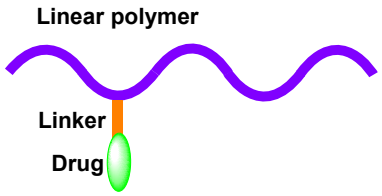

Figure 1.4. Graphic representation of a Drug-Polymer conjugate.

Certain physiological barriers do exist however they are reduced by selecting appropriate particle size, surface charge and hydrophobicity while designing the delivery systems. While overcoming the physiological challenges, biological obstacles arise that can be tackled if the nanoparticles are capable of vasculature, prolonged vascular circulation time, improved cellular uptake and endosomal-lysosomal escape. One example of drug-polymer conjugate to enter anti-cancer clinical trials is ProLindac (Figure 1.5). Chemically known as HPMA copolymer (N-(2-Hydroxypropyl) methacrylamide) platinate (AP 5346) (a cytotoxic diamino cyclohexane (DACH)-platinum moiety coupled to a biocompatible HPMA); this conjugate consists of a pH sensitive linker that causes the release of the drug in the extracellular space of the tumour [15].

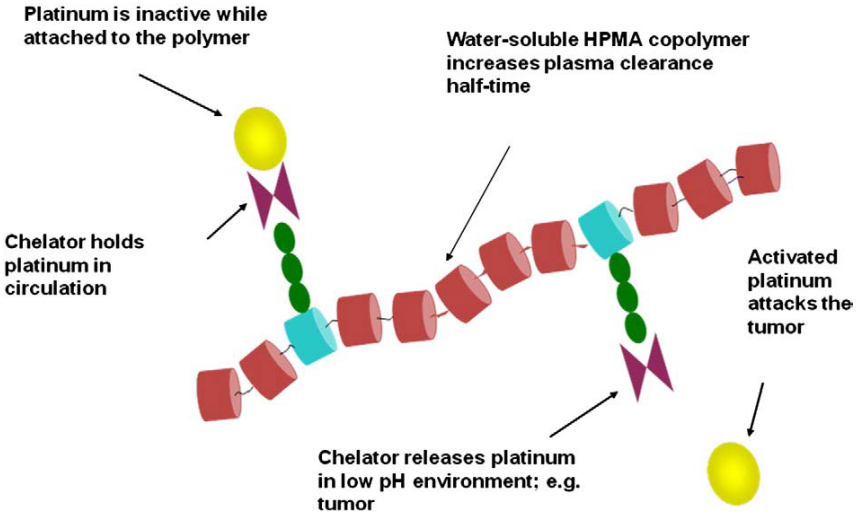

Figure 1.5. Graphical representation of ProLindac, a cytotoxic diamino cyclohexane (DACH)-platinum moiety coupled to a biocompatible hydroxypropylmethacrylamide copolymer (HPMA). Reprinted from Advanced Drug Delivery Reviews, 61 (13), David P Nowotnik, Esteban Cvitkovic, ProLindac™ (AP5346): A review of the development of an HPMA DACH platinum Polymer Therapeutic, 1214-1219, Copyright 2009, with permission from Elsevier.

The Platinum drug released causes cross-linking of the DNA by binding to it and initiating apoptosis. Also, the linear polymer chain has weight-average molecular weight of approximately 25 kDa ensuring appropriate tumour targeting through fenestrated endothelial cells besides acceptable renal clearance. Another novel method has found its way to clinical trials as a maintenance therapy for ovarian cancer patients by means of intravenous injection; known as IT-101 (Insert Therapeutics) [16]. This conjugate consists of camptothecin covalently linked to a cyclodextrin based polymer (CDP) using a glycine linker. This drug system exhibits high anti-tumour activity due to extended circulation time allowing repeated or prolonged access to the tumour. Also, its administration has shown considerably less side-effects on cancer patients thereby improving their quality of life.

Satchi-Fainaro et al, synthesized and studied a conjugate of HPMA and TNP-470 (O-(chloracetyl-carbomoyl) fumagillol)) covalently linked to Gly-Phe-Leu-Gly-ethylenediamine, a degradable bond [17]. Animal tests revealed that the modified linker underwent cleaving in the presence of intralysosomal cysteine proteases - cathepsin B (present excessively in tumour endothelial cells). This resulted in selective accumulation of the conjugate in the tumour vessels due to EPR (enhanced permeability retention) effect while increasing and prolonging the therapeutic activity of TNP-470. Also, the conjugate structure prevented drug from crossing the blood brain barrier which resulted in negligible neurotoxicity and hence, took the conjugate pro-drug from laboratory testing to pre-clinical trials as Caplostatin by SynDevRx [18, 19].

1.1.1.3 Bio-conjugated polymers

In Polymer Therapeutics, bio-conjugates are gaining popularity as preferred drug delivery vehicles. For having good pharmacokinetics, multifunctionality and circulation half-life; they are being rigorously researched for a breakthrough. Polyglycerols (PGs) make a good example of bio-conjugates since they are biocompatible and readily synthesized with controlled molecular weights while being multifunctional. Kizhakkedathu et al synthesized hybrid PGs consisting of both linear and hyperbranched polyglycerols in varying molar ratios using anionic ring opening multi-branching polymerization (ROMBP) and subsequently tested them for their biocompatibility and biodistribution in mice [20]. These hybrids exhibited excellent blood circulation half-life in mice when compared to well known drug Dextran and polymer polyvinyl alcohol (PVA) (table 1.1). In addition, the accumulation was found to be minimal within major organs explaining the non-existence of non-specific elimination pathways. With such results, hybrid PGs have gained attention as conceivable bioconjugates in the field of drug delivery systems.

At present diabetes is dangerously common disease leading to restricted lifestyle. Polymer therapeutics have been constantly researched for solution to this problem and a breakthrough might surface soon. In 2007, Ikumi et al managed to modify Poly (γ-glutamic acid)s (γ-PGA) with phloridzin (PRZ), creating the possibility of obtaining a cutting-edge oral anti-diabetic drug [21]. Phloridzin (Figure 1.6) is a compound that prevents the glucose transport extensively by binding the glucose moiety to the sodium-glucose cotransporter (SGLT1) located on the mucosal side of epithelial cells.

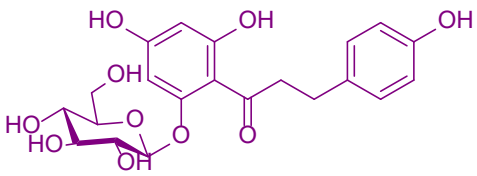

Figure 1.6. Chemical structure of Phloridzin.

This compound is found in the bark and stems of apple trees. Since, phloridzin exhibits hydrolysis (breaking of glucoside bond) by intestinal b-glucosidase and releases toxin phloretin, it cannot be used on its own. Hence, conjugation with γ-PGA yielded a bioconjugate γ-PGA-phloridzin (PGA-PRZ) (Figure 1.7) whose efficiency was researched upon by in vitro and in vivo experiments in rats. The results showed that the conjugated PRZ inhibited the glucose transport as strongly as intact PRZ while the hyperglycaemic effect was reduced remarkably, when administered orally. Also, replacing PGA-PRZ with excess intact PRZ;

didn't result in any fluctuation in the blood glucose concentration. This behaviour from the bioconjugate suggested that the glucoside bond of PRZ was stopped from degrading and stabilized by its conjugation to PGA. As a result, a potential anti-diabetic drug is witnessed in this γ-PGA-PRZ bio-conjugate.

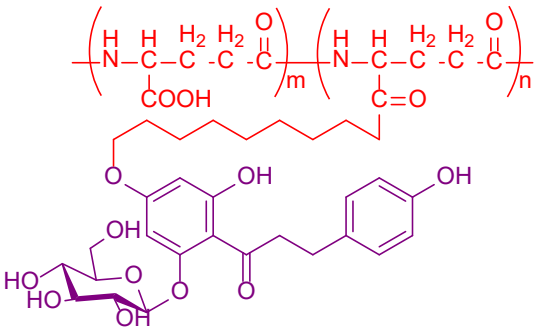

Figure 1.7. Chemical structure of γ-PGA-phloridzin conjugates (PGA-PRZs).

Moving forward, drug targeting and delivery (DTD) approach is a method being researched in which vectors are used to deliver cytotoxic agents specifically to tumour cells without affecting healthy cells. This ensures significant decrease in chemotherapy related side effects [22]. In 2012, Gaviglio et al reported the synthesis, characterization and biological evaluation of Pt-peptide (Platinum-peptide) bioconjugates (Figure 1.8) [23]. The Pt (IV)-peptide conjugates (Figure 1.8) were tested for their ability to hinder cellular proliferation in comparison to Pt (IV) parent compound. *cis,cis,trans*-diamminedichloridodiscuccinatoplatinum(IV) complex (Pt(IV)) releases cisplatin following reduction. Also, the succinate moieties consisting of terminal carboxylate groups at axial position are suited for coupling with biomolecules i.e. peptides post additional derivatization. The peptide(s) such as Neurotensin (NT) (tridecapeptide) over expresses itself in human pancreatic, prostate and lung cancers and so, its analogue Pseudo-neurotensin (pNT) was used whereas Octreotate (tate), was the analogue of somatostatin (cyclic tetradecapeptide found in hypothalamus), another peptide that over expresses itself in human breast and brain tumours.

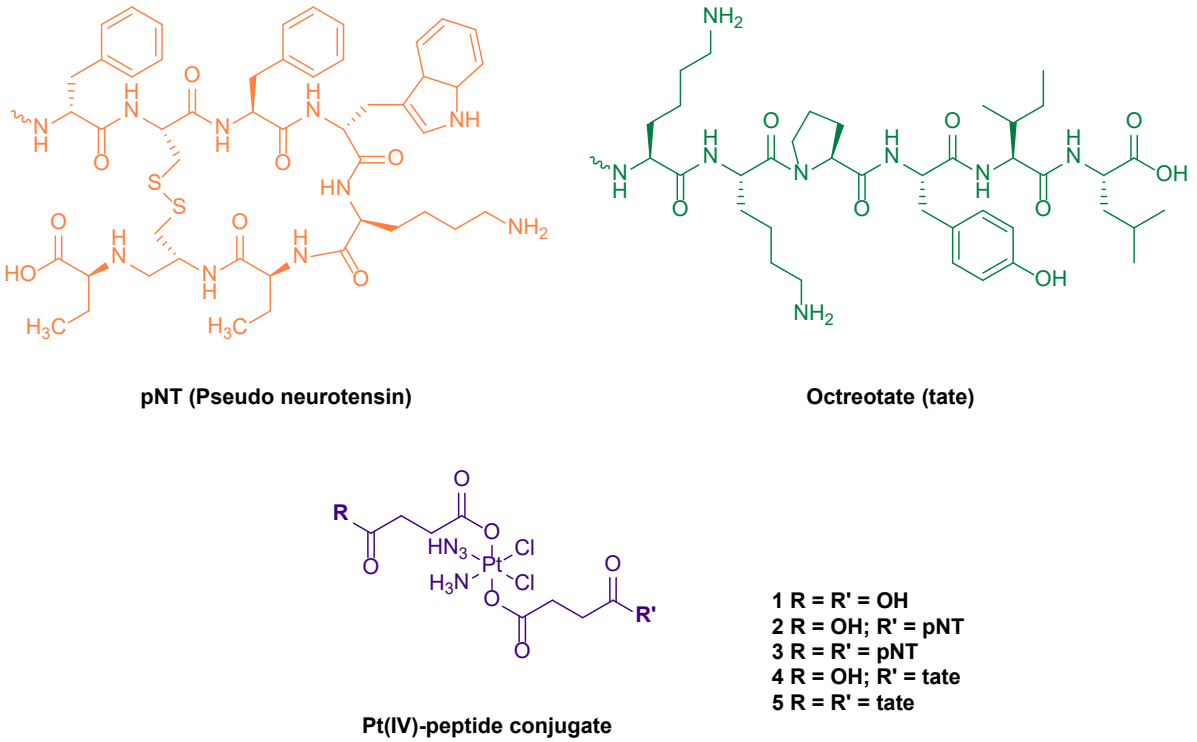

Figure 1.8. Chemical structures of Pt (IV)-peptide bioconjugates.

The study revealed that the bio-conjugates displayed enhanced cytotoxicity as the peptides readily cleaved making Pt (IV) an active species improving its anti-cancer effect incredibly. Further studies are being conducted on making this bio-conjugated an efficient pro-drug delivery system. With the above-mentioned studies, bio-conjugates find themselves useful for varied medical endeavours in a fight against lethal diseases by being effective on the human body.

1.1.1.4 Smart polymers

For decades, science and medicine has been looking for cures to deadly diseases and with new discoveries taking place, new types of materials are created. These materials are more specifically known as smart polymers that are capable of tuning themselves according to the environment they are put in. Such an innovative system leaves science and medicine with endless possibilities towards better drug administration and definitive answers to currently unanswered aspects of disease prevention. Smart polymers are capable of undergoing alteration with respect to application requirement without affecting self-efficiency hence, a popular choice for DDS [24]. The most popular class of smart polymers is Hydrogels; while being biocompatible, their swelling properties or state can be monitored permitting required amount

of drug release once administered [24]. Beside hydrogels, smart polymers commonly referred to as stimuli responsive polymers, can be broadly classified into three types, temperature controlled, pH-responsive and electro-responsive polymers (Figure 1.9) [25].

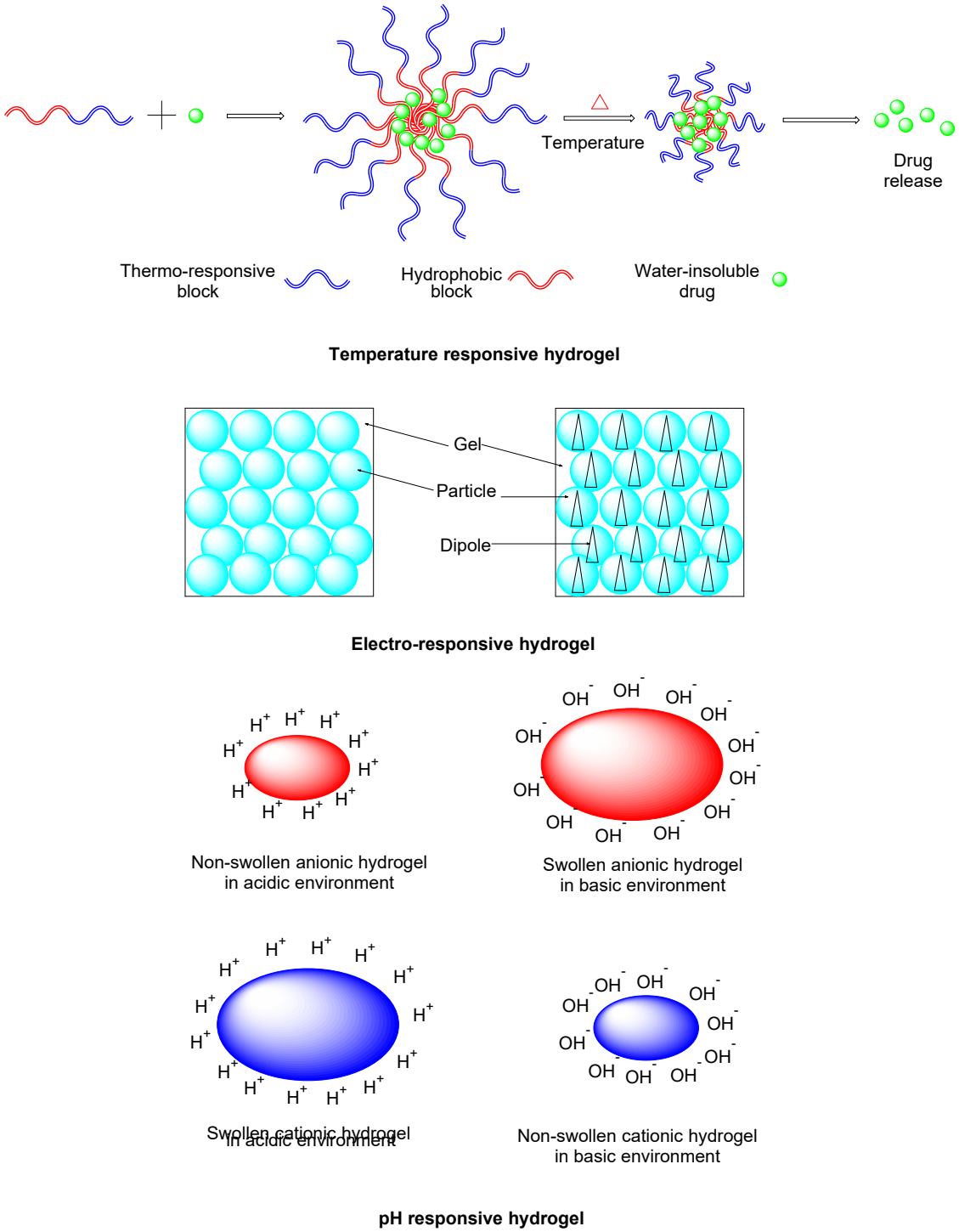

Figure 1.9. Graphical representation of stimuli responsive hydrogels.

Lowman et al studied a pH responsive hydrogel for the transport of orally administered insulin, a peptide drug that easily undergoes proteolytic degradation in the acidic stomach [26]. To prevent

this from happening, (P(MAA-g-EG)) (poly(methacrylic-g-ethylene glycol)) preformed polymer was synthesized and the drug absorbed within. The intermolecular interaction between the drug and polymer occurred resulting in the protection of the drug from the acidic environment in the stomach and finally facilitating its release at the target site i.e. the intestine. The chemical environment of the intestine being alkaline causes the intermolecular interactions to disappear, aiding the hydrogel to swell which ultimately leads to the release of insulin. This approach of treating diabetes provides enhanced quality of life for patients while reducing the need of taking unnecessary precautions during the treatment.

In another example of stimuli responsive polymers, Indomethacin (drug taken to reduce fever, pain and swelling) was used [27]. This was encapsulated inside PLGA microparticles which were later embedded into a chitosan-pluronic hydrogel matrix, a temperature sensitive hydrogel (Figure 1.11). The purpose of this study was to induce delayed drug release, based on two factors, the PLGA microparticles releasing slowly due the matrix formation and secondly temperature-controlled stimuli causing further controlled discharge of the drug. This delayed drug release ensures that the medicine is only released when the body temperature intends to rise (during fever) making certain that the optimal dose is sent out at the correct point without causing any unwanted side effects. Also, slow and gradual release of the drug would mean prolonged therapeutic influence without the need of drug top up.

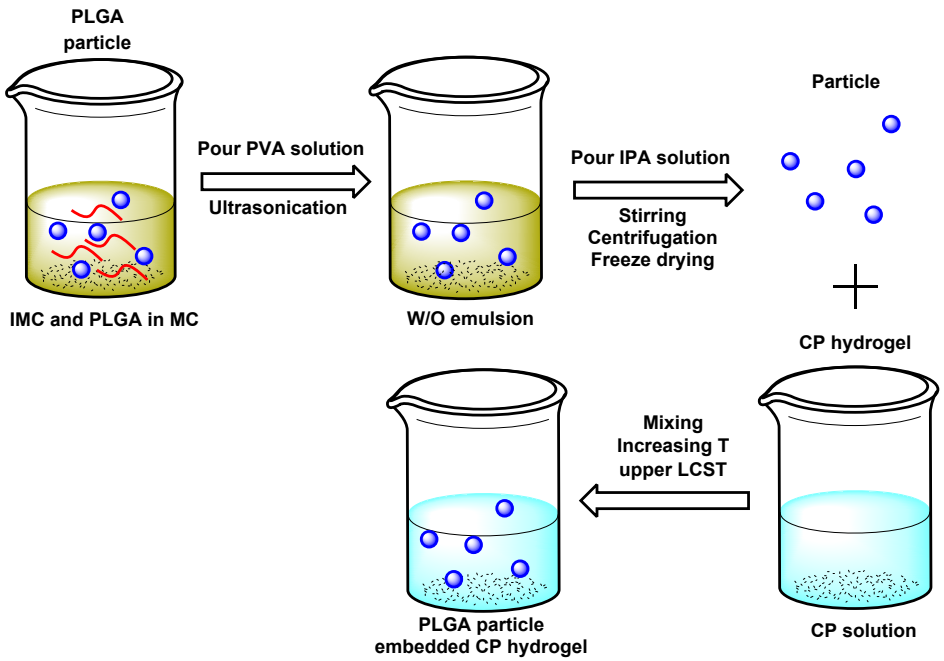

Figure 1.11. Graphical representation of the method for preparing the Indomethacin-PGLA drug conjugate using Chitosan-Pluronic hydrogel matrix.

The above-mentioned examples point out the possibility of smart or stimuli responsive polymers becoming the next generation drug delivery systems. However, while being tangible in their physiological properties and allowing the drug to reach the target site safely, major hurdles such as cytotoxicity, bio-degradability still need to be addressed. Nonetheless, with advancements taking place at tremendous speed, Smart Polymers indeed hold the key to the future of Polymer Therapeutics.

1.1.1.5 Micelles

In 1913 Dr McBain witnessed unusual behaviour exhibited by sodium palmitate solutions and coined the term 'colloidal ions' [28]. In a discussion paper published later that year, renowned scientists argued the conditions and context in which these colloidal ions were observed drawing similarities to phase separations. The foundation of new macromolecules was established based on these findings. Later into the century, as more studies were carried out, a more popular name 'micelles' was used [29]. The extensive aggregation of surfactants consisting of nonpolar groups avoiding contact with water i.e. hydrophobic and polar groups in contact with water i.e. hydrophilic form large aggregates known as micelles (Figure 1.12), from Latin *micella* meaning small bit [29].

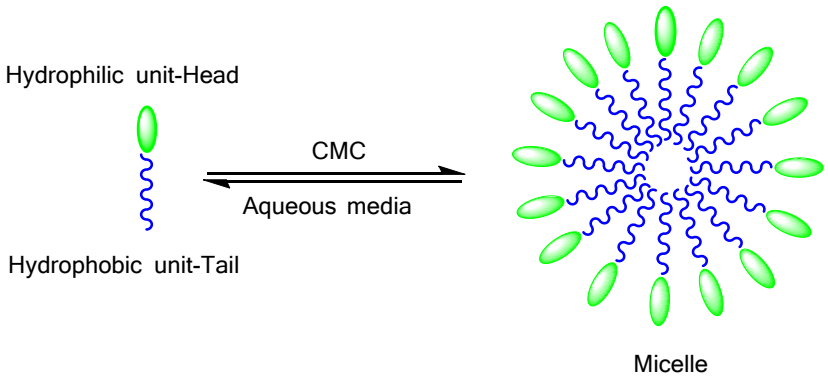

Figure 1.12. Graphical representation of micelle formation at or above critical micelle concentration. The surfactant molecule consists of a hydrophilic unit (head) and a hydrophobic unit (tail) that aggregate with decrease in surface free energy as the surface contact of the surfactant with aqueous media increases.

The aggregation behaviour is triggered when the surface tension or surface free energy of the surfactant decreases as the surface contact with aqueous solution increases. The surfactants decrease the contact area of the hydrophobic part by forming aggregates that causes the surface free energy to decrease. Once the critical threshold is passed, micelle formation occurs. This threshold is better known as Critical Micelle Concentration (CMC) [30] and is highly depend on

the concentration of the surfactants in an aqueous solution. Micelles are formed using surfactant molecules consisting of hydrophobic tail and hydrophilic head groups. Polymeric micelles result from amphiphilic di- or tri-block copolymers consisting of polar or solvophilic and non-polar or solvophobic blocks.

Quite often certain drugs are not very effective as they are unable to access the site of action due to high dosage requirement. So, even if the drug is sent to the site in small quantities, they don't prove to be very efficient. To get over this difficulty, modifications are done for the delivery of drugs, which in turn results in reduced efficacy and adverse effects. Undoubtedly micelles mimic natural carrier systems such as viruses and lipoproteins making them a preferable choice for drug delivery studies [30]. Besides they exhibit favourable characteristics of high drug loading while shielding hydrophobic drugs from the outside environment and maintaining interactions with aqueous media using hydrophilic head groups. Also, with the help of surface targeting groups targeted drug delivery using micelles with minimal adverse effects has gained popularity. In one of the studies, DOX (doxorubicin) was encapsulated within copolymers of poly (lactic acid) and poly (2-methacryloyloxyethyl phosphorylcholine) (PLA-*b*-PMPC) micelles and corresponding biocompatibility was tested [31]. Figure 1.12 gives a representation of intracellular release of encapsulated DOX within PLA-*b*-PMPC micelles.

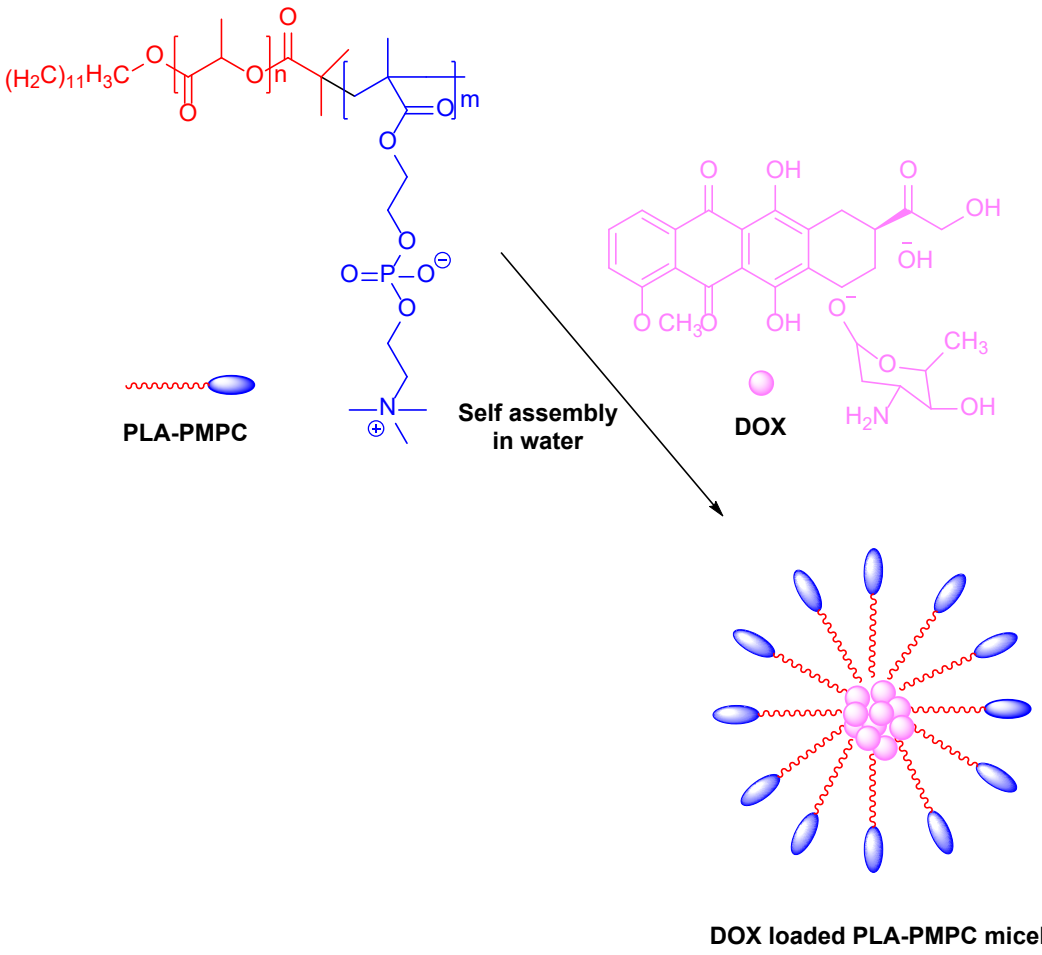

Figure 1.12. Graphical representation of DOX (doxorubicin) loaded PLA-*b*-PMPC (poly (lactic acid) and poly (2-methacryloyloxyethyl phosphorylcholine)) micelles formation in water.

Since, PLA (poly (lactic acid)) intends to form the hydrophobic core of the micelles; water insoluble drugs can be stored in the core without undergoing changes in their properties. Its biocompatibility and biodegradability plays a major role as well. On the other hand, PMPC are considered to have good blood compatibility with respect to the human body and prevents protein adsorption and platelet adhesion, all due to the presence of phospholipids, the building block of cell membranes [32]. In this study, the zwitterionic phosphorylcholine group increased the biocompatibility of the micelles greatly. Also, the cytotoxicity was found to be lower with effectual delivery and release of DOX within the cancer cells. Henceforth, it could be said that the copolymers of Poly (lactic acid) and poly (2-methacryloyloxyethyl phosphorylcholine) (PLA-*b*-PMPC) tend to be emerging as the new generation of drug delivering polymer micelles.

Sinn Aw et al in 2012, studied the delayed release of polymer micelles using TNT (Titania nanotube) arrays as drug eluting surfaces [33]. The TNT nanotube arrays were electrochemically generated on a titanium surface and drug encapsulated polymer micelles were loaded at the

bottom of the structure. On top of these loaded micelles, blank or unloaded micelles were added that caused the delayed drug releasing effect (Figure 1.13). This phenomenon was proved by using four types of polymer micelles regular and inverted with water insoluble indomethacin and water soluble drug gentamicin. The study revealed elevated strength, good stability and a better administration technique when regular and reversed micelles were put in together. This approach to facilitate time controlled and delayed release of drugs can be an effective way of suppressing and treating post-operative infections in orthopaedics and bone therapies besides providing enhanced bone integration.

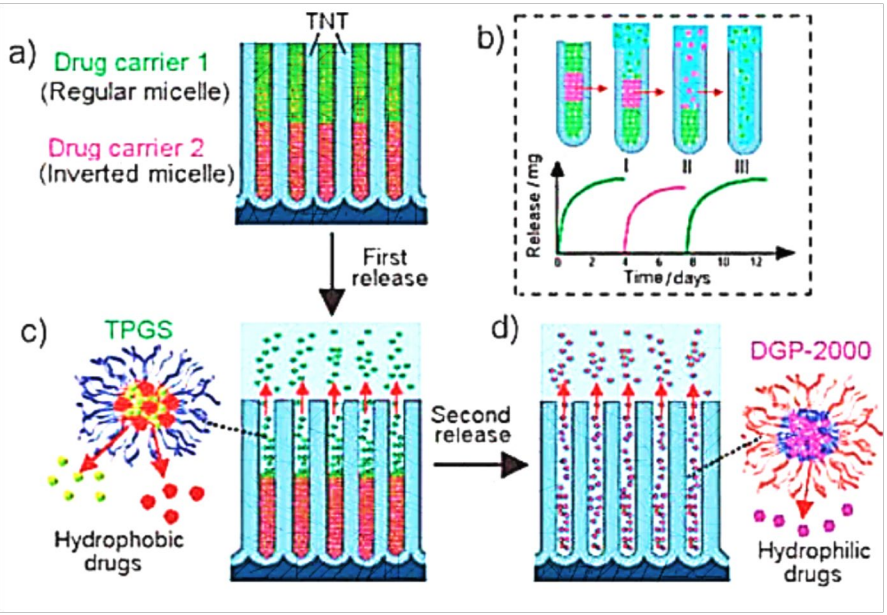

Figure 1.13. Graphical representation of multi-drug release using TNT nanotube arrays and polymer micelles. Four types of polymer micelles regular and inverted with water insoluble indomethacin and water-soluble drug gentamicin were studied. Republished with permission of Royal Society of Chemistry, from A multi-array delivery system with sequential release using titania nanotube arrays, Moom Sinn Aw, Jonas Addai-Mensah and Dunsan Losic, 48, 27, 2012; permission conveyed through Copyright Clearance Center, Inc.

1.1.1.6 Hyperbranched Polymers

In the end of 19th century, Berzelius reported the formation of a resin from tartaric acid (A_2B_2 monomer) and glycerol (B_3 monomer); this was the first hyperbranched polymer to be synthesized [34]. This discovery led to extensive studies by Watson Smith, who later published a report in 1901, stating detailed reaction between phthalic anhydride (latent A_2 monomer) or phthalic acid (A_2 monomer) and glycerol (B_3 monomer) [34]. Their work was further investigated by Callahan, Arsen, Dawson, Howell and Kienle, et al and their findings are still in use today [35]. Following all these discoveries, Kim and Webster in 1988 managed to synthesis

hyperbranched polyphenylene polymer and hence, the terminology 'Hyperbranched Polymers' (HBP) was coined [36]. A hyperbranched polymer consists of a functional core that leads out to the formation of branches that are not uniform. These branches expand to give more branches resulting in a supramolecular structure. These types of polymers are synthesized by AB_x type monomers (Figure 1.14). The core of a hyperbranched polymer controls the molecular weight distribution of the polymer besides tackling the degree of branching.

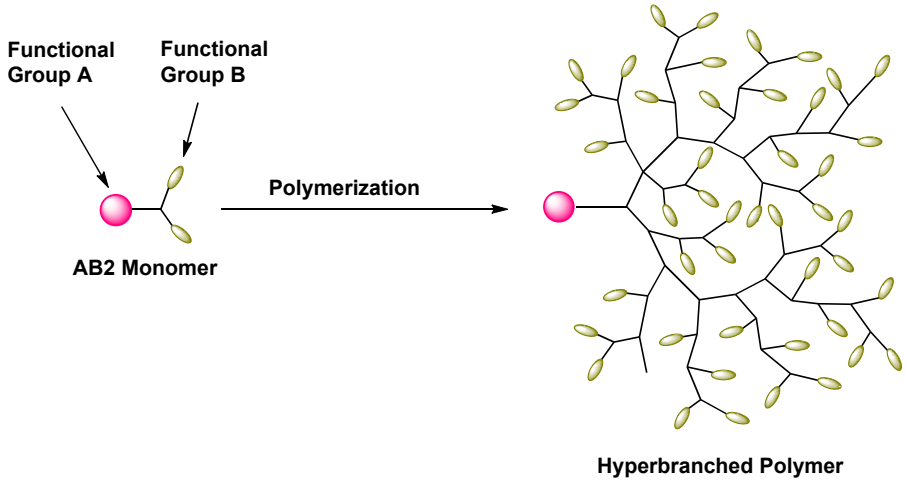

Figure 1.14. Graphical representation of hyperbranched polymer synthesized using an AB_2 monomer.

HBPs have since found various applications in drug and protein delivery, gene transfection, bio-imaging, cytomimetic applications and tissue engineering [36]. They are known to be efficient drug delivery transports because of their highly branched chemical structure and chemical stability even when the drugs are covalently attached to their surfaces. Drugs can be loaded within or on HBPs by forming drug complexes, unimolecullar micelles, multimolecullar micelles, responsive micelles and conjugates. Besides enhancing the aqueous solubility and bio-availability of the drugs, HBPs increase their circulation time with enhanced permeability and retention (EPR) effect [37].

Currently, theranostics are gaining popularity because of their approach to treating diseases. In theranostics, the efficiency of therapeutics is tracked using latest diagnostics such as imaging etc. In this paper, it has been described how biocompatible HBPs were synthesized and administered for treating prostate cancer cells with subsequent optical imaging [38]. The HBP was synthesized using reversible addition fragmentation chain transfer polymerisation (RAFT) of polyethylene glycol monomethyl methacrylate, with ethylene glycol dimethacrylate as the branching agent and internalised by the cancer cells with the help of prostate-specific membrane antigen (PSMA) targeting. The delivery system was a controlled delivery system which consisted of far-red fluorescent dye that allowed tracking of the polymer via optical

imaging. The fluorene 2-carboxaldehyde, model drug was attached to the HBP via hydrolytic degradable hydrazone linkage which intended to degrade at an endosomal pH of 5.5. At this pH, about 95% of the drug was released over a period of 4 hours compared to 5% released at physiological pH. The study revealed high uptake of the drug into the cancer cells where prostate specific membrane antigen was expressed compared to cancer cells without PSMA suggesting the increased efficiency of the targeting ligand.

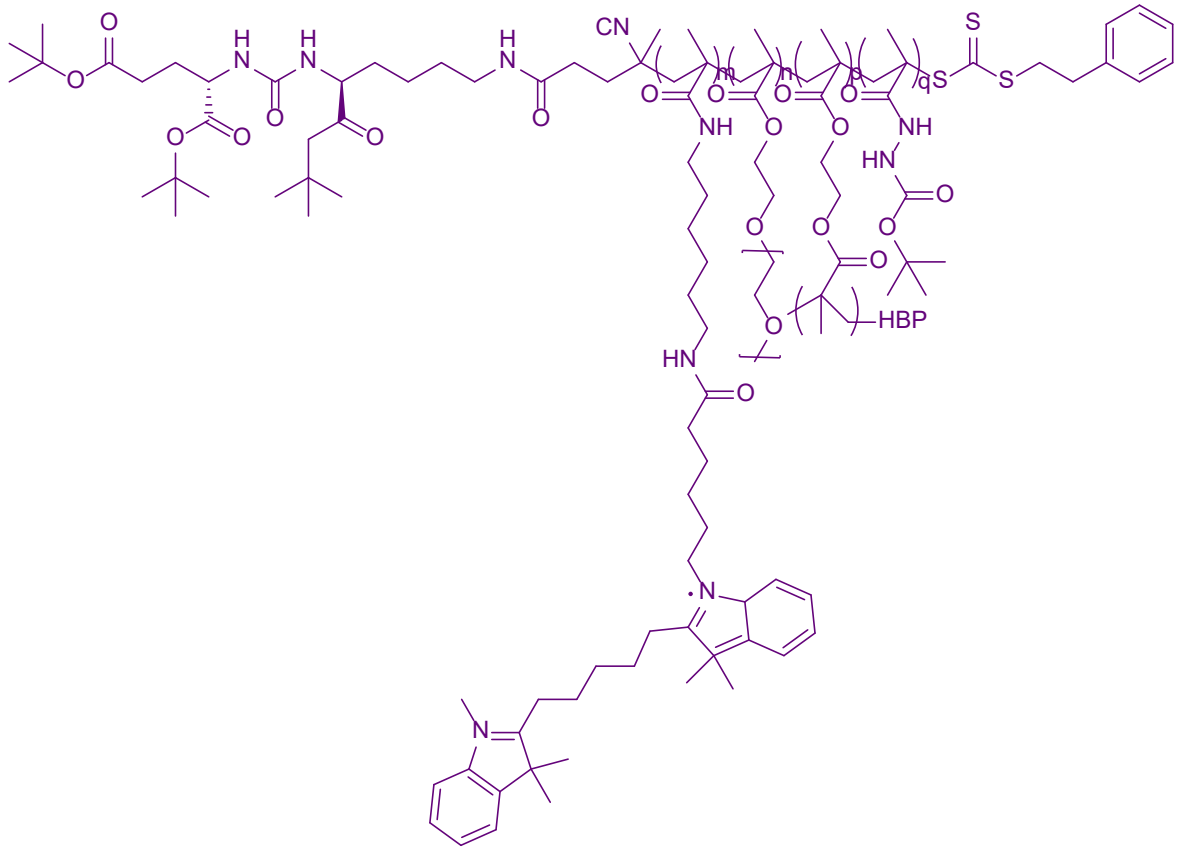

Figure 1.15. Chemical structure of prostate-specific membrane antigen (PSMA) targeted HBP.

In another study, the application of hyperbranched poly (citric acid) as an anticancer drug delivery system was researched. Since, citric acid intends to decompose easily, different ratios of citric acid and glycerol as AB3 and A3 monomers were used to synthesize HBP step by step to avoid degradation[39]. The HBPs were loaded with cisplatin and tested for their efficiency as delivery systems. The loading capacity was found to be high with increased stability in saline buffer solutions for several months. With IC_{50} (half maximal inhibitory concentration) values lower than that of free cisplatin over C26 cancer cell lines (murine colon adenocarcinoma), hyperbranched poly (citric acid) advanced as biocompatible cargos to transport anti-cancer drugs.

1.1.1.7 Dendrimers

Vogtle et al. in 1978 reported successful 'cascade' synthesis of polymers [40]. He reported that acrylonitrile was added to an amine by Michael addition reaction after which the nitrile groups were reduced to primary amines to yield a dendrimer. According to his work, this step could be infinitely repeated to give very highly branched macromolecular ligands. Following his work in 1985, Tomalia reconfigured the polymerization process to a step by step method to give highly branched polymers with low polydispersity [41]. That same year, Newkome et al. also reported the synthesis of highly branched polymers and named them arborols, meaning tree in Latin [42]. However, Dendrimers (dendron-tree and meros-parts) is a more popular word to dominate this class of polymers. After rigorous research, step by step synthesis of dendrimer with advancing generation was established. A dendrimer, in general, has a polyfunctional core, multiple branching units that consist of functional end groups that act as building blocks for high generation dendrimers (Figure 1.15).

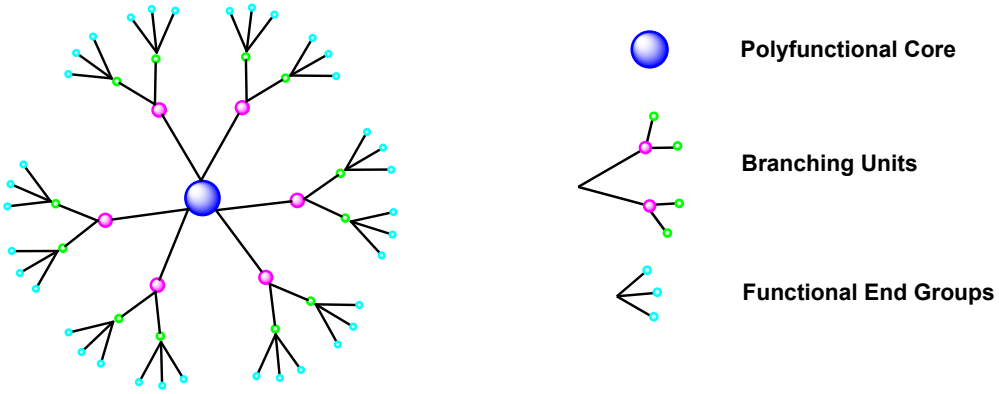

Figure 1.15. Graphical representation of a dendrimer structure.

Structural uniformity, multifunctional surface and internal cavities renders dendrimers applicable in pharmaceutical and biomedical research. Dendrimers can encapsulate the drug or protein molecule either externally via surface modifications or internally in the cavities-covalently and non-covalently or in the form of a core.

1.1.1.7.1 Applications with surface conjugation

In one of the studies, surface conjugation ability of dendrimers as vital anti-bacterial agents was studied. Cooper and co-workers synthesized PPI dendrimers (poly(propyleneimine)) with 16 quaternary ammonium compounds (QACs) with long alkyl chains known for their disinfectant properties by increasing cell permeation and cell membrane disruption [43]. These

QACs immobilized dendrimers exhibited enhanced antibacterial activity against both Gram-positive and Gram-negative bacteria when compared to QACs immobilized HBPs.

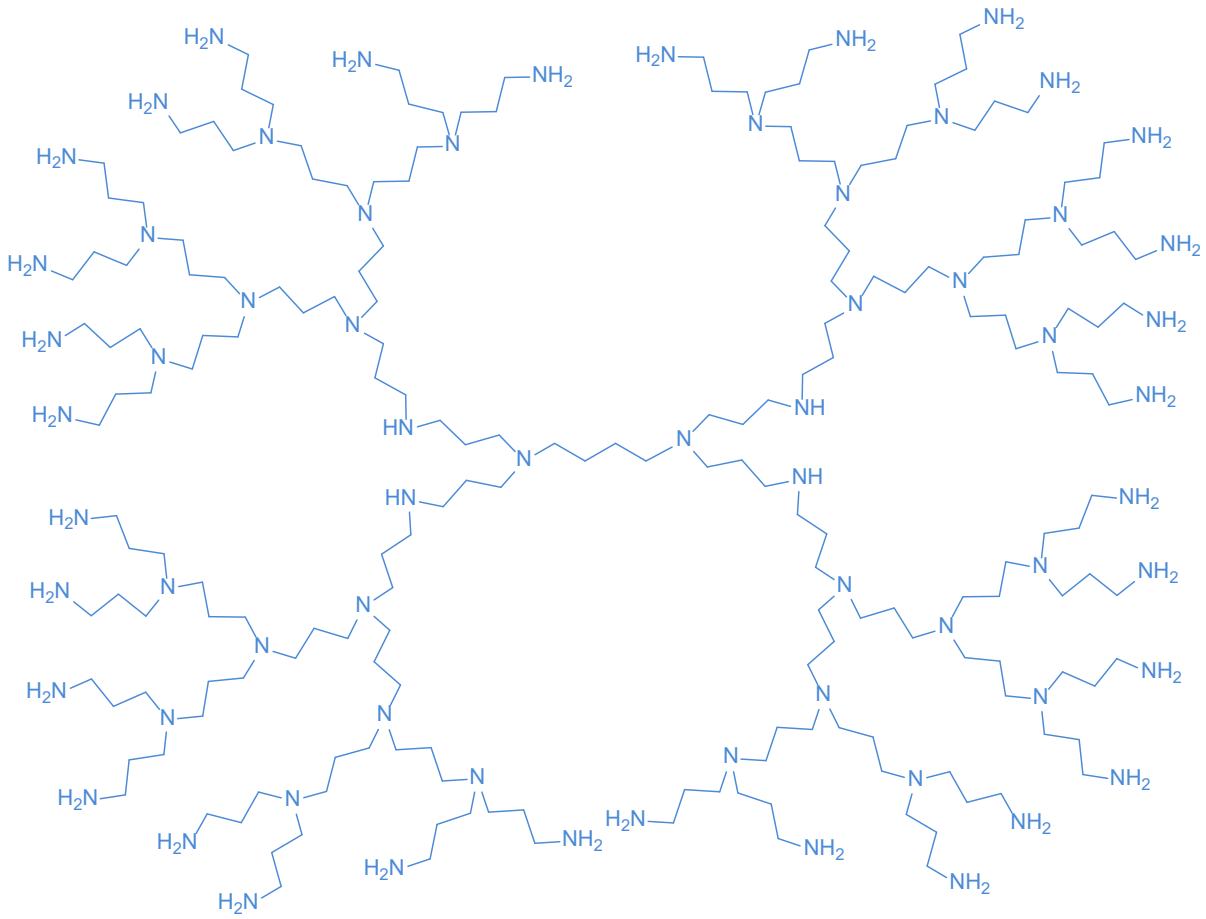

Figure 1.16. Chemical structure of Generation 4 poly(propyleneimine) primary amine terminated dendrimers.

1.1.1.7.2 Encapsulation within dendrimers

Generation 4-poly (glycerol succinic acid) dendrimers (G4-PGLSA) were used for the encapsulation of the naturally derived anti-cancer drug, camptothecin. their cytotoxicity was studied [44]. The G4-PGLSA-COONa modified dendrimers successfully encapsulated the drug 10-HCPT (10-hydroxycamptothecin). These encapsulated dendrimers were exposed to MCF-7 human breast cancer cells to show high cytotoxicity when compared to unloaded dendrimers. The research group led by Grinstaff, compared these dendrimers to PEG modified dendrimers, (G4-PGLSA-OH)2-PEG3400. Both the dendrimers were tested on HT-29 human colon cancer cells and similar results were obtained. This led to the conclusion that G4-PGLSA-COONa dendrimer was the most favourable delivery vehicle for 10-HPCT and 7-butyl 10-aminocamptothecin (BACPT), a highly potent lipophilic camptothecin derivative.

Kolhe et al. studied Ibuprofen an anti-inflammatory drug as a complexed guest molecule for encapsulation within 3rd and 4th generation poly(amidoamine) (PAMAM) dendrimers. According to the study, 78 ibuprofen molecules were seemingly encapsulated in the cavities of PAMAM dendrimer due to the complexation taking place between the amine groups of the dendrimers and carboxyl group of the drug i.e. electrostatic interactions. The in-vitro release of ibuprofen is graphically represented in Figure 1.17. In comparison to free ibuprofen, the release of encapsulated ibuprofen from within dendrimers' cavities was slower with swift access to A549 cells (adenocarcinomic human alveolar basal epithelial cells) [45].

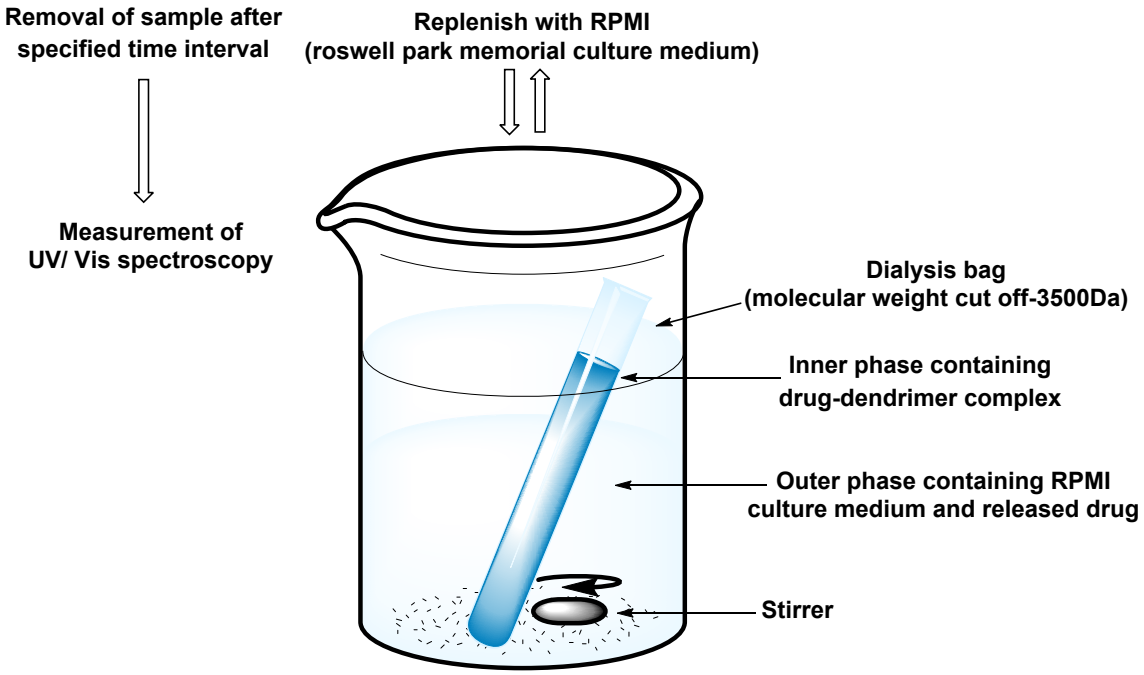

Figure 1.17. Graphical representation of in vitro release study of encapsulated ibuprofen from within PAMAM dendrimer in different solvent(s).

In another example involving PAMAM dendrimers, the core of the dendrimer used was Polypropylene oxide (PPO) to study the effect on the aqueous solubility of encapsulated hydrophobic non-steroidal anti-inflammatory drugs (NSAIDS) such as ketoprofen, ibuprofen and diflunisal (Figure 1.18) [46]. The study revealed that due the presence of PPO core, ketoprofen exhibited the highest solubility followed by diflunisal and ibuprofen. These results were significantly better when compared to solubility of the same drugs in EDA (ethylene diamine) cored PAMAMs suggesting that the solubility of a drug could be enhanced or challenged by changing the core and properties of the dendrimers, thereby creating cost effective designs for novel drug delivering dendrimers.

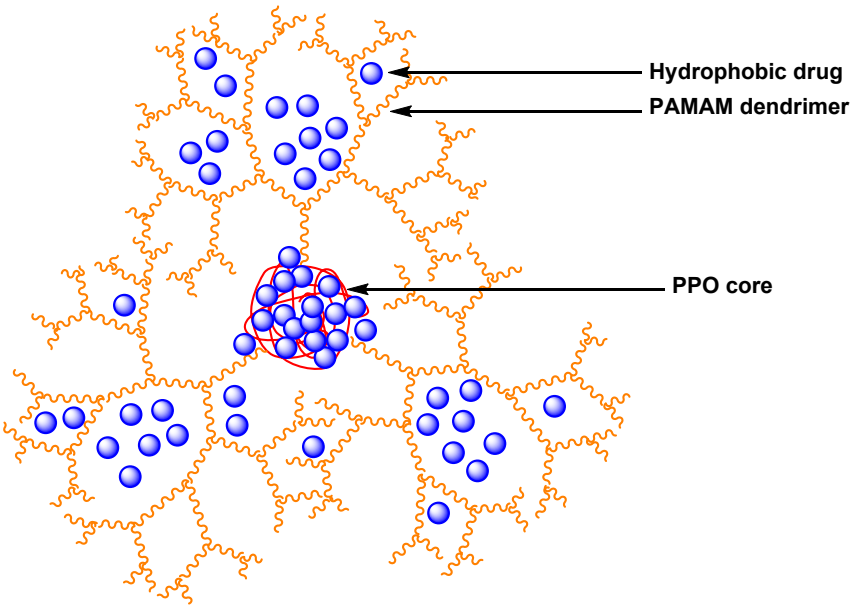

Figure 1.18. Graphical representation of PPO cored PAMAM dendrimers with high drug loading.

1.1.1.7.3 Dendrimers for functionalized Nano-particles and photosensitizers

Attempts to functionalize the core of dendrimers for applications in biomedicine have been recent. Although this aspect of dendrimer application is in its nascent stage, certain research studies highlighted the potential of functionalized cored dendrimers focused towards photodynamic therapy (PDT) (Figure 1.20) and photothermal therapy (PTT) [47, 48]. In PDT, visible light of specific wavelength activates a photosensitizer administered at the target site such as tumour cells. Highly reactive singlet oxygen species are generated following series of photochemical reactions resulting in heightened cytotoxicity in the tumour cells. This cytotoxic effect in the tumour cells is considered as a potential therapeutic strategy in curing cancer [48]. In PTT, removal of tumour occurs when high amounts of heat is generated by activating the photosensitizer using controlled near infrared (NIR) irradiation [47]. Most common examples of photosensitizers researched are porphyrins and gold nanoparticles. With dendrimer protection these photosensitizers can reach the targeted tumour site successfully.

In 2014, Li et al studied the benefits of PEG-modified PAMAM dendrimers (PEG-cys-PAMAM) with a spherical gold nanorod (GNR) core in photothermal therapy *in vitro* for cancer treatment (Figure 1.19) [47]. Surface plasmon resonance (SPR) at visible light around 530 nm is emitted by gold nanoparticles. However, it is difficult for SPR to reach the target site as the light is absorbed by bio-components such as haemoglobin. With the help of PEG-cys-PAMAM, the nanoparticles can reach the target site and NIR irradiation can be used to activate

the SPR i.e. removal of tumour cells with controlled release of heat. GNR cored PEG-cys-PAMAM dendrimer were studied for their effect on HeLa cells (immortal human cells-cervical cancer cells derived from cancer patient 'Henrietta Lacks' and tumour cells in mice. No damage to HeLa cells was observed whereas significant decrease in tumour volume was recorded.

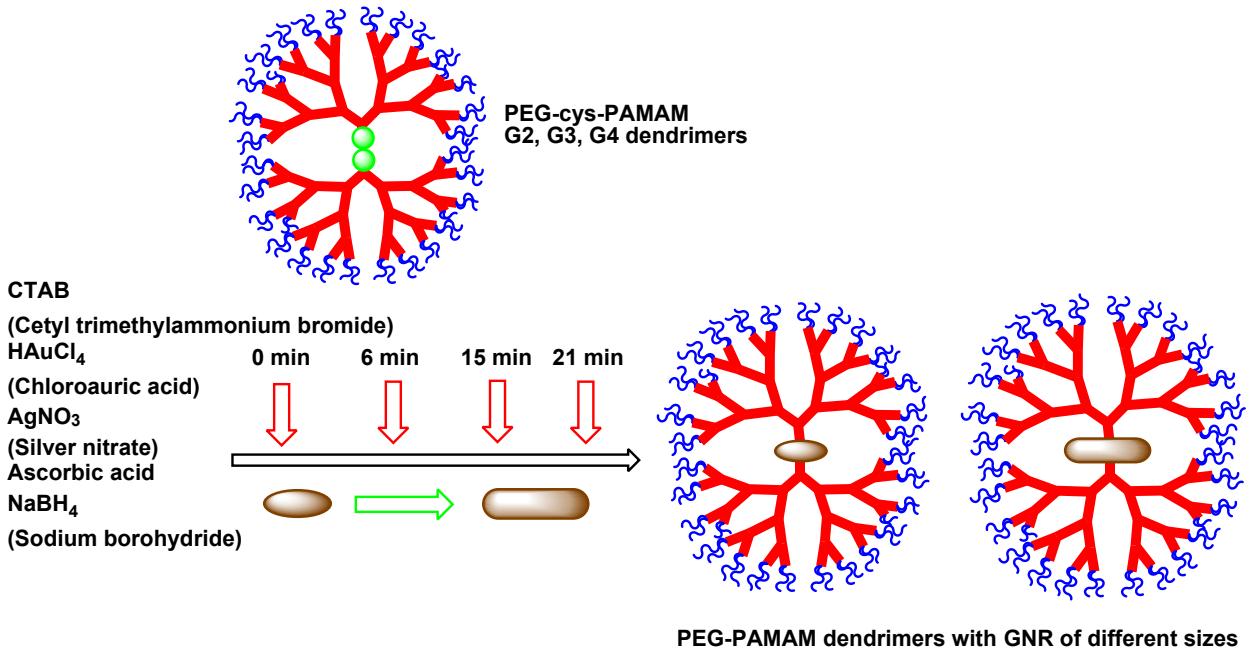

Figure 1.19. Graphical representation of PEG-PAMAM dendrimers with GNR obtained from PEG-cys-PAMAM dendrimers.

Studies using porphyrin cored G3.0 polyaryl ether dendrimers for PDT were conducted by Nishiyama et al [48, 49]. Porphyrin cored G3.0 polyaryl ether dendrimers with 32 quaternary ammonium groups and 32 carboxylate groups were synthesized. Both dendrimers exhibited endocytosis-mediated entry with cationic dendrimers being more evident. Compared to free Protoporphyrin IX (PpIX) both dendrimers exhibited lowered toxicity in intracellular organelles and membranes with high cytotoxicity in Lewis lung carcinoma (LLC) cells. Further studies looking into the dark toxicity of the dendrimers in comparison to free PpIX revealed lower levels of toxicity suggesting porphyrin cored dendrimers as potential targeted PDT agents.

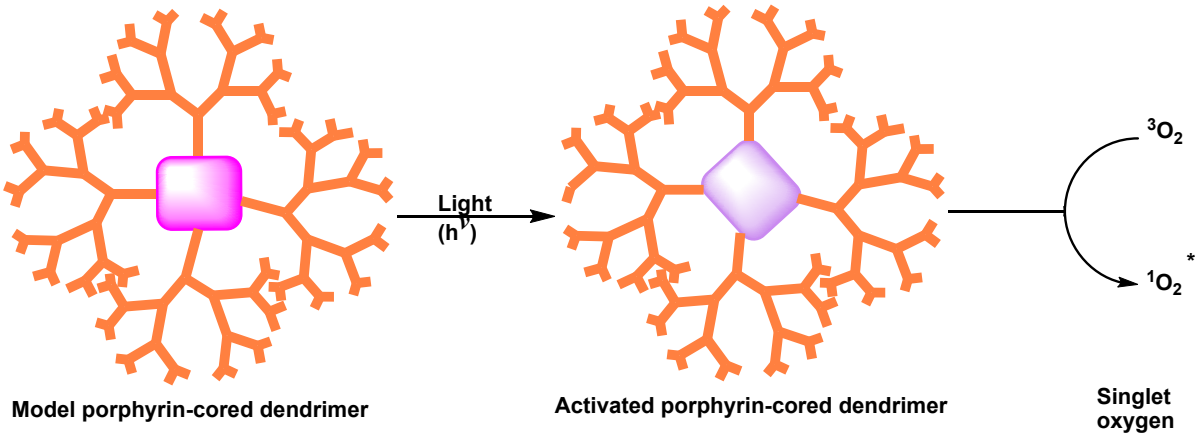

Figure 1.20. Schematic representation of porphyrin-cored dendrimers used for production of singlet oxygen for Photodynamic Therapy.

1.2 Conclusions

In this overview, prevalent polymer therapeutics and their utility as novel drug delivery systems is discussed. The era of polymer therapeutics started with linear polymers and continues to progress with advancements seen in their viability as drug delivery systems. They might not be able to have high drug payload nonetheless their straightforward synthesis, ability to form coils while encompassing drugs and; significance in responsive gene-delivery systems have been stepping stones towards advanced polymer therapeutics. Following through, drug-polymer conjugates ensure the transportation of the drug to target site using linkers that are labile towards digestive enzymes and acidic conditions. This property of drug-polymer conjugates makes them preferable for cancer treatments and studies looking into this specific use can be seen. However, physiological and biological challenges arise that require furtherance along with enhanced vasculature, prolonged vascular circulation time, improved cellular uptake and endosomal-lysosomal escape. Studies looking into prevention of diabetes and cancer treatments have focused on bio-conjugates for a breakthrough as the conjugates offer good pharmacokinetics, multifunctionality and circulation half-life.

The classification of smart polymers as part of polymer therapeutics is underlined by the fact that these polymers are stimuli-responsive and can undergo application-dependant alteration. These polymers are usually electro-responsive, pH-responsive and temperature-responsive finding applications in targeted drug administration and slow drug release studies. Conversely, cytotoxicity and bio-degradability remain an issue requiring research to further the use of smart

polymers for drug administration to clinical phase. With Dr McBain discovering colloid formations in sodium palmitate solutions, an era of micelles began. Their progress in the field of polymer therapeutics has been extensive. From suppressing and treating post-operative infections in orthopaedics and bone therapies along with enhanced bone integration by slow-multiple drug(s) release using TNT arrays to development of bio-degradable and blood-compatible micelle for efficient drug transport, micelles are headed forward as the future of polymer therapeutics.

Biocompatible HBPs were used to transport drugs to treat prostate cancer with optical imaging to follow the treatment progress. This type of treatment known as theranostics is gaining popularity with HBPs at its core. HBPs have strived to be the penultimate drug delivery systems due to their highly branched chemical structure and chemical stability even when the drugs are covalently attached to their surfaces. Studies using HBPs to transport drugs by forming drug complexes, unimolecular, multimolecular and responsive micelles and conjugates have and continue to provide promising results. HBPs have demonstrated enhanced aqueous solubility and bio-availability of drugs and increased circulation time with enhanced permeability and retention effect. However, dendrimers are the competing class of DDS. The contenders are structurally uniform with multifunctional surface and internal cavities making them applicable in pharmaceutical and biomedical research. Dendrimers can encapsulate the drug or protein molecule either externally via surface modifications or internally in the cavities-covalently and non-covalently or in the form of a core. Lately, dendrimers have been studied for encompassing functionalised nanoparticles for photothermal therapy for cancer treatment with encouraging results giving them a headway as the leading polymer therapeutics. Cancer treatments via photodynamic therapy and photothermal therapy to delivery of anti-inflammatory drugs, dendrimers are capable of various bio-medical applications with successful end-results. With advancements in the field of medicine with promising clinical trials, therapies etc. taking place, the decision of which drug delivery system is better between HBPs and dendrimers, remains indefinite.

1.3 References

1. Tiwari, G. et al., 2012. Drug delivery systems: An updated review. *International Journal of Pharmaceutical Investigation,* 02(01), pp. 02-11.

2. Duncan, R. & Vicent, M. J., 2013. Polymer therapeutics-prospects for 21st century: The end of the beginning. *Advanced Drug Delivery Reviews,* 65(01), pp. 60-70.

3. Uhrich, K. E., Cannizzaro, S. M., Langer, R. S. & Shakesheff, K. M., 1999. Polymeric Systems for Controlled Drug Release. *Chemical Review,* 99(11), pp. 3181-3198.

4. Pillai, O. & Panchagnula, R., 2001. Polymers in drug delivery. *Current Opinion in Chemical Biology,* 05(04), pp. 447-451.

5. Angelova, N. & Hunkeler, D., 1999. Rationalizing the design of polymeric biomaterials. *Trends in Biotechnology,* 17(10), pp. 409-421.

6. Brocchini, S. & Duncan, R., 1999. Pendant Drugs, Release from Polymers. *Encyclopedia of Controlled Drug Delivery,* Volume 02, pp. 786-816.

7. Colthurst, M. J., Williams, R. L., Hiscott, P. S. & Grierson, I., 2000. Biomaterials used in the posterior segment of the eye. *Biomaterials,* 21(07), pp. 649-665.

8. Mao, H. Q. et al., 2005. Biodegradable poly(terephthalate-co-phosphate)s: synthesis, characterization and drug-release properties. *Journal of Biomaterials Science, Polymer edition,* 16(02), pp. 135-161.

9. Fang, J., Nakamura, H. & Maeda, H., 2011. The EPR effect: Unique features of tumor blood vessels for drug delivery, factors involved, and limitations and augmentation of the effect. *Advanced Drug Delivery Reviews,* 63(03), pp. 136-151.

10. Pasut, G. & Veronese, F. M., 2009. PEG conjugates in clinical development or use as anticancer agents: An overview. *Advanced Drug Delivery Reviews,* 61(13), pp. 1177-1188.

11. Zhang, Q. F. et al., 2013. Linear polycations by ring-opening polymerization as non-viral gene delivery vectors. *Biomaterials,* 34(21), pp. 5391-5401.

12. Wang, Y. et al., 2011. Branched Polyethylenimine Derivatives with Reductively Cleavable Periphery for Safe and Efficient In Vitro Gene Transfer. *Biomacromolecules,* 12(04), pp. 1032-1040.

13. Villar, G., Puche, J. T. & Albericio, F., 2012. Polymers and Drug Delivery Systems. *Current Drug Delivery,* 09(04), pp. 367-394.

14. Panyam, J. et al., 2003. Fluorescence and electron microscopy probes for cellular and tissue uptake of poly(d,l-lactide-co-glycolide) nanoparticles. *International Journal of Pharmaceutics,* 262(01-02), pp. 01-11.

15. Nowotnik, D. P. & Cvitkovic, E., 2009. ProLindac™ (AP5346): A review of the development of an HPMA DACH platinum Polymer Therapeutic. *Advanced Drug Delivery Reviews,* 61(13), pp. 1214-1219.

16. Davis, M. E., 2009. Design and development of IT-101, a cyclodextrin-containing polymer conjugate of camptothecin. *Advanced Drug Delivery Reviews,* 61(13), pp. 1189-1192.

17. Satchi, F. R. et al., 2004. Targeting angiogenesis with a conjugate of HPMA copolymer and TNP-470. *Nature Medicine,* 10(03), pp. 255-261.

18. Chesler, L. et al., 2007. Malignant Progression and Blockade of Angiogenesis in a Murine Transgenic Model of Neuroblastoma. *Cancer Research,* 67(19), pp. 9435-9442.

19. Fainaro, R. S. et al., 2005. Inhibition of vessel permeability by TNP-470 and its polymer conjugate, caplostatin. *Cancer Cell,* 07(03), pp. 251-261.

20. Imran ul-haq, M., Lai, B. F. L., Chapanian, R. & Kizhakkedathu, J. N., 2012. Influence of architecture of high molecular weight linear and branched polyglycerols on their biocompatibility and biodistribution. *Biomaterials,* 33(35), pp. 9135-9147.

21. Ikumi, Y. et al., 2008. Polymer-phloridzin conjugates as an anti-diabetic drug that Inhibits glucose absorption through the Na+/glucose cotransporter (SGLT1) in the small intestine. *Journal of Controlled Release,* 125(01), pp. 42-49.

22. Gabano, E., Ravera, M. & Osella, D., 2009. The Drug Targeting and Delivery Approach Applied to Pt-Antitumour Complexes. A Coordination Point of View. *Current Medicinal Chemistry,* 16(34), pp. 4544-4580.

23. Gaviglio, L., Gross, A., Nolte, N. M. & Ravera, M., 2012. Synthesis and in vitro cytotoxicity of cis,cis,trans-diamminedichloridodisuccinatoplatinum(IV)–peptide bioconjugates. *Metallomics,* 04(03), pp. 260-266.

24. Katime, I., Guerrero, L. G. & Mendizabal, E., 2012. Size matters: smart copolymeric nanohydrogels: synthesis and applications. *Frontiers in Bioscience,* Volume E4, pp. 1314-1334.

25. Bawa, P., Pillay, V., Choonara, Y. E. & Toit, L. C., 2009. Stimuli responsive polymers and their applications in drug delivery. *Biomedical Materials,* 04(02), pp. 01-15.

26. Lowman, A. M. et al., 1999. Oral Delivery of Insulin Using pH-Responsive Complexation Gels. *Journal of Pharmaceutical Sciences,* 88(09), pp. 933-937.

27. Joung, Y. K., Choi, J. H., Park, K. M. & Park, K. D., 2007. PLGA microparticle-embedded thermosensitive hydrogels for sustained release of hydrophobic drugs. *Biomedical Materials,* 02(04), pp. 269-273.

28. Schryver, S. B. et al., 1913. Colloids and Their Viscosity. *Transactions of the Faraday Society,* Volume 09, pp. 93-107.

29. Lindman, B. & Wennerstrom, H., 1980. Amphiphilic Aggregations in Aqueous Solution. *Micelles-Topics in Current Chemistry,* Volume 87, pp. 01-83.

30. Kataoka, K. et al., 1993. Block copolymer micelles as vehicles for drug delivery. *Journal of Controlled Release,* 24(01-03), pp. 119-132.

31. Liu, G. Y. et al., 2011. Biocompatible Poly(D,L-lactide)-block-Poly(2-methacryloyloxyethylphosphorylcholine) Micelles for Drug Delivery. *Macromolecular Chemistry and Physics,* 212(06), pp. 643-651.

32. Chapman, D., 1993. Biomembranes and New Hemocompatible Materials. *The Langmuir Lectures,* 09(01), pp. 39-45.

33. Aw, M. S., Mensah, J. A. & Losic, D., 2012. Polymer Micelles for Delayed Release of Therapeutics from Drug-Releasing Surfaces with Nanotubular Structures. *Macromolecular Bioscience,* 12(08), pp. 1048-1052.

34. Gao, C. & Yan, D., 2004. Hyperbranched polymers: from synthesis to applications. *Progress in Polymer Science,* 29(03), pp. 183-275.

35. Kienle, R. H., van der. Meulen, P. A. & Petke, F. E., 1939. The Polyhydric Alcohol-Polybasic Acid Reaction. III. Further Studies of the Glycerol-Phthalic Anhydride Reaction. *Journal of the American Chemical Society,* 61(09), pp. 2258-2268.

36. Kim, Y. H. & Webster, O. W., 1990. Water soluble hyperbranched polyphenylene: "a unimolecular micelle?". *Journal of the American Chemical Society,* 112(11), pp. 4592-4593.

37. Kim, Y. H. & Webster, O. W., 1992. Hyperbranched Polyphenylenes. *Macromolecules,* 25(21), pp. 5561-5572.

38. Pearce, A. K. et al., 2014. Development of a polymer theranostic for prostate cancer. *Polymer Chemistry,* 05(24), pp. 6932-6942.

39. Adeli, M., Rasoulian, B., Saadatmehr, F. & Zabihi, F., 2013. Hyperbranched poly(citric acid) and its application as anticancer drug delivery system. *Journal of Applied Polymer Science,* 129(06), pp. 3665-3671.

40. Vogtle, F., Buhleier, E. & Wehner, W., 1978. "Cascade"- and "Nonskid-Chain-like" Syntheses of Molecular Cavity Topologies. *Synthesis,* Volume 02, pp. 155-158.

41. Tomalia, D. A. & Frechet, J. M. J., 2001. Discovery of dendrimers and dendritic polymers: A brief historical perspective. *Journal of Polymer Science Part A: Polymer Chemistry,* 40(16), pp. 2719-2728.

42. Newkome, G. R., Yao, Z., Baker, G. R. & Gupta, V. K., 1985. Micelles. Part 1. Cascade molecules: a new approach to micelles. A arborol. *The Journal of Organic Chemistry,* 50(11), pp. 2003-2004.

43. Chen, C. Z. et al., 2000. Quaternary Ammonium Functionalized Poly(propylene imine) Dendrimers as Effective Antimicrobials: Structure−Activity Studies. *Biomacromolecules,* 01(03), pp. 473-480.

44. Morgan, M. T. et al., 2005. Dendritic supramolecular assemblies for drug delivery. *Chemical Communications,* 0(34), pp. 4309-4311.

45. Kolhe, P., Misra, E., Kannan, R. M. & Lieh Lai, M., 2003. Drug complexation, in vitro release and cellular entry of dendrimers and hyperbranched polymers. *International Journal of Pharmaceutics,* 259(01-02), pp. 143-160.

46. Koc, F. E. & Senel, M., 2013. Solubility enhancement of Non-Steroidal Anti-Inflammatory Drugs (NSAIDs) using polypolypropylene oxide core PAMAM dendrimers. *International Journal of Pharmaceutics,* 451(01-02), pp. 18-22.

47. Li, X. et al., 2014. Preparation of PEG-modified PAMAM dendrimers having a gold nanorod core and their application to photothermal therapy. *Journal of Materials Chemistry B,* 02(26), pp. 4167-4176.

48. Tekade, R. K., Kumar, P. V. & Jain, N. K., 2009. Dendrimers is oncology: an expanding horizon. *Chemical Reviews,* 109(01), pp. 49-57.

49. Nishiyama, N. et al., 2003. Light-Harvesting Ionic Dendrimer Porphyrins as New Photosensitizers for Photodynamic Therapy. *Bioconjugate Chemistry,* 14(01), pp. 58-66.

Chapter 2

Synthesis of Polymers and Porphyrins

Chapter 3

Branched Macromolecules for Drug Delivery

Table of Contents

Abbreviations

5-FU – 5-Fluorouracil

A549 cells – Adenocarcinomic human alveolar basal epithelial cells

G0.5, G1.0 etc. – Generation of respective dendrimer(s)

GPC – Gel permeation chromatography

HBP(s) – Hyperbranched Polymers

HYPAM(s) – Hyperbranched Poly(amido)amines

IC_{50} – Half maximal inhibitory concentration

M – Molar

m/v – mass/volume

M^{-1} cm^{-1} – $Molar^{-1}$ $centimetre^{-1}$

mg/ml – milligram/milli-litre

MTX – Methotrexate

nm – nanometre

PAMAM(s) – Poly(amido)amine

PDT – Photodynamic Therapy

PEG – Polyethylene glycol

PG(s) – Polyglycidol

pH – power of hydrogen

pK – equilibrium of acid dissociation

THPP – meso-tetra(hydroxyphenyl) porphyrin/ 5,10,15,20-Tetra (4 hydroxy) phenyl porphyrin

TPP – 5,10,15,20-Tetraphenyl porphyrin

TRIS – tris(hydroxymethyl)amino methane

TRIS-PAMAM/PAMAM-TRIS – tris(hydroxymethyl)amido methane poly(amido)amine

UV-Vis – Ultraviolet-Visible

ZnTDHPP – Tetra (3,5 dihydroxyphenyl) porphyrin zinc

ZnTDMPP – Tetra (3,5 dimethoxyphenyl) porphyrin zinc

ZnTHPP – 5,10,15,20-Tetra (4 hydroxyphenyl) porphyrin zinc

ZnTPP - 5,10,15,20-Tetraphenyl porphyrin zinc

List of Figures

List of Tables

List of Graphs

List of Equations

3.1 Introduction

After the inception of dendrimers as the new class of macromolecules, research contemplating their synthesis gained momentum. Once the synthetic routes for dendrimers were identified and accepted by the scientific community, the focus switched to their applications. Dendrimers in general, are macromolecules with a globular, well-defined, mono-dispersed structures. Their physiochemical properties make them one of the most suited therapeutic polymers. Some of their most advantageous properties consist of bio-distribution and pharmacokinetic characteristics. These can be modified by controlling the size, functionality, and conformation of the dendrimers. With increments in their generations, the molecular weight continues to grow in a controlled manner giving them the identity of single molecular system. The potential of strengthened ligand-receptor binding is exploited as the multivalent ligand density increases with incrementing generations. And finally, with the use of self-immolative dendrimers capable of functionality modification, their self-degradation is kept in check [1].

With numerous benefits connected with dendrimers' properties, their interactions with drugs has been a topic of wide-spread research [2]. In this brief introduction, advancements in dendrimer-drug interactions will be presented with PAMAM dendrimers as the focal point. Broadly, two well-researched interactions exist: non-covalent and covalent interactions.

Covalent interactions represent the conjugation of drugs with relevant functional groups of the dendrimers which can later be released by cleaving hydrolytic labile bonds chemically or enzymatically [3]. Acetylated PAMAM dendrimers were conjugated with 5-Fluorouracil (5-FU), an antitumor drug (Figure 3.1), transporting them safely to the target tumour site and releasing it slowly with reduced toxicity [4]. Although the toxicity results for this study were good, the modification of the PAMAM dendrimers was rather time consuming if not difficult. Another example highlighting this issue was the use of G5-PAMAM dendrimers for targeted drug delivery by their conjugation to folic acid was studied by Baker group [5]. The terminal amines of the dendrimer were glycidol capped to form ester linkages with methotrexate (MTX). The slow drug release by the dendrimer system on comparison to free drug release was reported to be less than ~5% over 2.5 hours, making the dendrimers the ideal drug delivery system. With blockage and under-expression of folic acid receptors, the conjugates ended up losing their anti-proliferative effect. To get better results and avoid under-expression, improvement in the synthesis of the conjugate were carried out, reflecting on the drawbacks of covalent interactions with dendrimers in drug delivery systems.

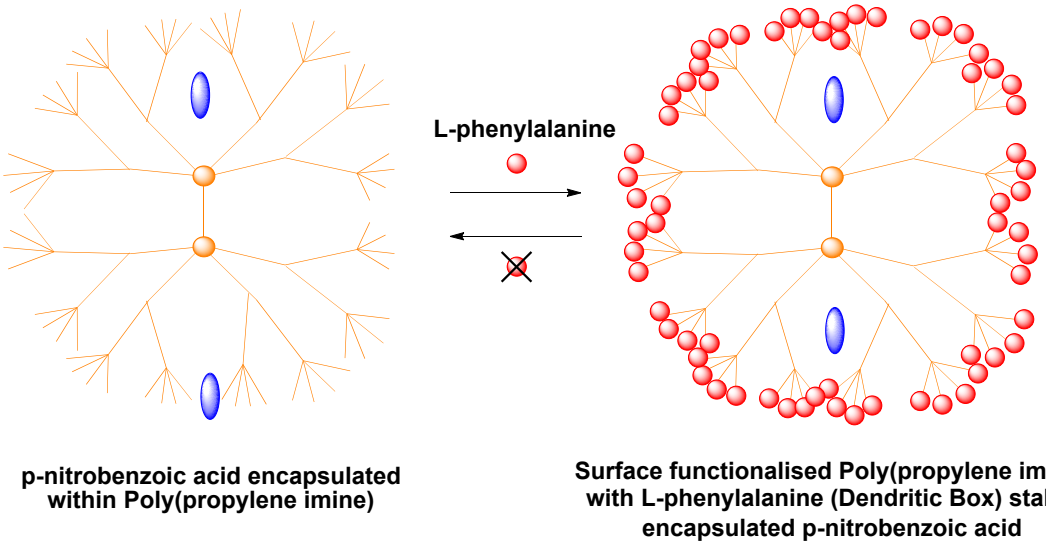

Figure 3.1. Graphical representation of a (host-guest) dendritic box with surface functionalised poly (propylene amine) with L-phenylalanine encapsulated with p-nitrobenzoic acid.

The IC_{50} toxicity (the half maximal inhibitory concentration measuring the potency of a substance in inhibiting a specific biological or biochemical function) of anticancer drug, Paclitaxel was reduced 10-fold on comparison to free Paclitaxel, upon conjugation with G4-PAMAM dendrimers [6] while the PEG-ylated dendrimers demonstrated a reduction of ~25-fold. Even though PAMAMs were able to reduce the toxicity, on comparison to PEG-ylated dendrimers, they lacked potential. The application of dendrimers in photodynamic therapy (PDT) can be seen as well. For example, study involving prophyrin cored carboxylated glycodendrimers for PDT, showed significant results [12] (Figure 3.2).

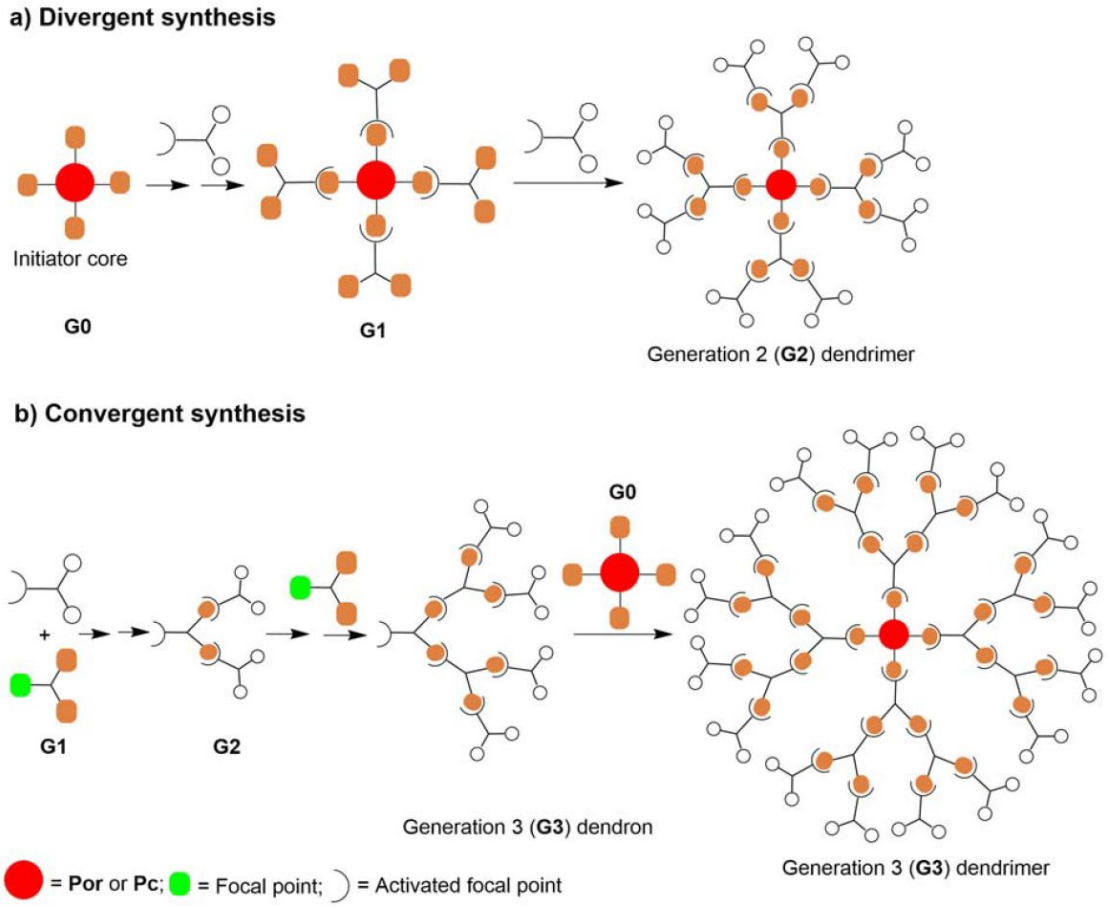

Figure 3.2. Graphical representation of synthesis drug cored dendrimers such as porphyrin or phthalocyanine containing carbohydrate glycodendrimers, for Photodynamic Therapy (PDT). Republished with permission of Current Organic Synthesis, from Porphyrins and Phthalocyanines Decorated with Dendrimers: Synthesis and Biomedical Applications, Figueira F, Pereira MR, Silva S, Cavaleiro J AS, Tome J, 11 (01) 2014; permission conveyed through Copyright Clearance Center, Inc.

Overall, the above said examples of covalent dendrimer-drug interactions show good potential however, their complicated synthesis serves as a major drawback. Changes to the properties of the drug as reported with folic acid receptors due to conjugation with the dendrimer also makes this method for encapsulation studies less favourable. Twyman et al reviewed various types of covalent dendrimer-drug interactions primarily based upon their conjugated synthesis which were found to be difficult and time-consuming [7].

Having said that, non-covalent interactions, is another approach to drug delivery. Hydrophobic interactions besides electrostatic and secondary interactions govern the encapsulation and solubility of the drug in this approach. The need for structural modifications is minimal except the modification of terminal functionality modifications to lower cyto-toxicity of the system. With this approach, hydrophobic drugs can easily be encapsulated without the need of complicated modifications to the dendrimer or the drug.

This form of drug encapsulation also facilitates host-guest interactions where a drug can be enticed to reside in the hydrophobic cavity of the dendrimer under aqueous media conditions. The following examples reflect on the noncovalent PAMAM dendrimer-drug interactions that have been successful.

Up to 78 ibuprofen molecules per PAMAM dendrimer (G3 and G4) were encapsulated and their release in vitro was studied [8]. The release of Ibuprofen was found to be slower than that of free Ibuprofen. Also, the dendrimer-drug complex could enter A549 cells faster than free Ibuprofen. This studied proved that dendrimer had the potential to deliver drugs to the target sites, safely. In another example, dendrimers behaved as vectors for gene delivery by forming transfection complexes upon interacting with the phosphate groups of the nucleic acids [9]. The dendrimers could carry large amount of genetic material mainly because of their well-defined shape and low pK of amines. Size dependant solubility of hydrophobic drug, nifedipine, calcium channel-blocking agent, was studied with varying generations of PAMAM dendrimers in aqueous media [10]. The study revealed as the size of the dendrimer increased, the solubility of the drug increased as well.

3.2 Aims and Objectives

After discussing the shortfalls of covalent interactions and benefits of non-covalent interactions briefly, understanding the aims of this research will be straightforward. This chapter discusses the application of PAMAM dendrimers and its analogues as drug delivery systems. The studies were carried out using one small and one large drug along with their respective analogues.

As we know, amine PAMAMs on their own are toxic and cannot be used for drug delivery without modifications [7, 14]. Hence, neutral TRIS PAMAMs consisting of terminal OH groups were synthesised from G2.0 to G5.0. Their synthesis and characterisation are described in detail in Chapter 2 Section 2.2.2.3. Following the successful synthesis, determining which generation gives the highest loading of a drug was conducted using the model drug, Ibuprofen. This was followed by determination of the best suitable concentration of the dendrimer for all the encapsulation studies. To do that, varying concentrations of the selected PAMAM generation were encapsulated with excess Ibuprofen and studied via UV-Vis Spectroscopy to give the loading of Ibuprofen in each concentration. The concentration giving the highest loading was set as the standard dendrimer concentration for all future encapsulation experiments.

The next aim was to compare TRIS PAMAMs to a hyperbranched polymer to determine whether dendrimers are better or hyperbranched polymers. Another reason for comparison of the two macromolecules was to understand the role of secondary interactions in the encapsulation of drugs and increase in their respective solubility. Four drugs were chosen, although, five were tested with TRIS PAMAMs alone to understand the effect of hydrophobicity in dendrimers, only four were studied with polyglycidol. The first two drugs were Ibuprofen and THPP followed by their analogs Cuminol and ZnTHPP. These were selected to study whether secondary interactions between the drug and the dendrimer, if at all it occurs, maximises the solubility of the drug or not.

As polyglycidol does not contain any internal amines, it did not mimic the internal interactions that would take place between a drug and TRIS PAMAM dendrimer. Therefore, the third and the final aim of the research involved comparing hyperbranched PAMAMs (HYPAMs) with Amine PAMAMs in their efficiency as drug delivery systems. Since, HYPAMs consists of terminal amines, they could not be compared to TRIS PAMAMs. As a result, a direct assessment between HYPAMs and Amine PAMAMs was done.

In the end, evaluation to determine which of the four polymers studied displayed overall good solubility with all the above-mentioned factors at hand, was done.

3.3 Results and discussion

Part 1 TRIS PAMAM vs Polyglycidol

3.3.1 Polymer selection

PAMAM dendrimers were synthesized from the starting generation G0.5 to G5.0 for studying their ability as drug delivery systems. The beginning of the study involved in understanding how good drug encapsulations were as the size of the dendrimer increased. In other words, determining the ability of successfully encapsulating drugs with increasing dendrimer generation was the first milestone of this study. So as discussed in chapter 2 section 2.2.2.3, upon successful synthesis, PAMAMs underwent surface modification to suit the needs for respective drug delivery applications. To understand which generation works best in encapsulating drugs, TRIS PAMAMs were chosen (Figure 3.4). TRIS PAMAMs have neutral surfaces with the presence of TRIS-OH groups making them the preferable choice for drug delivery studies.

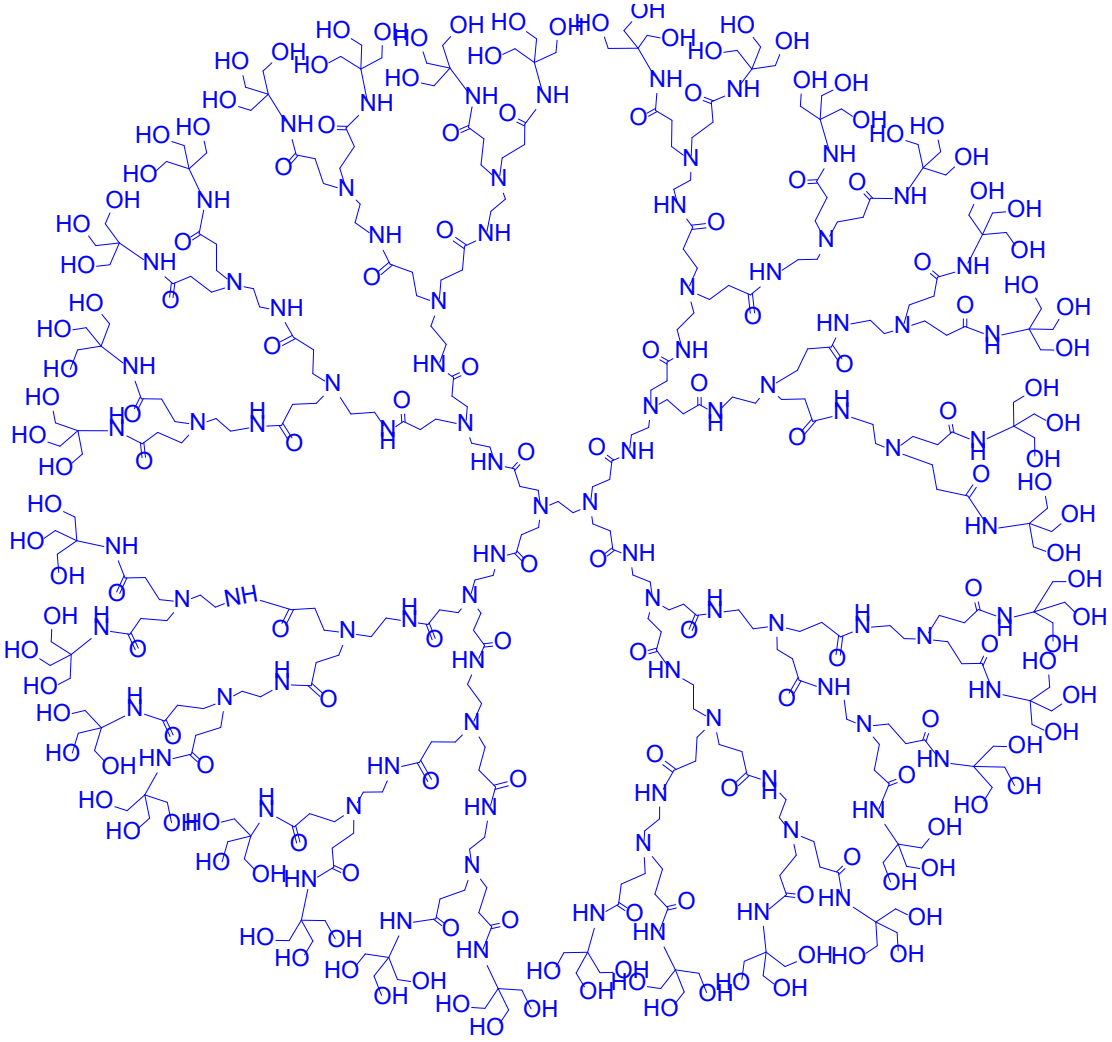

Figure 3.4 Structure of G4.0 TRIS PAMAM

To conduct the study, successive TRIS PAMAMs i.e. G2.0, G3.0, G4.0 and G5.0 were used to encapsulate excess Ibuprofen at a concentration of 1 x 10^{-4} M via co-precipitate method. Methanol was used as the common solvent and TRIS buffer with 0.01 M concentration was used as the buffer system. UV-Vis Spectroscopy was used for determining the extent of encapsulation within each dendrimer generation. Ibuprofen was chosen for this study as it has been extensively studied in Twyman group as a model drug [13]. It is a small drug with low aqueous solubility and good hydrophobic interactions with PAMAMs. It has a characteristic wavelength at 264 nm with a molar extinction co-efficient of 320.70 $M^{-1}cm^{-1}$. Also, the maximum solubility of Ibuprofen in buffer was determined beforehand. These values were used to calculate the concentration of Ibuprofen after encapsulation obtained. The maximum loading of Ibuprofen i.e. maximum number of Ibuprofen molecules incorporated per dendrimer were calculated by dividing the concentration of Ibuprofen by the concentration of the dendrimers. The results for this study are tabulated below (Table 3.1).

Table 3.1 Concentration and loading of Ibuprofen encapsulated within successive TRIS PAMAMs

TRIS-PAMAMs (1×10^{-4} M)	Obtained Concentration of Ibuprofen using Molar Extinction Coefficient (ε =320.60 $M^{-1}cm^{-1}$) ($\times 10^{-3}$ M)	Maximum loading of Ibuprofen obtained (stoichiometry of loading/dendrimer)
G 2.0	0.48	4.80
G 3.0	1.33	13.29
G 4.0	3.07	30.66
G 5.0	2.16	21.61

From the results, we notice that as the generation increases, the encapsulation ability also as well. It was certain that G 4.0 TRIS PAMAM encapsulated the highest number of Ibuprofen molecules. However, the argument here is why doesn't G 5.0 encapsulate more than its predecessor? After all, the encapsulation seems to be size dependant. The reason is that as the dendrimer size increases, an increase in dense shell packing is witnessed as well. As a result, less space is available for the drugs to occupy. Therefore, a significant drop in drug loading is seen (Graph 3.1). As for G 4.0 TRIS PAMAMs, they encapsulated the highest number of Ibuprofen proving that they have the perfect structure with good steric packing.

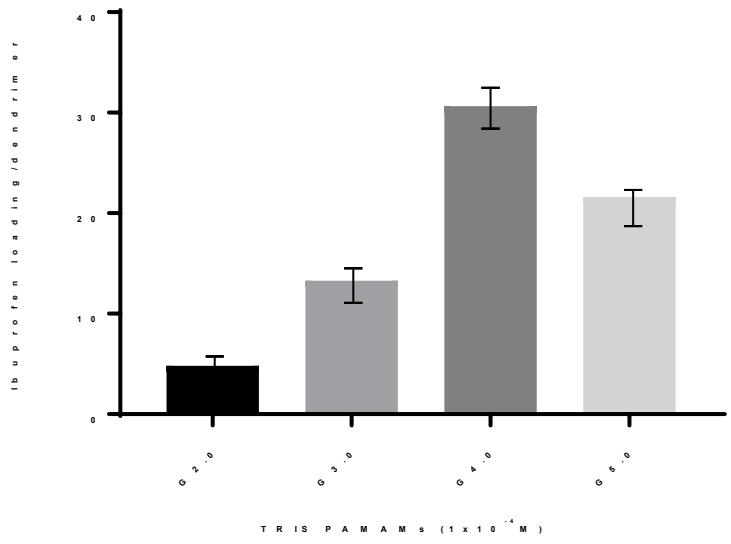

Graph 3.1. Loading of Ibuprofen within different generations of TRIS PAMAMs

The study described above provided with which generation of TRIS PAMAMs to proceed further. This was clearly, G 4.0 TRIS PAMAMs. The encapsulation ability of the dendrimer at a fixed concentration was to be studied. To determine the optimal concentration, varying concentrations of G 4.0 TRIS PAMAM were used to encapsulate excess Ibuprofen. The concentration of the dendrimer varied from $1x10^{-5}$ M to $1x10^{-3}$ M. The loading of Ibuprofen obtained are presented in the Graph 3.2 below.

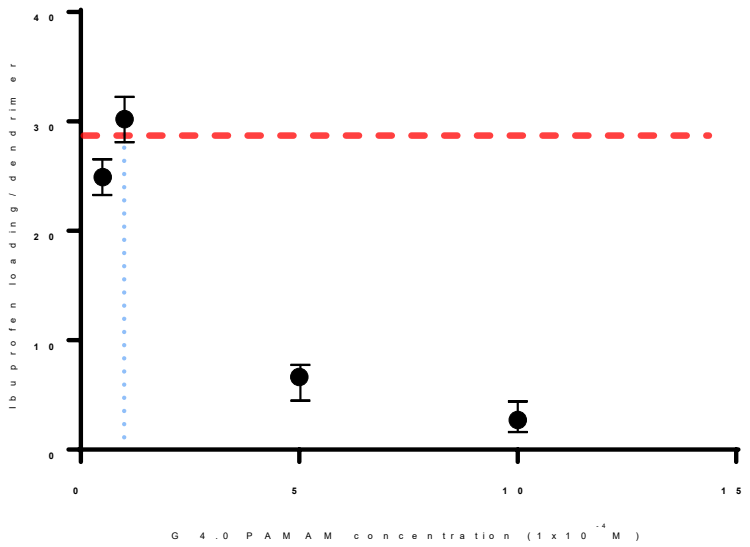

Graph 3.2. Loading of Ibuprofen per G4.0 TRIS PAMAM molecule.

The data showed that the G4.0 TRIS PAMAM performed best at a concentration of 1×10^{-4} M. As the concentration of the dendrimer increments, the loading of ibuprofen should ideally be constant i.e. plateauing off. To the contrary, the loading drops significantly. One possible hypothesis for this experiment is aggregation. This phenomenon was studied shoulder to shoulder by another researcher in the Twyman group[15]. However, the focus of my study was on selecting the perfect dendrimer concentration with maximum loading. This concentration dependant study showed exactly that and $1x10^{-4}$M concentration for G 4.0 TRIS PAMAMs was chosen to be used for all future encapsulation studies.

3.3.2 Drug(s) selection

To study the encapsulation ability of G4.0 TRIS PAMAMs, five drugs were carefully selected. The selection was based upon their solubility in buffer and their primitive hydrophobicity. The solubility of drugs needs to be poor or very low in water/aqueous media. If we take a moment to think about this, one of the important properties of a good drug delivery system is to carry a drug which cannot tolerate aqueous media on its own. The dendrimers provide a safe environment for these drugs while they are transported to specific (target) sites.

Building on this, drugs with poor aqueous solubility naturally have good hydrophobic properties. This makes their encapsulation furthermore simple. The internal amines of the dendrimer interact with the drug (host-guest) helping the drug stay in place without undergoing structural modifications. A series of drugs were tested and studied specifically in consideration with the above two requirements. The chosen drugs were Ibuprofen, Warfarin, and THPP. The other two drugs studied were Cuminol and ZnTHPP (Figure 3.5). Ibuprofen, Warfarin and Cuminol were commercially sourced whereas THPP and ZnTHPP were synthesised in laboratory (Chapter 2 Section 2.3). Cuminol and ZnTHPP are important as they undergo secondary interactions while encapsulated. A stronger interaction with the dendrimer should result in higher drug loading. Also, Cuminol is an analogue of Ibuprofen while ZnTHPP is the analogue of THPP. So, the performance of Ibuprofen and THPP to that of their respective analogues was studied and compared. Table 3.2 below provides with characteristic wavelength, molar extinction coefficient and the maximum solubility of the drugs tested in the laboratory.

Table 3.2. Drugs with their respective UV-Vis properties.

Drug	Characteristic wavelength (nm)	Molar extinction coefficient ($M^{-1}cm^{-1}$)	Maximum Inherent solubility in TRIS buffer (M)
Ibuprofen	**264**	**320.70**	**6.02×10^{-3}**
Cuminol	**263**	**5837.60**	**6.66×10^{-4}**
THPP	**418.5**	**297922**	**4.04×10^{-7}**
ZnTHPP	**424.5**	**15379**	**8.71×10^{-7}**
Warfarin	**306.5**	**14934**	**3.80×10^{-4}**

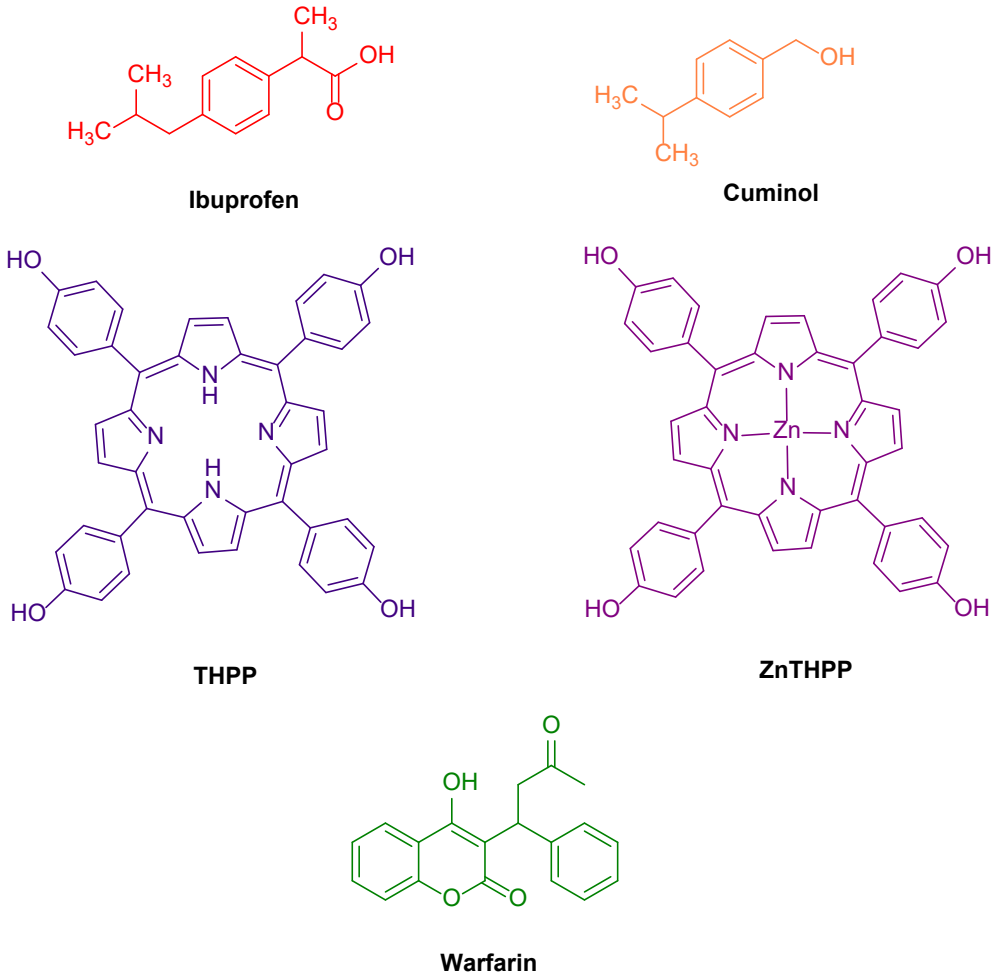

Figure 3.5. The chosen drugs for future encapsulation studies with G4.0 TRIS PAMAMs

3.3.3 Encapsulation studies for TRIS PAMAMs

Having determined the optimum dendrimer for encapsulation, the next step was to investigate how well it could encapsulate and dissolve some other drug molecules and five drugs were chosen. The encapsulation was done as previously described via the co-precipitate method (Figure 3.6). The obtained concentration (c) for each drug was calculated by using their maximum absorbance (A) at characteristic wavelength(s), respective molar absorption coefficient (ε) and correcting for any dilutions and inherent solubility in the TRIS buffer. The molar extinction coefficient for respective drugs is obtained by following the Beer Lambert Law (the length (l) of quartz cuvette is 01 cm);

$$A = \varepsilon c l \qquad \textbf{Equation 3.1}$$

The maximum loading obtained was calculated by dividing the concentration obtained by the concentration of the dendrimer. At this point, it is important to mention that a high buffer concentration was used. Specifically, a TRIS buffer with a concentration of 0.01M (and a pH of 7.4 was required). This relatively high concentration was required to ensure that it was strong enough to cope with the dendrimer's basic amines. This is important as many of the drugs have acidic protons and could be deprotonated, which would enhance their inherent solubility. The results for each of the drugs encapsulated are listed in the Table 3.3.

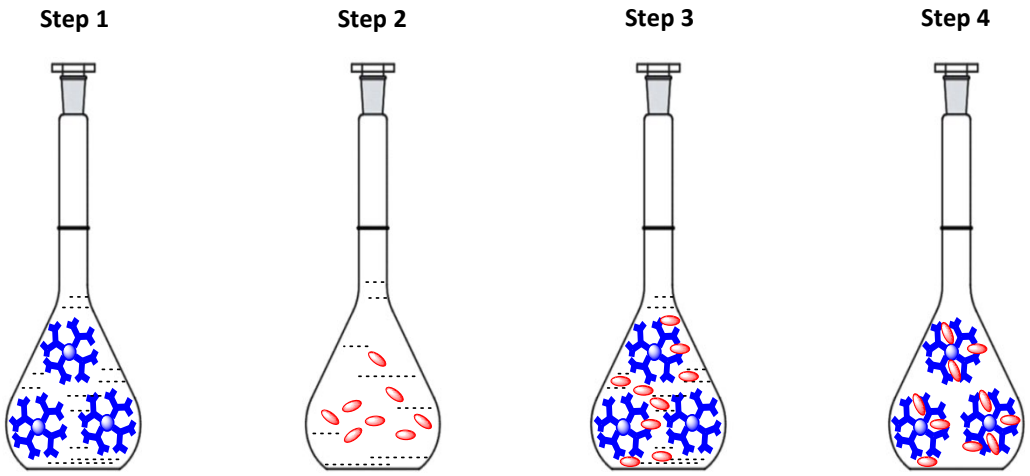

Figure 3.6. Graphical representation of co-precipitate encapsulation method. Step 1 and Step 2 represent polymer solution with a concentration of $1x10^{-4}$ M (TRIS PAMAMs) and excess drug(s) solution, respectively. Hereafter, the polymer and drug solutions are mixed and stirred vigorously for an hour (Step 3) following which the solvent (methanol) is removed *in vacuo* and TRIS buffer of 0.01M concentration is added to give polymer-drug complex (Step 4).

Table 3.3. Drugs with respective loading per dendrimer molecule

Drugs	Concentration of encapsulated drugs ($x10^{-3}$ M)	Maximum Drug loading/ dendrimer
Ibuprofen	3.06	30.66
Cuminol	0.64	6.40
THPP	Negligible	Negligible
ZnTHPP	0.019	0.19
Warfarin	3.60	35.96

The table above lays out the concentration and the loading for each of the five drugs encapsulated and studied. Interestingly, when comparing Ibuprofen and Cuminol, higher loading with ibuprofen was achieved, with ~31 Ibuprofen molecules encapsulated per dendrimer. Cuminol, which does not possess a carboxylic acid group, gave a loading of six per dendrimer. The reason the dendrimer can encapsulate so much more ibuprofen, is due to the acid group, which can be deprotonated by the dendrimer's internal amines to form a salt; this interaction is not possible for the Cuminol. As such, 5-6 times more ibuprofen can be encapsulated than the neutral Cuminol. If we look at the porphyrins, THPP loading was almost non-existent and could not be reported in numerical form hence, reported as 'negligible'. However, ZnTHPP can co-ordinate to the dendrimers internal amines, which accounts for the increase in encapsulation efficiency (with respect to the non-metallated porphyrin). Overall, these results show how important secondary interactions are with respect to drug loading and encapsulation efficiency. And finally, almost forty molecules of warfarin per dendrimer could be encapsulated.

3.3.4 Encapsulation studies with Polyglycidol

To get a deeper insight into the effect of secondary interactions between guest and host, encapsulation studies using a new polymer that does not possess any internal amines (that gave rise to the secondary interactions observed in the PAMAM dendrimer) were needed to be studied. Although we wanted a polymer with little to no secondary interactions, it still needed to be water soluble and provide a suitable hydrophobic environment to encapsulate drug molecules. For this part of the study, polyglycidol was chosen as the polymer (Figure 3.7).

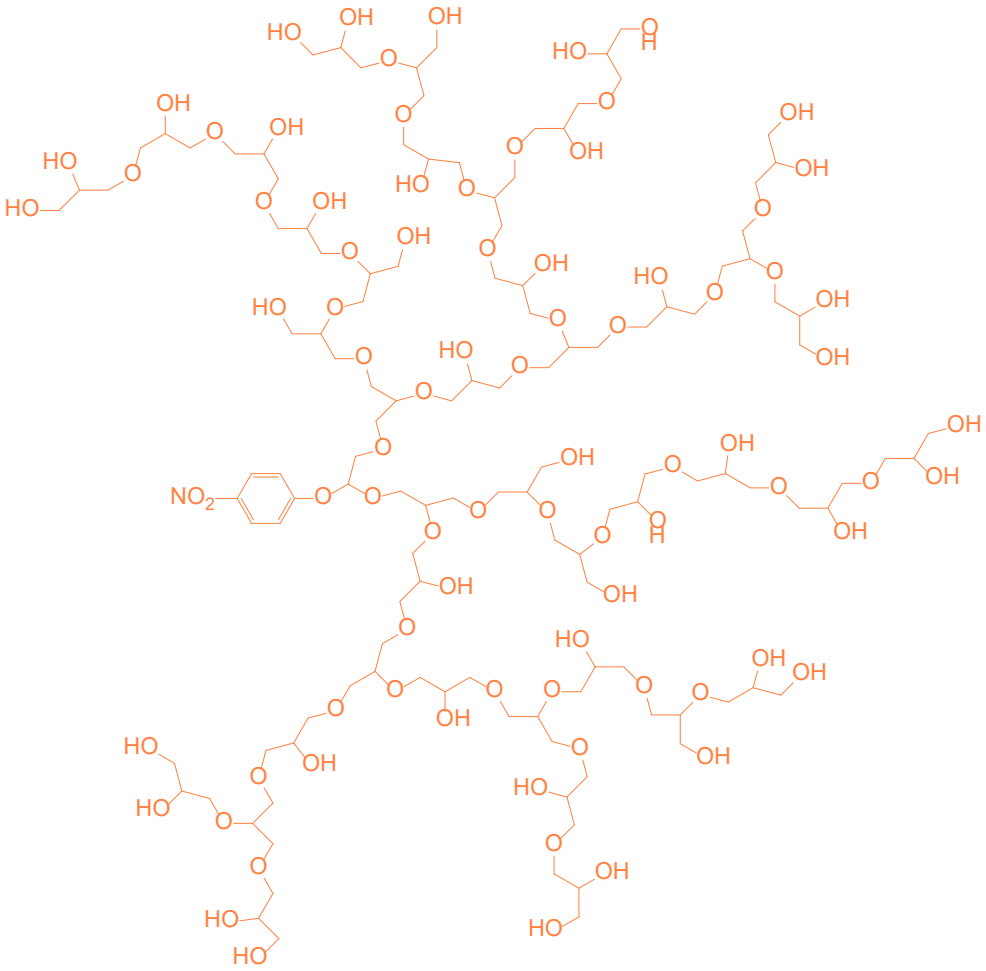

Figure 3.7. Structure of polyglycidol with presence of internal ether oxygens

A significant advantage of using HBPs instead of dendrimers is their significantly simpler synthesis. However, as discussed in the previous Chapter 2 Section 2.2.3, characterization with respect to molecular weights from GPC is not accurate. This is key, as molecular weight is important when calculating concentration. Obtaining a dendrimer solution with an accurate molar concentration is easy, as dendrimers are mono-disperse and have a unique and identifiable structure. This is not possible with HBPs as they are poly-dispersed and do not have defined molecular weight; making molar concentrations impossible to calculate. Therefore, when studying polymers, we use mass per volume (m/v) as the units for concentration. For the work described in the following sections, an m/v concentration or 0.83 mg/mL has been used, as this corresponds directly to the $1x10^{-4}$ M concentration used for the G4.0 TRIS PAMAM dendrimer. This will enable us to make a reasonable comparison between the two systems.

For the encapsulation studies, we selected the acidic Ibuprofen molecule and its neutral analogue Cuminol and a metallated and non-metallated porphyrin (ZnTHPP and THPP). As

polyglycidol does not possess any internal amines, which were essential for the secondary interactions (observed in G 4.0 Tris PAMAM dendrimer), we were not expecting to see any significant differences in the encapsulation efficiency. HBPs-drug complexes were made using the same co-precipitate method that was used for PAMAM experiments. They were later analysed via UV-Vis Spectroscopy to give the obtained concentration of respective drugs (with the use of Beer Lambert law (Equation 3.1)). The results obtained are shown below in Table 3.4.

Table 3.4. Concentration of drugs obtained after encapsulation within PG 1:10

Drugs	Obtained concentration of the drugs encapsulated ($x10^{-2}$ M) using Eq. 3.1
Ibuprofen	1.11
Cuminol	0.35
THPP	Negligible
ZnTHPP	Negligible

If we consider the porphyrin pair first, we observe that the HBP does not appear to be a good host for either, despite the possibility of a weak interaction between the ether oxygens and the metallated porphyrin. Presumably because of the poor coordination ability of ether oxygen, and Polyglycidol's open structure. Also, unlike dendrimers where open structure helps in better encapsulation, the level of branching in HBP means they are more dynamic and structurally flexible whereas dendrimers are static. As a result, the data for the porphyrins could not be reported in numerical form. We initially predicted that the HBP would bind ibuprofen and cuminol with a similar efficiency, as the HBP does not possess the internal functionality capable of contributing to any meaningful secondary interactions. However, ibuprofen was encapsulated very well, with a dissolved concentration akin to that recorded for the PAMAM dendrimer. In addition, if we compare the concentration with that recorded for cuminol, we notice that the HBP encapsulates ibuprofen 3-4 times better than cuminol. This is less than the ratio observed for the PAMAM dendrimer, which could encapsulate ibuprofen 5-6 times better than cuminol. This therefore provides good evidence for secondary interactions within the PAMAM dendrimer. We also predicted that overall binding efficiencies would be low for both molecules, as the HBP has a poorly defined and relatively open structure. However, the concentration of dissolved cuminol was around 5 times higher than the value obtained using the PAMAM dendrimer. Now, we are not sure why, could be due to the polarity of

polyglycidol that can be linked to the presence of internal hydroxyl groups which get deprotonated to O^-. It could also be due to the strong buffer system.

3.3.5 Comparing TRIS PAMAM to Polyglycidol

After conducting encapsulation studies with polyglycidol, the next step was to compare the results to that of TRIS PAMAMs. To do that, obtained concentrations of Ibuprofen, Cuminol and ZnTHPP after encapsulation within G4.0 TRIS PAMAMs and PG1:10 were compared, respectively. The first drug to be compared was Ibuprofen (Graph 3.3).

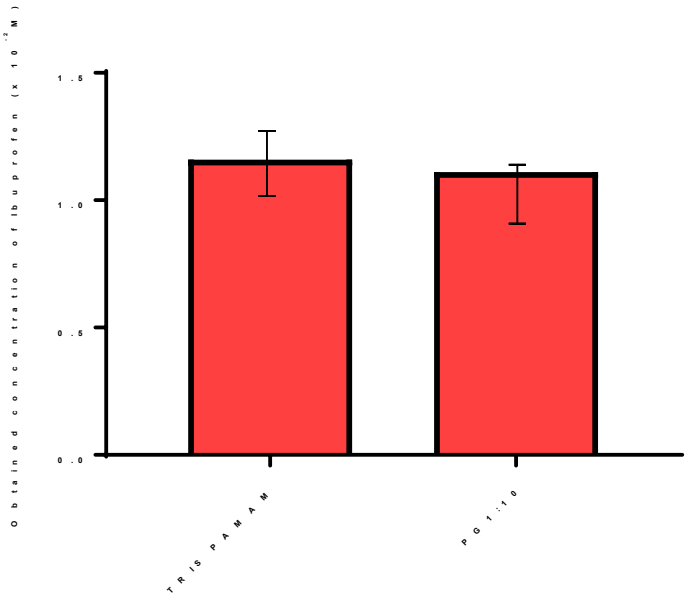

Graph 3.3. Comparing the encapsulation results for Ibuprofen between TRIS PAMAM and PG 1:10

It was evident that difference in encapsulation of Ibuprofen was not significant however, TRIS PAMAMs were able to encapsulate slightly more than PG1:10. This result didn't really prove if secondary interactions were needed to get more drugs inside a polymer. The next comparison was made for cuminol, analog of ibuprofen (Graph 3.4). For cuminol, the story was different. Polyglycidol incorporated more cuminol than TRIS PAMAM did.

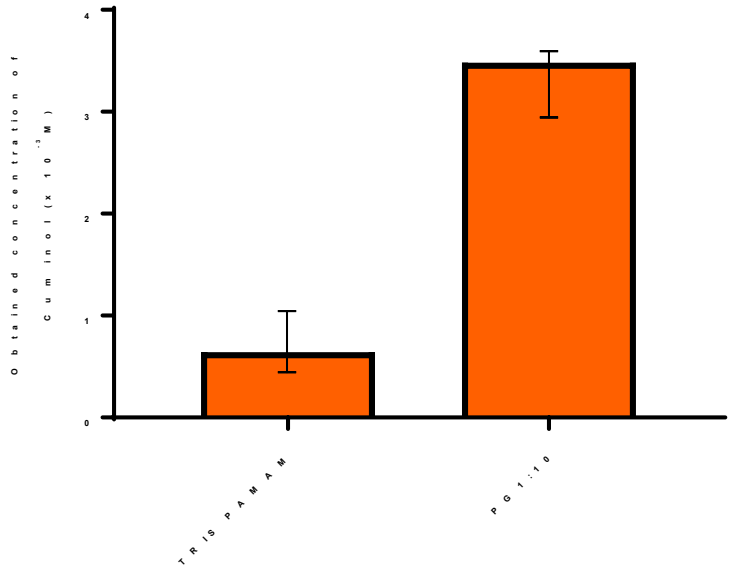

Graph 3.4. Comparing the encapsulation results for Cuminol between TRIS PAMAM and PG 1:10

To sum up, Table 3.5 compares the concentration of all the drugs encapsulated in both, G4.0 TRIS PAMAM and PG 1:10.

Table 3.5. Comparison of concentration of drugs encapsulated within TRIS PAMAM and PG 1:10

Drugs	Obtained Concentration after encapsulation (x 10^{-2}M)	
	G4.0 TRIS PAMAM	PG 1:10
Ibuprofen	1.16	1.11
Cuminol	0.06	0.35
THPP	Negligible	Negligible
ZnTHPP	0.0019	Negligible

With the encapsulation of drugs compared between the two polymers; it was clear that polyglycidol could encapsulate ibuprofen and cuminol. The importance of secondary interactions was highlighted. While ibuprofen showed a sixteen-fold increase in its loading, relatively low encapsulation for cuminol was reported. In conclusion, polyglycidol did not show superior encapsulation abilities. This was due to the absence of secondary interactions which are important for attaining high drug loading. TRIS PAMAMs on the other hand, could engage in secondary interactions leading to higher encapsulation efficiencies. Therefore, for a

better comparison, it was decided to look at a polymer that possessed similar internal functionalities to the PAMAM dendrimer. This formed the second milestone of the encapsulation studies which will be discussed in the next section.

Part 2 HYPAMs vs Amine PAMAM dendrimer

In the previous section, conclusions were drawn based on the encapsulation results that polyglycidol was no good when compared to TRIS PAMAMs. Preferably a hyperbranched polymer with internal functionalities, capable of secondary interactions should be studied. So, the question was, what type of hyperbranched polymer would be able to compete with TRIS PAMAMs. The idea of fracturing an already synthesised amine terminated PAMAM dendrimers i.e. G2.0, G3.0 and G4.0 was put into action. Upon thermal condensation, the dendrimers would undergo retro Michael addition internally. This would result in structural imperfections forming hyperbranched polyamidoamines. As discussed previously in Chapter 2 Section 2.2.4, the GPC analysis was not accurate. It seems as the condensation reaction progressed with time, fluctuation in the polydispersity of the polymer was observed. With repeated analysis, recurrent results proved the same. This brought us to the conclusion that instead of forming a structurally imperfect hyperbranched polymer, the dendrimer was shrinking down to its predecessor, a smaller dendrimer.

At that juncture, it was decided that instead of fracturing PAMAM dendrimers, hyperbranched PAMAMs (HYPAMs) would be synthesised and their encapsulation abilities will be subsequently studied. The detailed synthesis and characterisation of these polymers is discussed in Chapter 2 Section 2.2.5. As stated, two monomers AB_2 and AB_4 were synthesised. These monomers underwent retro Michael addition via thermal condensation to give AB_2 HYPAM and AB_4 HYPAM, respectively (Figure 3.8). Since, their characterised molecular weights were not definite due to their poly-disperse nature, concentration was calculated using mass/volume (m/v) or 0.82mg/ml. This matched the concentration of 1×10^{-4}M for TRIS PAMAMs. However, HYPAMs consist of terminal amine groups therefore, they were compared to amine terminated G4.0 PAMAM (Figure 3.9).

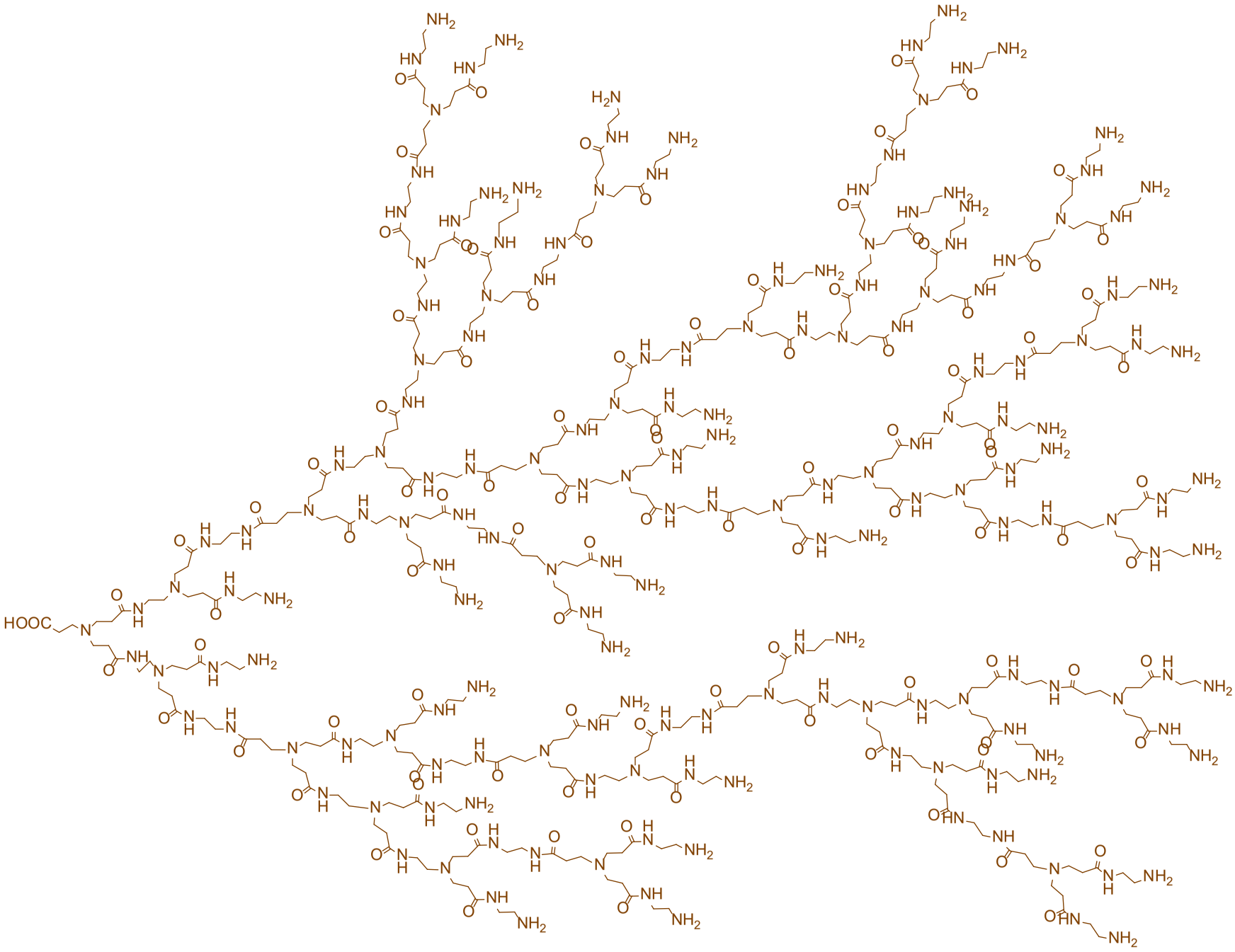

Figure 3.8 Structure of AB_4 HYPAM.

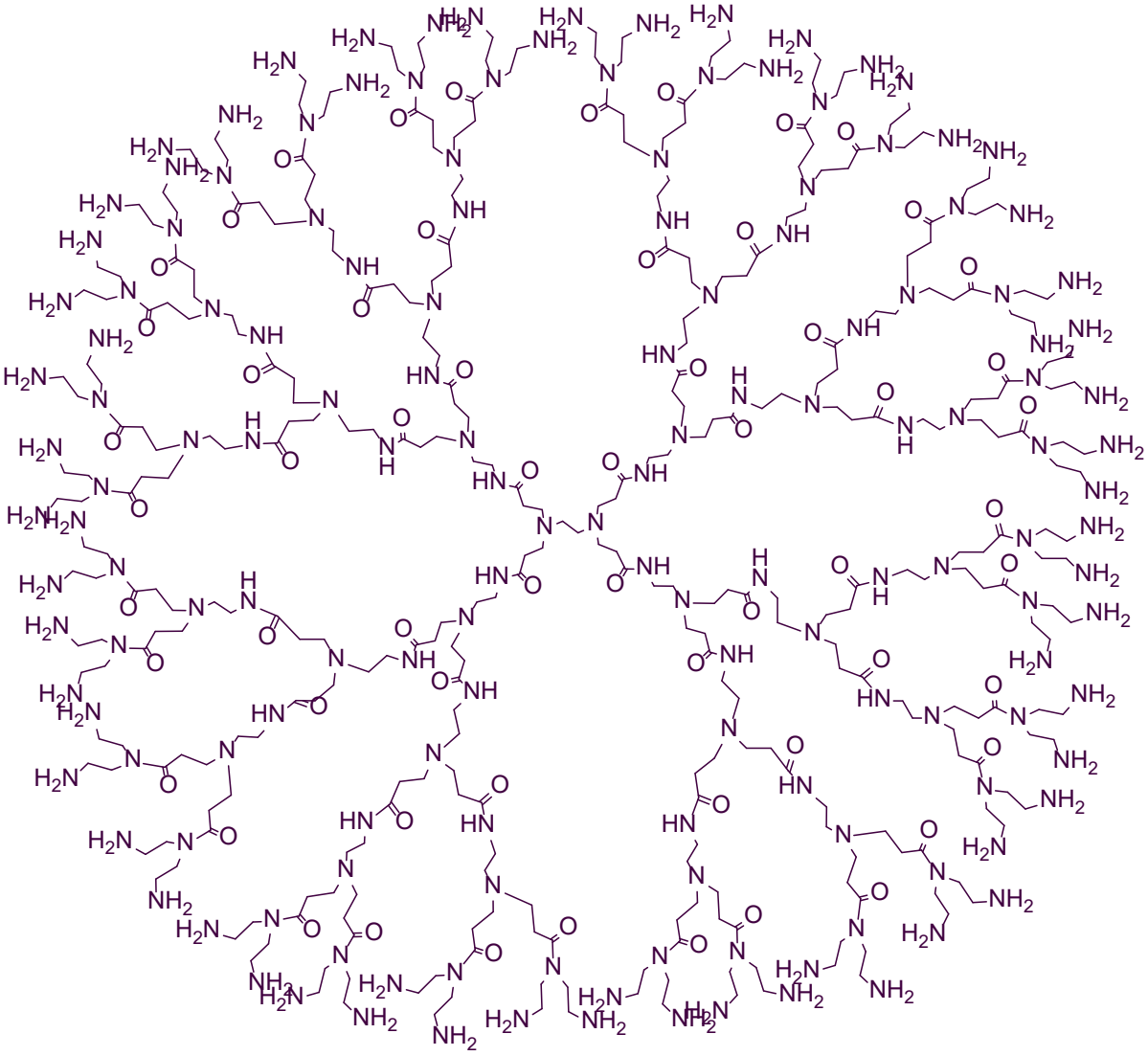

Figure 3.9 Structure of G4.0 PAMAM dendrimer

3.3.6 Encapsulation studies with HYPAMs and G4.0 Amine PAMAM

Since, the secondary interactions were the focus of this study, Ibuprofen and THPP along with their respective analogs were chosen (i.e. cuminol and ZnTHPP). Here as well, co-precipitate method was used to prepare the complexes. While the concentration of polymers was constant excess quantity of drugs was used. Hereafter, the complexes were analysed using UV-Vis Spectroscopy at each drug's characteristic wavelength. The concentration of the encapsulated drug was determined by using its molar coefficient, dilutions, and respective inherent solubility in TRIS buffer. The drugs with their characteristic UV-Vis properties are mentioned in table 3.2 previously. The first polymer to be studied was AB_2 HYPAM with the above-mentioned drugs. The table 3.6 below gives the concentration of the encapsulated drugs obtained.

Table 3.6 Concentration of drugs obtained after encapsulation within AB_2 HYPAM

Drug(s)	Obtained Concentration of the drugs encapsulated (x 10^{-2} M)
Ibuprofen	1.00
Cuminol	0.91
THPP	Negligible
ZnTHPP	0.15

For AB_2 HYPAM, encapsulation of THPP was very low and hence, it could not be reported. On the contrary, the concentration of ZnTHPP was well-observed. Reason being this polymer experiences good secondary interactions with the metallated porphyrin due to the presence of internal amines. Another reason is the open structure of the polymer. For Ibuprofen and Cuminol, the obtained concentrations for both encapsulated drugs were similar. It could be said that, number of cuminol molecules encapsulated were equal to that of ibuprofen. This was an interesting result proving the efficiency of secondary interactions which were absent in the previously discussed polyglycidol. The next polymer to be studied was AB_4 HYPAM. Although its molecular weight could not be determined successfully, a high degree of branching resulting in high drug loading was still expected. Table 3.7 below details the concentration for the drugs encapsulated.

Table 3.7. Concentration of drugs obtained after encapsulation within AB_4 HYPAM

Drug(s)	Obtained Concentration of the drugs encapsulated (x 10^{-2} M)
Ibuprofen	1.18
Cuminol	0.72
THPP	Negligible
ZnTHPP	0.2

Comparing Ibuprofen to cuminol, solubility of the former seemed high. As for THPP and ZnTHPP, very low values of THPP were obtained and hence could not be reported. On the other hand, ZnTHPP showed good solubility.

As the GPC did not give good results (Chapter 2 Table 2.7 and Table 2.8), the presence of monomers and small oligomers could not be ruled out. If this was the case, possible interactions would take place between the AB_4 monomer and the metallated porphyrin. Therefore, a control experiment had to be done using methanol as the solvent followed by TRIS buffer (Figure 3.10). To do that, mass/volume concentration of the monomer was prepared at 0.82mg/ml. Complex of the ZnTHPP and the monomer was formed. UV-Vis Spectroscopy and Beer Lambert law (Equation 3.1) were used to analyse this complex. Originally, if the interactions were taking place between the monomer and the drug, similar absorbance would be observed. However, when the complex was analysed, the solubility was like the inherent solubility of ZnTHPP (Table 3.2). As a result, the spectrum could not be analysed and reported in the form of data. This proved that the AB_4 HYPAM was indeed a polymer and not a monomer. Also, it was more likely to have a high degree of branching making it behave like a dendrimer. This would mean a more controlled environment with the presence of internal amines (comparable to TRIS PAMAMs). Hence, good performance in terms encapsulating drugs and increasing their solubility was seen.

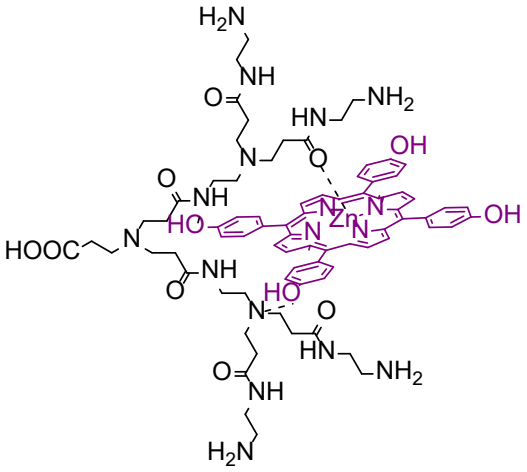

Figure 3.10 Graphical representation of possible interactions occurring between ZnTHPP and AB_4 monomer. A control experiment was performed to test the hypothesis whether interactions were taking place between the monomer and the drug. The co-precipitate encapsulation method was applied to form a monomer-drug complex in TRIS buffer which was analysed via UV-Vis Spectroscopy to reveal if the drug was encapsulated within the monomer or not.

Finally, the studies were repeated with G4.0 PAMAM as well and are reported in the table 3.8 below. G4.0 TRIS PAMAMs could have been used for comparison however, since its terminal functionalities are different to that of HYPAMs; G4.0 PAMAM was good choice as the competitor. The concentration values suggested the solubility of Ibuprofen was ten times better than that of cuminol. Again, the emphasis was made on the acid groups of ibuprofens that

enhanced the interactions with the dendrimer. As cuminol doesn't have any acid groups present, the encapsulation is relatively lowered. Between THPP and ZnTHPP, the encapsulation of THPP was unsuccessful. Nonetheless, incorporation of ZnTHPP was possible with enhanced solubility.

Table 3.8 Concentration of drugs obtained after encapsulation within G4.0 PAMAM

Drug	Obtained Concentration of the drugs encapsulated (x 10^{-2} M)
Ibuprofen	1.10
Cuminol	0.01
THPP	Negligible
ZnTHPP	0.02

Now, assessment of each of the polymer's efficiency in increasing the solubility of the drugs is studied. Although, AB_4 HYPAMs gave really good results, as their characterisation remained problematic, they will not be used for comparison. Instead, AB_2 HYPAM will be compared to G4.0 PAMAM. Table 3.9 does the comparison.

Table 3.9. Assessment of encapsulation efficiency between AB_2 HYPAM and G4.0 PAMAM

Drugs	Obtained Concentration after encapsulation (x 10^{-2}M)	
	AB_2 HYPAM	G4.0 PAMAM
Ibuprofen	1.00	1.10
Cuminol	0.91	0.01
THPP	Negligible	Negligible
ZnTHPP	0.15	0.02

Overall, the HYPAM seems to give better results than G4.0 PAMAM. Almost constant solubility is observed for Ibuprofen. However, for cuminol, AB_2 HYPAM provides good solubility than G4.0 PAMAM. Similarly, ZnTHPP encapsulates better in AB_2 HYPAM as compared to G4.0 PAMAM. One possible explanation for G4.0 PAMAM to give low solubility is its compact structure i.e. dense shell packing that hinders incorporation of the drug molecules. Literature reports that at neutral pH, primary amines are protonated, and the

dendrimer is significantly smaller than a corresponding dendrimer in high or low pH[11] due to the basic nature of HYPAMs and PAMAMs, we need the pH to be controlled with buffer.

3.4 Conclusions and Future work

To begin with, the generation with highest drug loading for TRIS PAMAM dendrimers was determined. The model drug used was Ibuprofen. The complexes were made via co-precipitate method and analysed using UV-Vis spectroscopy. G4.0 TRIS PAMAM was found to be the best between G2.0, G3.0 and G 5.0 TRIS PAMAMs. Following this, the optimum concentration for all the future encapsulation studies was determined. Varying concentrations of G4.0 TRIS PAMAM ranging from $5x10^{-3}$ M to $5x10^{-5}$ M were used. Co-precipitate method with Ibuprofen as the model drug was repeated. The optimal concentration for G4.0 TRIS PAMAM was found to be $1x10^{-4}$M with ~31 Ibuprofen molecules encapsulating per dendrimer.

Now, five drugs were chosen including Ibuprofen, from which four drugs were used to study encapsulation ability of polymers other than G4.0 TRIS PAMAMs. The drugs chosen were Ibuprofen and THPP with their respective analog Cuminol and ZnTHPP. The fifth drug was warfarin but was only studied with G4.0 TRIS PAMAMs. TRIS PAMAMs consist of internal amines that provide secondary interactions besides creating hydrophobic cavities for the drug to stay safe in. This results in high drug loading with these dendrimers. However, to know for sure, we needed to test this with a polymer of comparable molecular weights and without the presence of internal amines. Polyglycidol is one such polymer. It consists of internal ether oxygen which provide weak interactions however, the interactions tend to be strong enough to hold drugs in the cavity.

The encapsulation studies with the above state drugs were conducted to find that out of the four drugs, THPP did not encapsulate at all. However, its analog, ZnTHPP had enhanced solubility because due to its zinc core providing better secondary interactions. G4.0 TRIS PAMAM, showed to encapsulate the porphyrin while PG 1:10 failed to do so. Cuminol should exceptional solubility with PG1:10 but we couldn't understand why. As for Ibuprofen, in dendrimer a slightly higher concentration was found compared to PG1:10. Overall, G4.0TRIS PAMAMs could encapsulate more due to the presence of secondary interactions as driving force. To verify the role of secondary interactions, we decided to use hyperbranched PAMAMs. With similar chemical structure and presence of internal amines, which polymer encapsulate more, could be determined.

Firstly, the amine PAMAMs were subjected to thermal condensation to give fractured PAMAMs resembling hyperbranched PAMAMs. However, their fracture wasn't successful (Chapter 2 section) and then it was decided that hyperbranched PAMAMs (HYPAMs) will be synthesised. Their synthesis was successful and upon characterisation, they were studied for their encapsulation abilities and related with Amine PAMAMs instead of TRIS PAMAMs due to their terminal functionality.

With the encapsulation results obtained, it was suggested that HYPAMs were better to Amine PAMAMs as they possessed a more flexible structure with strong secondary interactions; especially with ZnTHPP. This also proved that metallated porphyrins tend to bind better than their non-metallated counterparts. Having said that, the encapsulation ability of the polymers studied above should be investigated with other types metallated porphyrins perhaps ZnTDHPP (Tetra (3,5 dihydroxyphenyl) porphyrin zinc) or ZnTDMPP (Tetra (3,5 dimethoxyphenyl) porphyrin zinc) to name a few.

Ibuprofen also gave good encapsulation results, but it was perceived to be so high, due to the presence of acidic groups on Ibuprofen. However, Cuminol also encapsulated well but the reason for its unusually high loading could not be understood. It was found necessary that the encapsulation studies with this drug are reiterated. The use of drugs with minimal to no solubility in water should be studied as well. As TPP and ZnTPP have also been studied with the latter performing better, different types of drugs other than porphyrin need to be looked at, such as metal-free Phthalocyanines, another class of large hydrophobic photosensitizers towards PDT [14] (Figure 3.11).

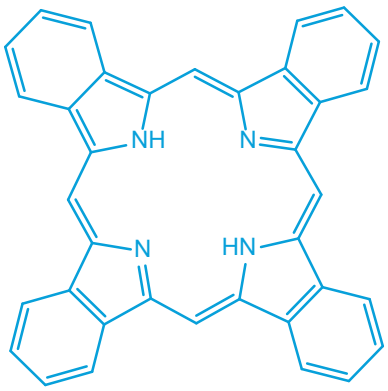

Figure 3.11. Structure of metal-free phthalocyanine

To conclude the results obtained from all the encapsulation studied performed using the four types of polymers or macromolecules, Graph 3.5 details the concentrations of the drugs studied

by the three polymers. While G4.0 TRIS PAMAM proves best for Ibuprofen, AB_2HYPAM comes out as the winner between the three polymers. Clearly these encapsulation studies need to be performed with much more hydrophobic drugs to assess if AB_2 HYPAM still works best or not.

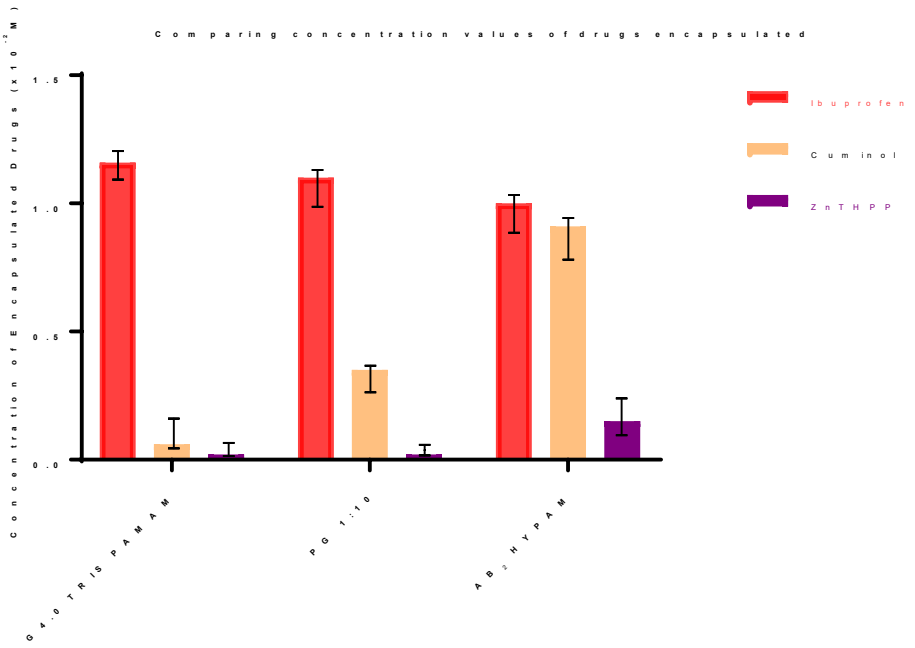

Graph 3.5. Evaluating the best polymer or macromolecule out of the three: G4.0 TRIS PAMAM, PG 1:10 and AB_2HYPAM, in terms of encapsulation and solubility enhancers at a concentration of 1 x 10^{-4} M, respectively.

3.5 Experimental section

3.5.1 General experimental considerations

3.5.1.1 UV/Vis spectroscopy

The UV/Vis spectrum was recorded on an Analytik Jena AG Specord s600 UV/Vis Spectrometer and analysed by the Software (WinASPECT).

3.5.1.2 pH measurement

The pH of the buffer solutions prepared (section 3.5.2.1) was substantiated using a pH 210 Microprocessor pH Meter from Hanna Instruments Ltd. (Leighton Buzzard, UK). The device was calibrated using pH 4.0 and pH 10.0 standard solutions.

3.5.1.3 Source of solvents, chemicals, and drug(s)

All the solvents and chemicals were sourced from Sigma-Aldrich and VWR. Cuminol was sourced from VWR. Ibuprofen and Warfarin were sourced from Sigma-Aldrich.

3.5.2 Encapsulation Studies

3.5.2.1 Molar extinction coefficient(s) of drug(s)

Solutions of known concentration(s) were made up using methanol for each drug, respectively. Using a quartz cuvette, the solution for each drug was analysed for maximum absorbance via UV-Vis spectroscopy at respective characteristic wavelengths. Dilutions were carried out to obtain a set of readings between maximum absorbance of ~0.3-1.5, respectively. For each drug, a Beer lambert plot between the maximum absorbance and corresponding concentrations was plotted to give the molar extinction coefficient (ε).

3.5.2.2 Buffer Solution

In a 1000ml volumetric flask, 12.1g (0.01M) of TRIS buffer solution was dissolved in 1 litre of distilled water. The pH was maintained ~7.4.

3.5.2.3 Inherent solubility tests for drug(s)

Excess drug(s) were dissolved in 5ml of methanol and vigorously stirred at 400-500 rpm for about 10 mins. The solvent was removed in vacuo followed by addition of 5ml buffer solution. The drug solution(s) were filtered into clean sample vial(s) using cotton wool. Inherent

solubility for each respective drug was determined by using the Beer lambert equation (1) with pre-determined molar extinction coefficient(s) and maximum absorbance (A) of the drug(s) obtained by analysing the filtered drug samples via UV-Vis Spectroscopy.

3.5.2.4 G4.0 TRIS PAMAM Solution

In a 250ml volumetric flask, 203.72mg of G4.0 TRIS PAMAM was dissolved in methanol to give the required solution ($1x10^{-4}$M).

3.5.2.5 Hyperbranched Polymer Solutions

For AB_2 and AB_4 HYPAMs, PG1:10 and G4.0 PAMAM; a concentration of 0.82mg/ml (m/v) was used to make up solutions in 250ml volumetric flasks using methanol.

3.5.2.6 Encapsulation of drugs

In a clean sample vial, 5ml of the polymer solution was mixed with excess of the drug being studied. After rigorous stirring for approximately an hour at 400-500 rpm, the solvent was removed in vacuo following which 5ml of TRIS buffer (0.01M) was added. The complex solution was filtered into a clean sample vial(s) using cotton wool and analysed via UV-Vis Spectroscopy at characteristic wavelengths for each drug, respectively.

3.6 References

1. Lee, C. C., MacKay, J. A., Fréchet, J. M. J. & Szoka, F. C., 2005. Designing dendrimers for biological applications. *Nature Biotechnology,* , 23(12), pp. 1517–26.
2. Thatikonda, S., Yellanki, S. and Charan, D., 2013. Dendrimers - a new class of Polymers. *Int. J Pharma Sci Res*, 4(6), pp. 2174-2183.
3. Dwivedi, D. K. & Singh, A. K., 2014. Dendrimers: a novel carrier system for drug delivery. *Journal of Drug Delivery and Therapeutics,* 4(5), pp. 1-6.
4. Klajnert, B. & Bryszewska, M., 2001. Dendrimers: properties and applications.. *Acta Biochimica Polonica,* , 48(1), pp. 199-208.
5. Wolinsky, J. B. & Grinstaff, M. W., 2008. Therapeutic and diagnostic applications of dendrimers for cancer treatment. *Advanced Drug Delivery Reviews,* , 60(9), pp. 1037-1055.
6. J. J. Khandare, S. Jayant, 2006, Dendrimers Versus Linear Conjugates, 15, 1464-1477
7. Peter J. Gittins, Lance J. Twyman, 2003. Dendrimers and Supramolecular Chemistry, Supramolecular Chemistry, 15:1, 5-23
8. Kolhe P, Misra E, 2003. Drug Complexation, in vitro release and cellular entry of dendrimers and hyperbranched polymers, 259, 143-160
9. Tang MX, Redeman CT, 1996. In vitro gene delivery by degraded polyamidoamines dendrimers, Bioconjug Chem., 7,203
10. Devarakonda B, Hill RA, 2004. The effect of PAMAM dendrimer generation size and surface functional group on the aqueous solubility of nifedipine, Int J Pharm, 284, 133-140
11. Maiti PK, Cagin T, 2004. Effect of solvent and pH on the structure of PAMAM Dendrimers, Macromolecules, 38, 979-991
12. F Figueira, Porphryin and phthalocyanine decorated with dendrimers (2014), Current Organic Synthesis, 11, 110-126
13. Shamsudin S, 2012. The Synthesis and Characterisation of Dendritic Macromolecules for Drug Delivery Application, PhD Thesis, *Department of Chemistry, The University of Sheffield*.
14. Aboshnaf F, 2018. The Synthesis and Application of Dendritic Polymer for Photodynamic Therapy, PhD Thesis, *Department of Chemistry, The University of Sheffield.*

Chapter 4

Non-covalent approaches to improve dendrimer interaction and to quantify binding strength

Table of Contents

Abbreviations

µM – micromolar

^{13}C NMR – carbon nuclear magnetic resonance spectroscopy

^{1}H NMR – proton nuclear magnetic resonance spectroscopy

COOH-PAMAM/PAMAM-COOH – Carboxylate terminated poly(amido)amine

Cyt c – Cytochrome C

d – doublet

ES-MS – Electron Spray Ionisation-Mass Spectrometry

FT-IR – Fourier transformed Infrared Spectroscopy

G0.5, G1.0 etc. – Generation of respective dendrimer(s)

K_a – Acid dissociation constant/equilibrium constant for weak acids in chemical reactions

m – multiplet

OH-PAMAM/PAMAM-OH – Neutral/ Hydroxyl terminated poly(amido)amine

PAMAM – Poly(amido)amine

pH – power of hydrogen

ppm – parts per million

R_f – Retention factor

s – singlet

t – triplet

TCPP – meso-tetra(carboxyphenyl) porphyrin/ 5,10,15,20-Tetra (4 carboxy) phenyl porphyrin

THPP – meso-tetra(hydroxyphenyl) porphyrin/ 5,10,15,20-Tetra (4 hydroxy) phenyl porphyrin

TRIS-PAMAM/PAMAM-TRIS – Tris(hydroxymethyl)amidomethane terminated poly(amido)amine

UV-Vis – Ultraviolet-Visible

v/v – Volume by volume percent

ZnTCPP – 5,10,15,20-Tetra (4 carboxyphenyl) porphyrin zinc

ZnTHPP – 5,10,15,20-Tetra (4 hydroxyphenyl) porphyrin zinc

List of Figures

List of Graphs

List of Tables

List of Schemes

4.1 Introduction and Aims

Many biological processes in a human body are driven by protein-protein interactions. At times, these interactions are uncontrolled leading to diseases [1]. Polymers or macromolecules acting as scaffolds with charged surfaces have the potential to stop these interactions from occurring [2]. The charged macromolecules bind to the hot spot of the proteins [2]. Proteins with small interfacial area have been studied so far. Twyman et al in 2008, made attempts to study the protein binding efficiency of dendrimers as size selective ligands [3]. Acid dendrimers synthesized via divergent route ranging from G0.5 to G4.5 were studied (Figure 4.1) (synthesis and functionalisation discussed in Chapter 2 Section 2.2.2.1). The surface area of the dendrimers complimented the interfacial area of the chosen proteins; α-Chymotrypsin and Cytochrome C. From the study, it was found that with α-Chymotrypsin bound best with G3.5 while Cytochrome C bound best with G2.5, due to its smaller interfacial area [4, 5]. This study reflected on the concept of size selective binding proving that the size of the dendrimer played an important role in protein binding.

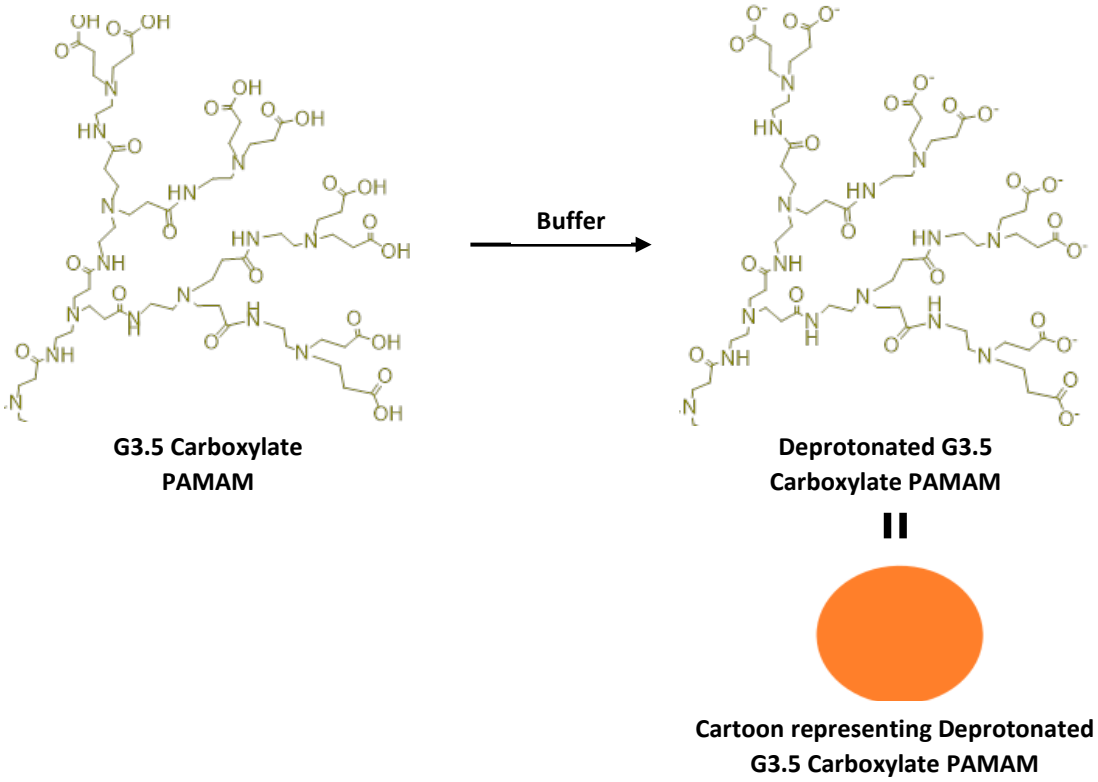

Figure 4.1. The carboxylate PAMAM deprotonates to give negative charge on its surface that enhances its ability to bind with the protein.

Shifting focus from the established size-selective studies done in the past, the less understood binding efficiency of Carboxylate PAMAMs with our model protein, Cytochrome C, was

studied and hence, is discussed in this chapter. Initial protein binding studies were conducted between Cytochrome C, porphyrin and G3.5 Acid PAMAM. This was a competition experiment. To monitor the binding between the protein and dendrimer, TCPP was used as the probe. In theory, when bound to Cytochrome C, the porphyrin will quench with no emission recorded. With the addition of the dendrimer, protein will bind to the dendrimer displacing the porphyrin. The displaced porphyrin would become fluorescence active again, hence, emission

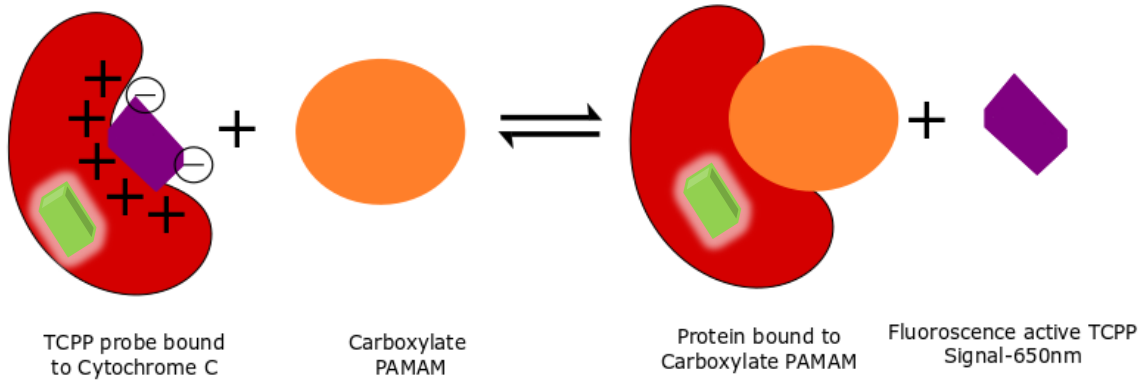

Figure 4.2. Competition experiment-When TCPP is bound to Cytochrome C the fluorescence is quenched. Upon displacement by Carboxylate dendrimers it becomes free and fluorescence-active .

However, this cannot be the only possibility. There is no surety that the dendrimer is binding with the protein. It could simply mean that the dendrimer encapsulates the porphyrin and does not bind to the protein. The porphyrin will still be fluorescence active and emit signals at ~650nm (Figure 4.3). The more dendrimer added to the porphyrin-protein solution, the more porphyrin molecules are released therefore, heightened emission.

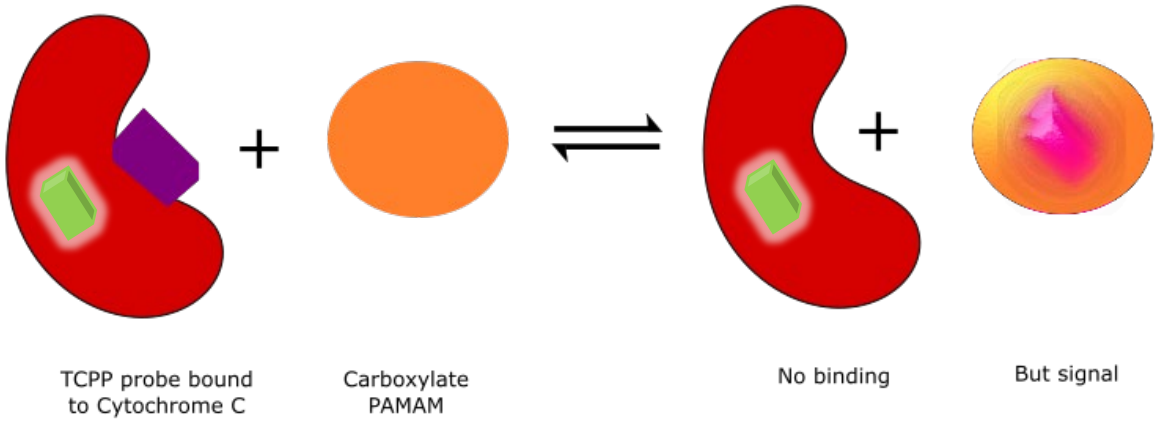

Figure 4.3. The bound TCPP is encapsulated by the carboxylate dendrimer making it fluorescence active without binding to the dendrimer.

This leads us to consider how we quantify protein binding. Covalent approaches for encapsulating the porphyrin can be used. Fixing or holding the porphyrin in one place or better,

using porphyrin cored dendrimers, hyperbranched polymers. These approaches have been studied in the Twyman group and turned out to be very time consuming with minimal success rate. Henceforth, non-covalent approach for encapsulation of the porphyrin shall be utilised (Figure 4.4). This approach is supposed to be efficient as it does not involve complicated chemistry. Once encapsulated within the dendrimer, the probe should have minimum to no solubility in aqueous media. Binding with protein will only be facilitated via interaction between surface functionalised dendrimer (discussed in section 4.2.9) and the protein.

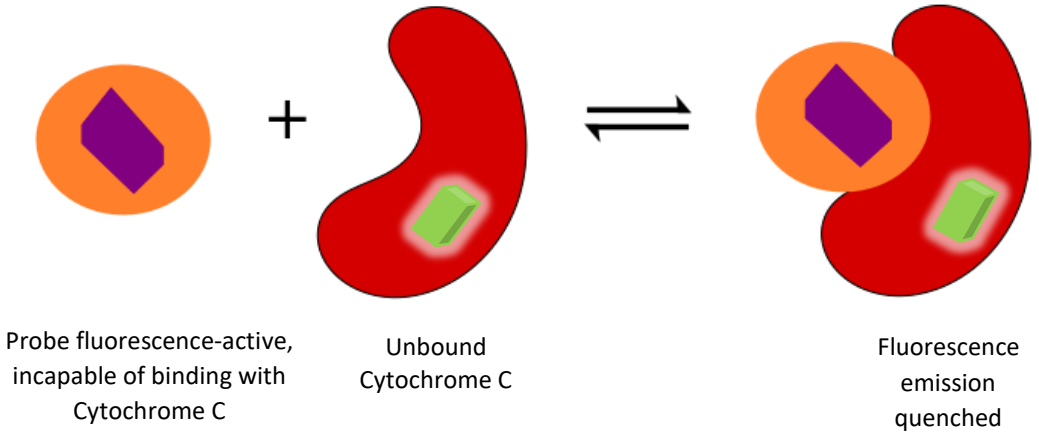

Figure 4.4 New method of quantifying Protein-dendrimer binding.

Having said that, targeting groups for protein binding studies could be another, better option. Adding targeting groups on the surface of the dendrimer using non-covalent approach, the binding affinity of the dendrimer-protein can increase manifold. This was the other half of the study; using targeting groups to quantify binding between dendrimers and proteins. To achieve this, a linear chain with a hydrophobic tail that is incorporated easily within the dendrimer cavity and hydrophilic head, so that the overall solubility of the system is enhanced, was desired (Figure 4.5).

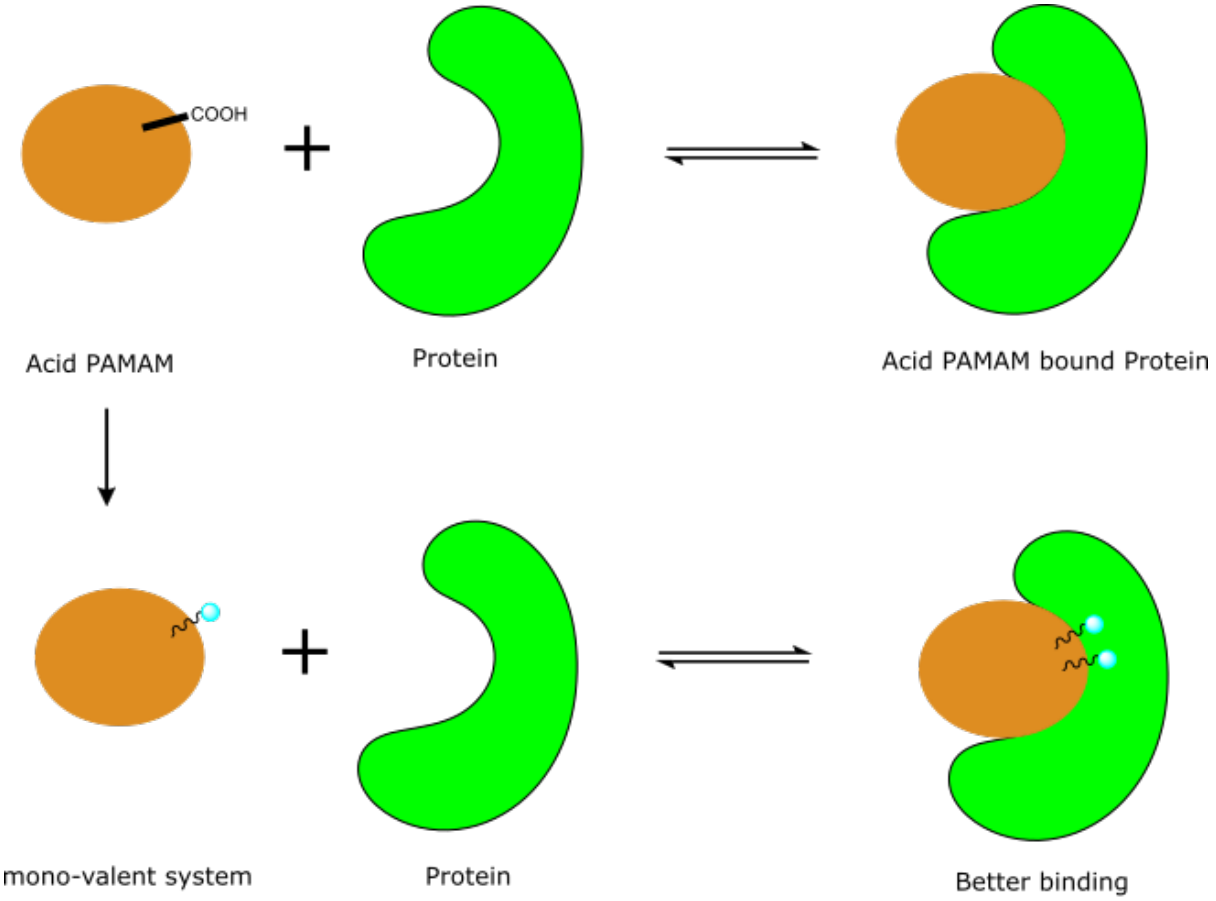

Figure 4.5. Mono-valent system-consisting of a targeting group, preferably an amino acid. Increase in binding affinity can be studied.

The targeting group chosen was an amino acid chain. Mono-valent system i.e. one amino acid working as the targeting group. However, as good binding affinity with a mono-valent system is reported [6], why not use two or three chains of amino acid to strengthen the binding further. Twyman group has studied the effect of terminal groups' functionality on the ability of dendrimers to bind proteins [6]. To the contrary, as predicted there wasn't any increase in the binding affinity instead, a drop was observed. The use of multiple targeting groups w.r.t. a mono-valent system was found to be a complete mess.

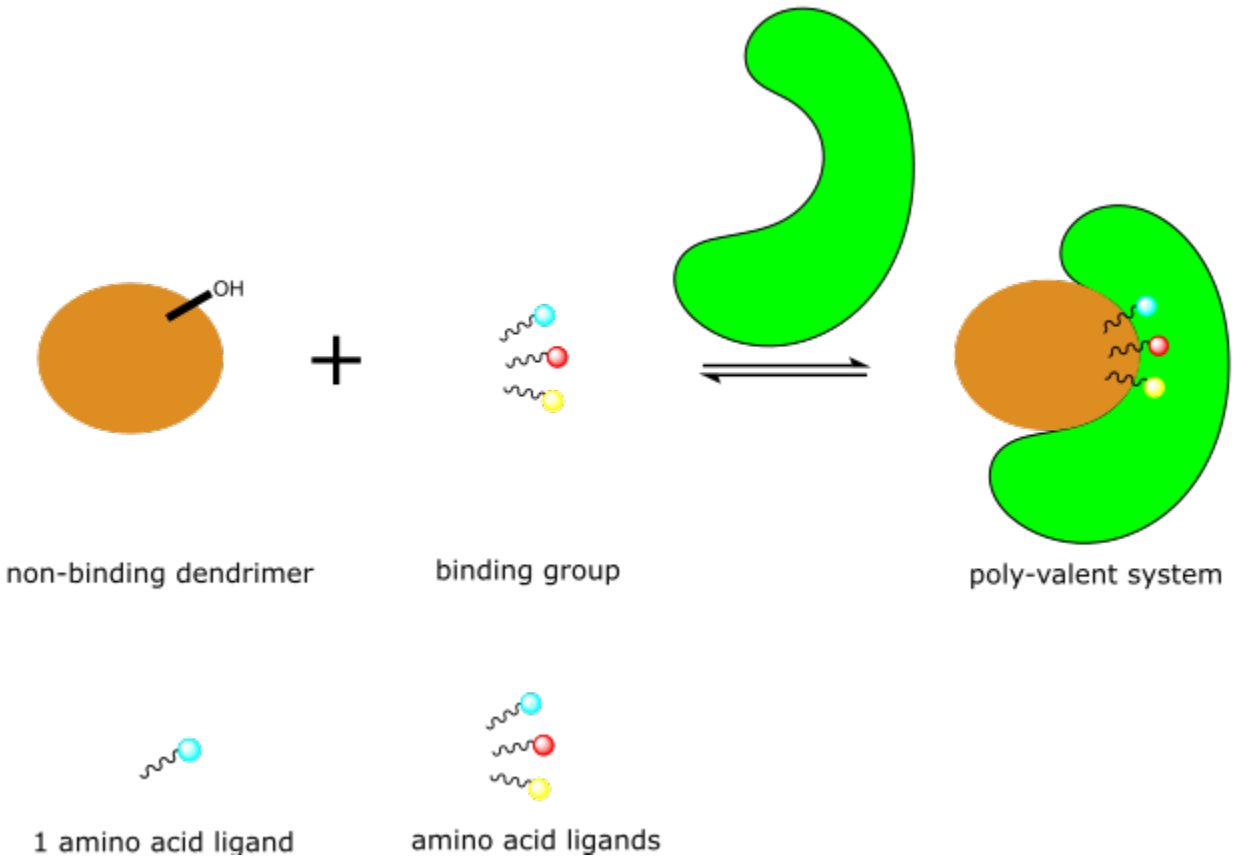

Figure 4.6. Poly-valent system in protein binding i.e. Dynamic Combinatorial Library

Therefore, a poly-valent system was thought of as an exemplary idea. A non-binding dendrimer for instance, G4.0 neutral PAMAM is added to a mixture of model protein and three amino acid ligands (targeting groups). The model protein will be bound to the dendrimer by the utilisation of one of the many ligands or targeting groups available, also known as 'best-fit' or Dynamic Combinatorial Library [6] (figure 4.6).

4.2 Results and discussion

Part 1 Adding Targeting group to the dendrimer for Improved Binding

4.2.1 Synthesis of the targeting groups

The first part of this research as outlined in the aims was to improve the binding between a model protein and the dendrimer. As the protein involves a range of different. This was done by incorporating a targeting group within the surface of a neutral dendrimer non-covalently. Subsequently, the binding properties of the system were studied. Hence, the first step involved the synthesis of a targeting group that could be easily encapsulated. Since the inner cavities of the dendrimer provides a safe hydrophobic environment (as shown in Chapter 2), a targeting group with a hydrophobic tail and hydrophilic head was required. The hydrophilic head must comprise an aromatic group to help interact with the solvent system. Therefore, with these considerations in mind, a targeting group was synthesised. The general synthesis mechanism is given in the Scheme 4.1 below.

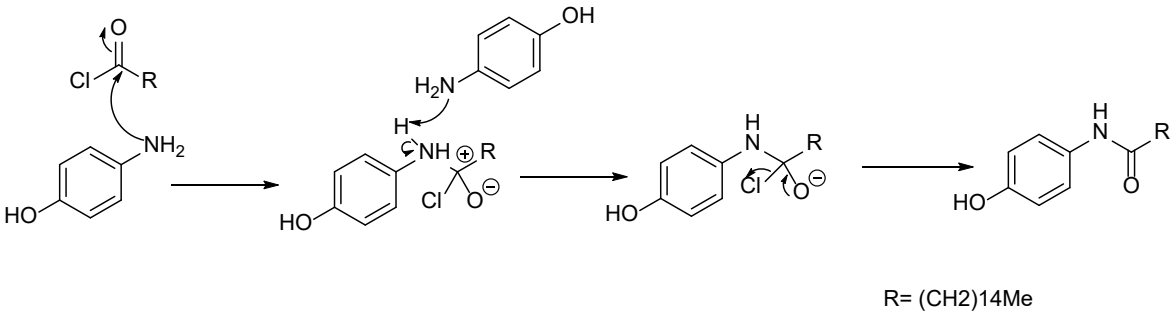

Scheme 4.1. General synthesis mechanism for the targeting groups

As the nitrogen of the amine is more nucleophilic than the oxygen, chemo-selectivity results in formation of an amide. At this stage, the nitrogen of the amide becomes more electronegative than both the hydrogen and carbon. This results in an increased electron density pull making it more delta negative and nucleophilic. Also, the acid chloride next to the amide is attacked by its active lone pair.

Hereafter, the carbon bound to the chloride and oxygen becomes prone to a nucleophilic attack as the electron density is pulled towards the electronegative chloride and oxygen. As a result, deprotonation of the nitrogen occurs by 4-aminophenol and since chloride is a good leaving group, it comes off next.

4.2.2 Characterisation of the targeting groups

To verify the successful synthesis of the targeting group, standard characterisation techniques were utilised. In ^{1}H NMR, a singlet peak around 9.15 ppm was seen. This corresponded to the amide-proton. The proton directly attached to the nitrogen is deshielded due to high electron withdrawing power of nitrogen. Hence, a shift towards the low field in the signal is observed. Aromatic signal around 6 ppm was also visible. The presence of aliphatic carbons was confirmed by the presence of corresponding protons around 2 ppm.

With ^{13}C NMR, peak at 170 ppm corresponding to the carbonyl peak next to the amide confirmed the synthesis to be successful. To reconfirm the NMR results, FT-IR was performed. Signals around 1650 cm^{-1} for the amide carbonyl stretch and 1500 cm^{-1} for the aromatic C-C bend were obtained. ES-MS was also used to characterize the targeting group. Molecular ion peak at 236.2 was visible, confirming successful synthesis of N-(4-hydroxyphenyl) hexadecanamide.

4.2.3 Encapsulation studies

After the successful synthesis of the targeting group, its encapsulation within the dendrimers was the next phase of this study. The dendrimers for this study were to have neutral surface functionality. Previously synthesised neutral OH-PAMAMs and TRIS-PAMAMs were selected (Chapter 2 Section 2.2.2.2 and Section 2.2.2.3). G4.0 OH PAMAM and G4.0 TRIS PAMAM (32 end groups) were chosen as the perfect generation for the encapsulation studies. They were perfect as small dendrimers would not have the structural integrity to incorporate the groups while larger dendrimers would hinder encapsulation due to their dense shell packing.

Having said that, co-precipitate method was used for encapsulating the targeting group within both the neutral dendrimers. Methanol was used as the common solvent followed by the addition of TRIS buffer at a pH of 7.36, 0.1 M. UV-Vis Spectroscopy was used for analysing the complexes formed.

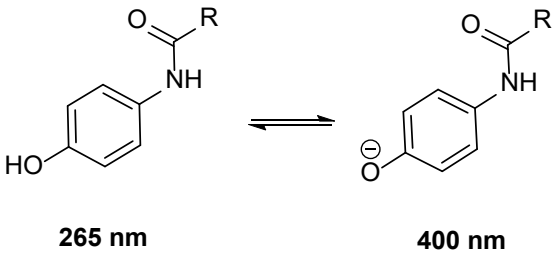

Figure 4.7. Targeting group's protonated and deprotonated form with different UV absorbances.

The first study using G4.0 OH PAMAM showed absorbance at 265 nm and 400 nm corresponding to the targeting group's protonated and deprotonated form (Figure 4.7). However, with G4.0 TRIS PAMAM, no absorption was recorded (Graph 4.1).

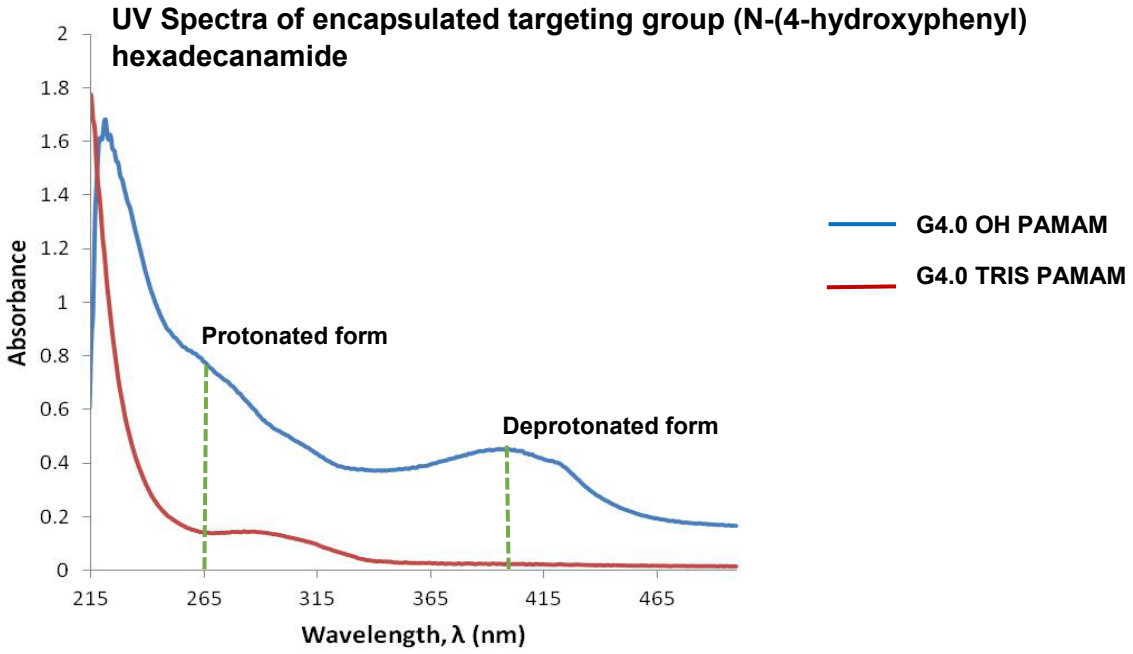

Graph 4.1. The absorption recorded for the targeting group encapsulated within the G4.0 OH PAMAM and G4.0 TRIS PAMAM, respectively. The protonated and deprotonated form of the targeting group at 265nm and 400nm when encapsulated with G4.0 OH PAMAM can be observed whereas for G4.0 TRIS PAMAM, no such absorbances were recorded.

A possible reason for this result was thought to be the formation of a complex between the deprotonated anion with amines or hydroxyl groups on the surface of the dendrimers. Since, G4.0 TRIS PAMAM consists of polar hydroxyl terminal groups, higher chances of complexation within this dendrimer must have resulted in poor absorption. However, if this was the case, the buffer system should have been able to sort this out. On the contrary, due to the presence of acidic head groups, the buffer facilitated the internal complexation between the targeting group and the internal amines of the dendrimer (Figure 4.8).

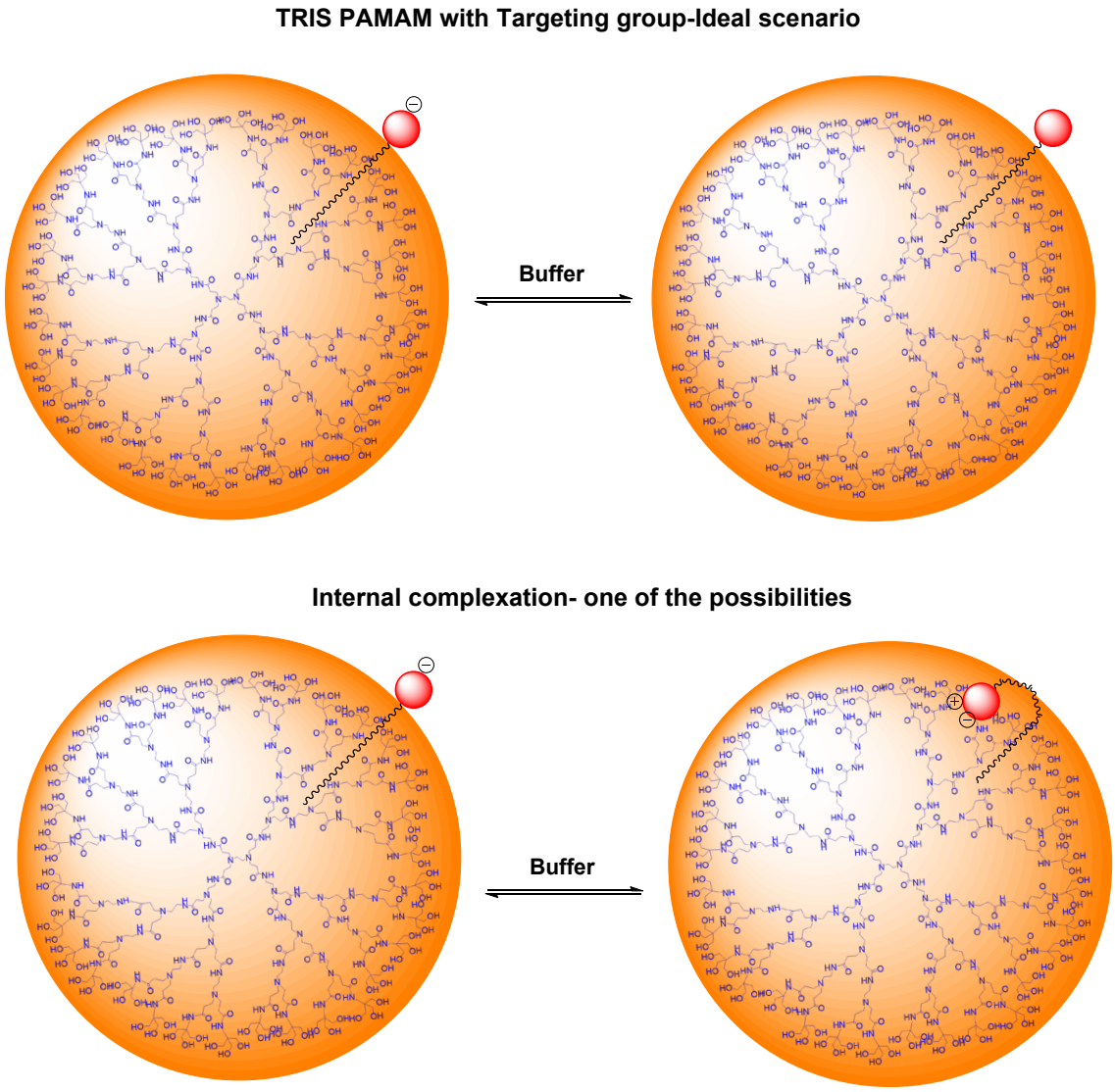

Figure 4.8. Graphical representation depicting internal complexation between the targeting group and TRIS PAMAM dendrimer.

Even though, encapsulation of the targeting group was successful within G4.0 OH PAMAM, the conclusion was derived that better hydrophobic interactions between the targeting group and the dendrimer were needed. Also, the failed encapsulation with G4.0 TRIS PAMAM clearly suggested that the targeting groups are required to be less acidic i.e. less prone to deprotonation at a certain pH to avoid internal complexation. The future studies with targeting groups were continued by a new PhD researcher in the Twyman's group.

Part 2 Protein-binding Studies

4.2.4 Probe selection

As discussed in the aims, various types of probes have been studied by the Twyman group for protein binding. One of the extensively researched probes are porphyrins. Up till now the challenge was the encapsulation of porphyrins. From Chapter 3 Section 2.2.3, we understood that the encapsulation of porphyrins can be made successful by co-ordinating them with metals. We studied the encapsulation of 5,10,15,20-Tetra (4 hydroxyphenyl) porphyrin zinc (ZnTHPP) with different polymers and all of them were able to encapsulate the porphyrin successfully, even if the loading was low. For protein binding studies, the loading of the probe i.e. the porphyrin within a polymer should be measurable. Preferably, in 1:1 ratio or greater. Nonetheless, if the loading is low, we can compensate for that by controlling the concentration of the probe-binding ligand system. In this study, dendrimers act as the binding ligand. Having said that, ZnTHPP gave good encapsulation results with the previously studied drug delivery systems and hence, was selected to be the probe for protein binding studies (figure 4.9).

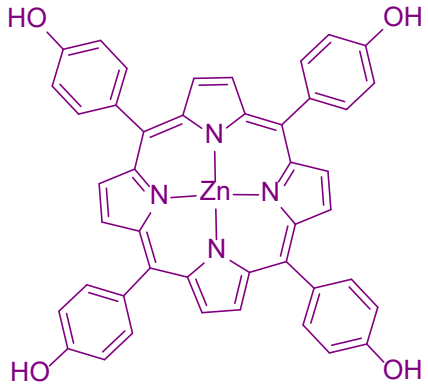

Figure 4.9. Structural representation of ZnTHPP

4.2.5 Binding ligand

Protein binding involves a range of different interactions including π-π, H-bonding and simple electrostatic interactions. The proteins we are targeting have binding areas that have a positive charge at neutral pH. Hence, the protein ligand should possess negative charge on its surface. Carboxylate PAMAMs consist of terminal acid groups that get deprotonated under basic conditions. In other words, in the presence of buffer, the dendrimer obtains negative charge on

its surface and hence, binds better than other dendrimers or polymers with the protein. Therefore, previously synthesised half generation PAMAM dendrimers were hydrolysed to give Carboxylate PAMAM dendrimers. Their synthesis and characterisation are detailed in Chapter 2 section. With the series of Carboxylate PAMAMs synthesis, the generation with a comparable surface area to that of model proteins was used for the studies. This was chosen to be G3.5 Carboxylate PAMAM (Figure 4.10).

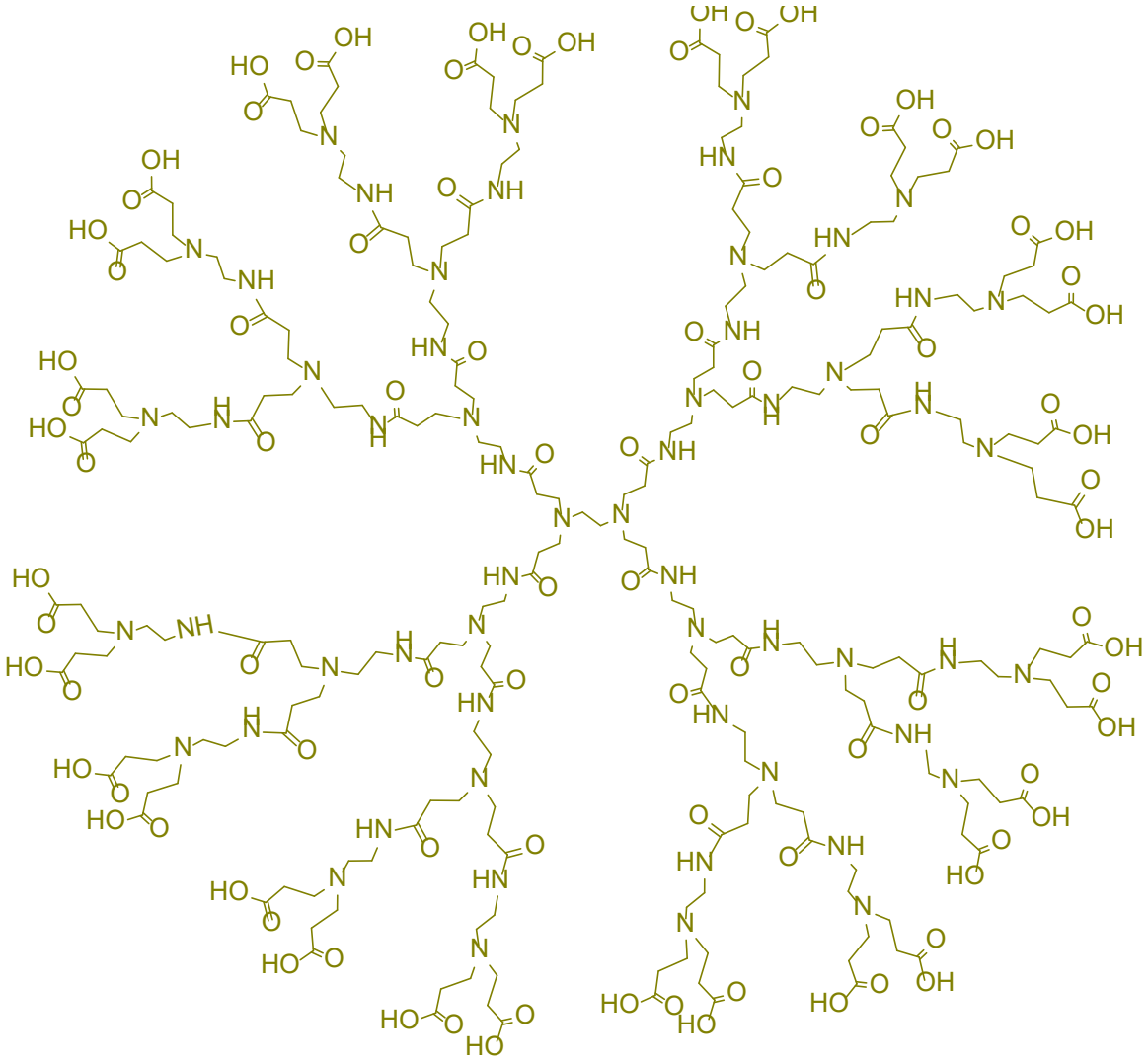

Figure 4.10. Structure of G3.5 Carboxylate PAMAM dendrimer

4.2.6 The Model Protein-Cytochrome C (Cyt c)

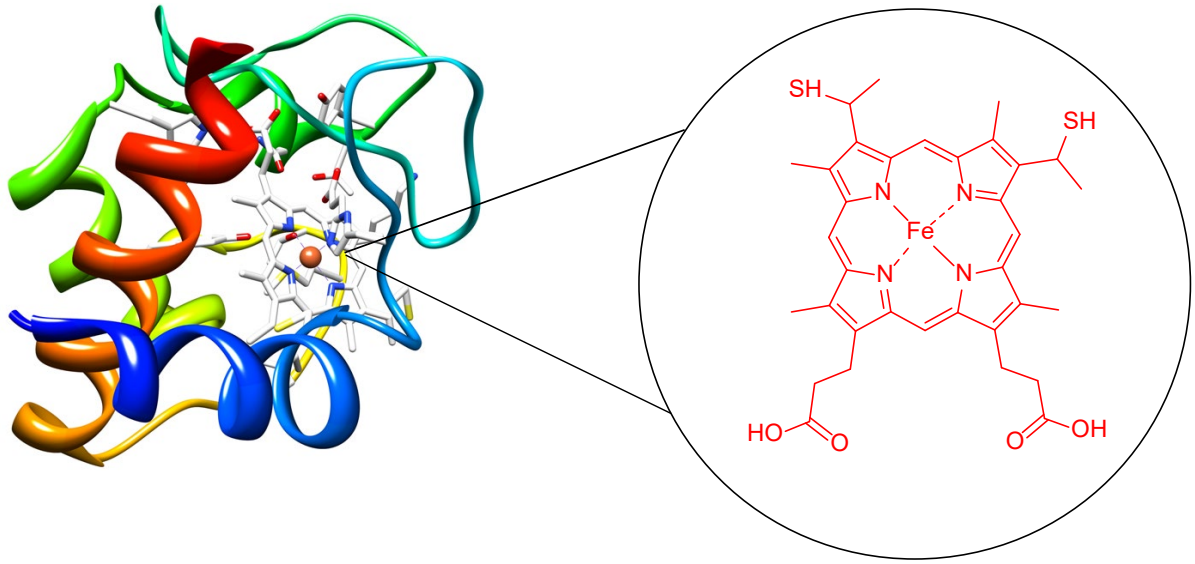

Figure 4.11. 3D structure of Cytochrome C alongside its chemical structure [7]. 3D structure of Cytochrome C reprinted from Journal of Molecular Biology, 214/2, Bushnell, G., Louie, G. and Brayer, G, High-resolution three-dimensional structure of horse heart cytochrome c, 585-595, Jul 20, 1990, with permission from Elsevier.

As stated in the introduction and aims of this chapter, protein binding studies had been using small proteins with much smaller interfacial area. With the progress of macromolecules in the field of protein binding, it was found necessary to start studying larger proteins with larger interfacial area (hotspots). Twyman group have studied Cytochrome C (Figure 4.11) as the model protein extensively as it has an interfacial area comparable to that of dendrimers' surface area [8]. Cytochrome C has an interfacial area of ~1000Å and it binds best with a G2.5 carboxylate PAMAM dendrimer with surface area of ~1200Å[7]. However, there hasn't been definite proof that this is the case due to multiple possibilities when studying protein-dendrimer binding, Cytochrome C was chosen as the model protein to be studied with a dendrimer generation higher than G2.5 carboxylate PAMAM i.e. G3.5 Carboxylate PAMAM dendrimer.

4.2.7 Encapsulation of ZnTHPP

The first step for the protein binding study was the encapsulation of ZnTHPP within G3.5 Acid PAMAM. This was done via co-precipitate method. Methanol was used as the common solvent followed by the addition of TRIS buffer (0.01 M, pH 7.4). A porphyrin-dendrimer complex was formed that was analysed by UV-Vis Spectroscopy. The absorption of the complex with encapsulated porphyrin was recorded at the characteristic wavelength of 430.5 nm with a molar extinction coefficient of 200500 $M^{-1}cm^{-1}$ (molar extinction coefficients specific to individual spectrometers). The absorption spectrum was used to determine the loading of ZnTHPP per dendrimer (Table 4.1).

Table 4.1. Concentration and loading of ZnTHPP obtained after encapsulation within G3.5 Carboxylate PAMAM.

Dendrimer concentration ($x10^{-4}M$)	Concentration of ZnTHPP ($x10^{-4}M$)	Ratio of dendrimer to porphyrin
1.00	0.54	1:0.54

A loading of five porphyrin molecules in every ten acid dendrimers was obtained. This was lower than the required stoichiometry of 1:1 i.e. one porphyrin per dendrimer (Figure 4.12). It meant one in two dendrimers binding with Cyt c, would contain a porphyrin.

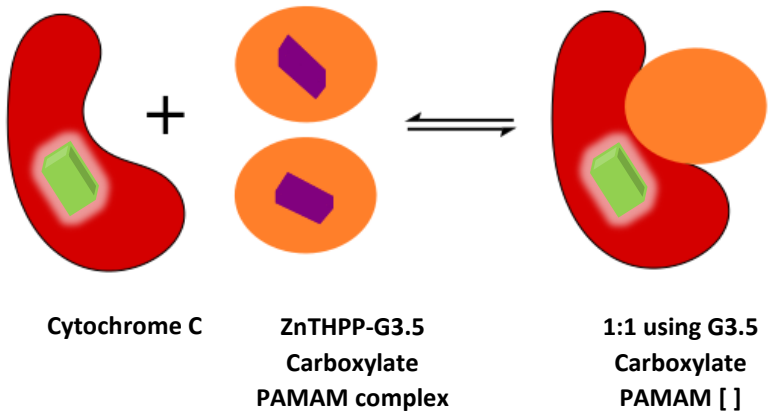

Figure 4.12. The ideal stoichiometry expected for protein-binding studies to achieve one porphyrin per dendrimer.

However, if the porphyrin loading is low, it can be worked out. In our case, the loading was one porphyrin in two dendrimers, to compensate for this, the total complex concentration was $2x10^{-5}$ M after dilution, but measurable as $1x10^{-5}$M (Figure 4.13). However, dendrimers without porphyrin will still bind though they won't be detected. This will be considered when K_a will be calculated.

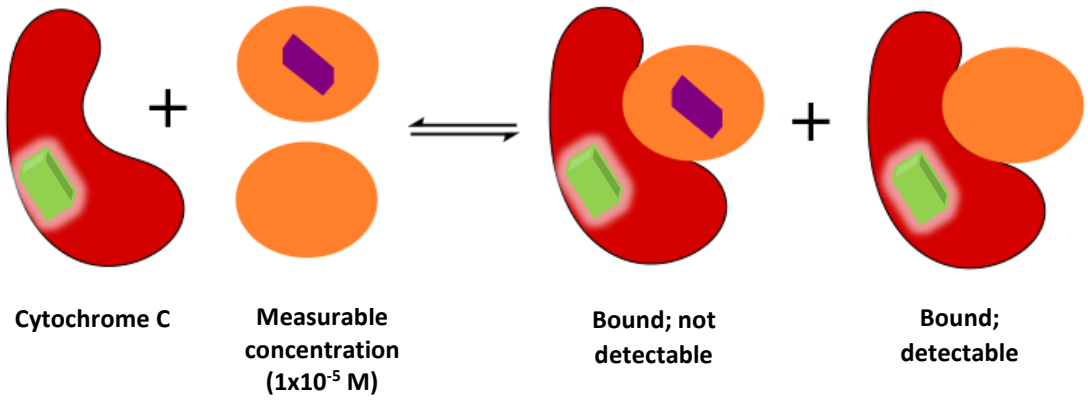

Figure 4.13. The dendrimer without the porphyrin will be detectable upon binding as no quenching will occur due to absence of encapsulated porphyrin. Hence, G3.5 Carboxylate PAMAM [ ]/2.

4.2.8 Fluorescence studies

Following the complex formation, the next step was to study interactions between Cyt c and the porphyrin-dendrimer ligand. Since, Cyt c and porphyrins, in general are fluorescence active, fluorescence spectroscopy was used to study the same. Titrations of Cyt c were carried out in the complex solution. Concentration of 400 µM for Cyt c was made up using the complex solution. This ensured that during titration, the concentration of porphyrin remained constant. A quartz cuvette contained 2ml of the complex solution to which for each titration, 10µl of the Cyt c solution was added and the fluorescence spectrum recorded. The fluorescence spectrum recorded was that of ZnTHPP porphyrin at an emission wavelength of ~610nm (with an excitation wavelength of 350nm).

It was predicted, upon protein-ligand binding, quenching in the fluorescence would occur due to the presence of the encapsulated porphyrin acting as the probe. This quenching effect would increase with every titration as more Cyt c would bind with the probe-ligand system. A fall in intensity for the probe would mean quenching was taking place. This could later be used to obtain the binding constant for the protein-ligand system. The quenching effect is plotted as a graph between intensity of the probe-protein ligand recorded at the emission wavelength of the probe at ~610 nm (Graph 4.2).

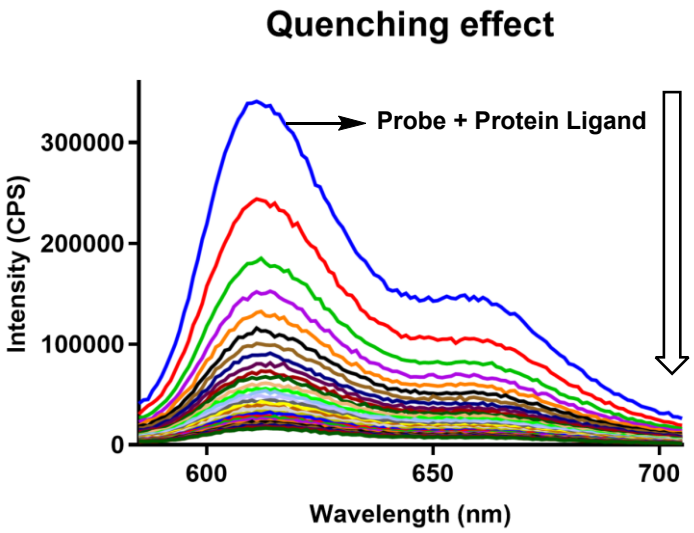

Graph 4.2. Quenching effect recorded for probe-protein ligand titration with Cc

The results were better than expected. With every titration, quenching occurred with a fall in the intensity of the probe-ligand system. This also meant that the binding between the protein and the ligand system was quite strong. To understand this better, the change in intensity was plotted against the concentration of the protein used (Graph 4.3). This gave us a binding constant for the protein-ligand system. Higher the value, better the binding between the protein and the ligand (dendrimer).

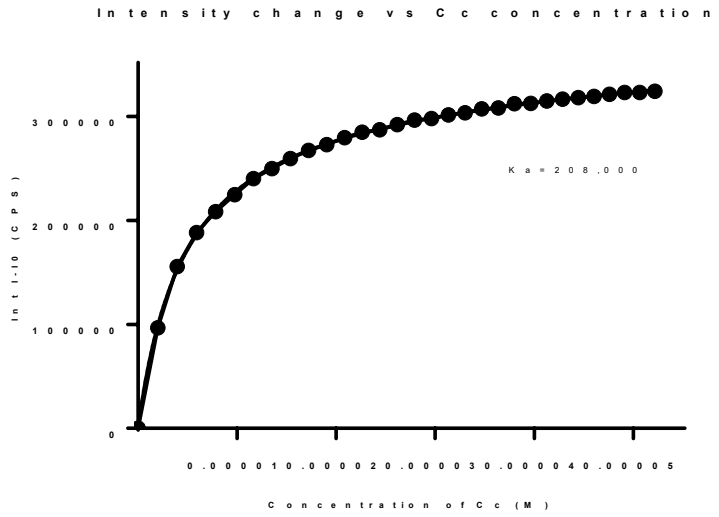

Graph 4.3. Intensity change vs concentration of Cytochrome C to give a K_a of 2.08 x 10^5

From the graph 3.3, the *apparent* K_a was found to be $2.08x10^5$ with an almost perfect R square value of 0.999. This gave us the binding constant of $4.16x10^5$ after taking the stoichiometry of porphyrin incorporation into account (Figure 4.13). The binding constant was close to the original experiments using porphyrin cored dendrimers and/or porphyrin competition experiments. The spotlight on the fact that to study effective protein binding, non-covalent approach worked equally well when compared to covalent approaches, was an important find. The conclusions deduced from this study were that any hydrophobic probe can be incorporated non-covalently inside the dendrimers to follow and study the binding affinity between the protein and the ligand. Also, the use of metal co-ordinated porphyrin as a probe was found to be quite useful as its loading was relatively higher than previously studied porphyrins.

Since, the porphyrin used for this study was different to those studied in the past, there was the possibility of the porphyrin falling out or coming out of the dendrimer complex system and interact with the protein, hence, the quenching effect. To be certain, a control experiment of Cytochrome C and ZnTHPP was carried out. ZnTHPP was dissolved with five times excess Cytochrome C in TRIS buffer (0.01M, pH 7.4). Firstly, the protein-probe control was UV-Vis analysed. The absorbance for the porphyrin was similar to its inherent absorbance in TRIS buffer, confirming that it was a hydrophobic probe.

Secondly, fluorescence emission of the control was run with the emission wavelength at ~610nm. No decrease in the intensity was noticed. This confirmed that the porphyrin was indeed not interacting or binding with the protein and validated the protein binding results discussed above. The importance of using a hydrophobic probe with minimal interactions with the proteins was established.

4.3 Conclusions and Future work

The protein binding study focused on two individual topics: using targeting groups to enhance binding affinity of the dendrimers and quantifying protein binding by exploiting secondary interactions between the dendrimer and metallated porphyrin. Both topics had a thing in common, non-covalent approach for encapsulation.

In the first study, targeting group, N-(4-hydroxyphenyl) hexadecanamide, with an acidic-aromatic hydrophilic head and hydrophobic tail was synthesized. This followed its encapsulation in two terminally functionalised PAMAM dendrimers. These were G 4.0 neutral OH PAMAM, and G 4.0 TRIS PAMAM. The complexes were analysed via UV-Vis Spectroscopy. For neutral dendrimers, the encapsulation of the targeting groups was successful with an absorbance for its deprotonate state recorded. However, for TRIS PAMAMs, the encapsulation did not work with no absorbance recorded. It was postulated that the targeting group's acidic-aromatic head group might have deprotonated forming a complex salt internally with the internal amines of the TRIS PAMAMs. For future studies, the use of non-acidic head groups was to be explored to avoid internal complexation. This part of the study was handed over to a new fellow PhD student.

On the other hand, it might have just been that the hydrophobic interactions between the dendrimer and the targeting group were weak and modifications to the linear chain would be needed to resolve this issue, possibly by introducing secondary interactions.

In the second study, quantification of protein binding between a model protein, Cytochrome C and a protein ligand, G3.5 carboxylate PAMAM was carried out. This was successfully achieved by using a probe, ZnTHPP with good secondary interactions. These interactions were exploited by encapsulating the porphyrin non-covalently previously with TRIS PAMAM as part of designing a perfect drug delivery system (Chapter 3). The same was followed here with better loading achieved in Carboxylate PAMAMs. Fluorescence spectroscopy was used to study the binding study the probe was fluorescence active with an emission at ~610nm. Cytochrome C solution was titrated into a solution of the protein ligand-probe complex solution. With increasing concentration of the protein, the emission intensity of the porphyrin declined verifying the strong binding affinity between the protein and the dendrimer. The values were accumulated to give a binding constant of 4.16×10^5 with a K_a of 2.08×10^5. These values were almost same as those of competition experiments.

The successful study was concluded with the understanding that, secondary interactions play an important role in protein binding studies. Different types of metallated porphyrins can now be studied for their role as probes helping quantify protein binding to more accurate levels.

Finally, the most important future work arisen from the conclusions drawn by the two studies, is to combine both the approaches and study their effect on the interaction between the protein and its ligand (Figure 4.14).

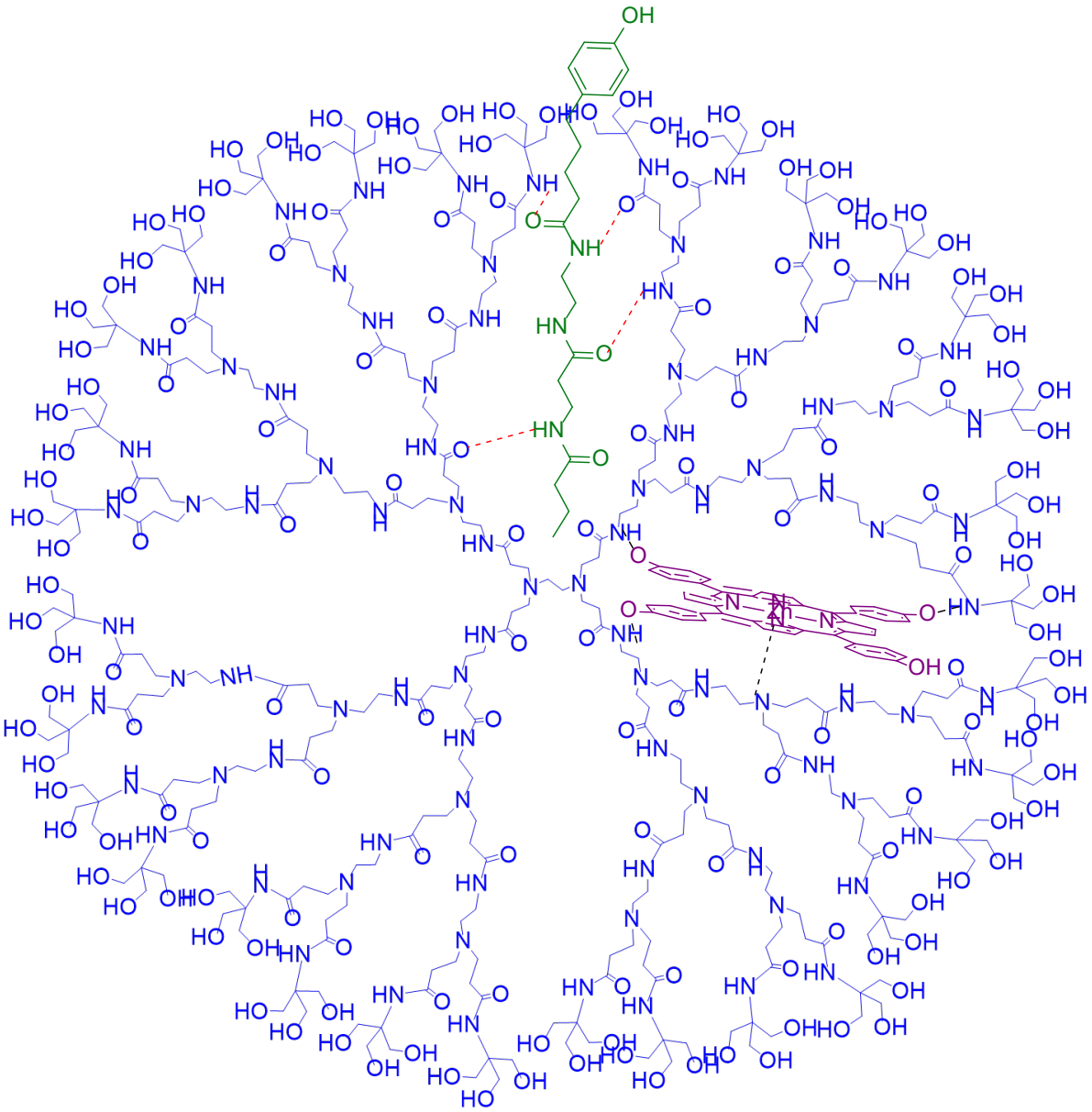

Figure 4.14. Graphically representation of secondary interactions between a modified targeting group, metallated porphyrin and G4.0 TRIS PAMAM (the dendrimer i.e. protein ligand for protein binding will be G3.5 carboxylate PAMAM). Between tertiary amines and the internal oxygen of the carboxylate PAMAM, the amines are better electron donors making binding between the zinc core of ZnTHPP and the tertiary amines possible.

4.4 Experimental

4.4.1 Instrumentation

4.4.1.1 NMR Spectroscopy

All deuterated solvents were supplied by Sigma Aldrich. ^{1}H NMR and ^{13}C NMR spectra were recorded using instruments of Brucker AV1400 MHz, Brucker AVX400 MHz and Brucker HD400 MHz. The NMR spectra were analysed by using Topspin 3.0 NMR software.

4.4.1.2 Infrared (IR) Spectroscopy

IR spectra were recorded using a Perkin-Elmer UATR Infrared spectrometer. Spectra were analysed with Spectrum100 software and spectra are stated using %Transmittance and wavenumber (cm^{-1}).

4.4.1.3 Mass Spectrometry

An Electrospray ionisation (ES) was used to give the mass spectra. The instrument used was a WATERS LCT mass spectrometer.

4.4.1.4 UV/Vis spectroscopy

The UV/Vis spectrum was recorded on an Analytik Jena AG Specord s600 UV/Vis Spectrometer and analyzed by the Software (WinASPECT).

4.4.1.5 Fluorescence Spectroscopy

Fluorescence results were obtained using a HORIBA Scientific Fluoromax-4 spectrofluorometer and analyzed by the software (FluorEssence V3).

4.4.1.6 pH measurement

The pH of the buffer solutions prepared was substantiated using a pH 210 Microprocessor pH Meter from Hanna Instruments Ltd. (Leighton Buzzard, UK). The device was calibrated using pH 4.0 and pH 10.0 standard solutions.

4.4.2 General synthetic procedures

4.4.2.1 Synthesis of N-(4-hydroxyphenyl) hexadecanamide

The general procedure was followed where a solution of THF and 4-aminophenol (2.16 g, 19.8 mmol) was added dropwise to the cooled toluene and palmitoyl chloride (0.54 g, 1.98 mmol) solution to give a pink mixture. The reaction mixture was stirred for 2 hours and then diluted with DCM and water. The organic layer was separated and the solvent was removed under reduced pressure. The crude product was chromatographed on silica gel (eluting with ethyl acetate/pet ether 1:3 vv^{-1}) to give the final product (670 mg, 98%) as a white solid.

R_f 0.4 [ethyl acetate/40-60 petroleum ether (1:3)]; λ_{max}/cm^{-1}(FTIR) 3313 (O-H stretch), 2916 and 2850 (C-H stretch), 1652 (amide, C=O stretch), 1611 (aromatic, C=C bend), 1548 (N-H bend); δ_H(ppm, 400 MHz; DMSO) 9.14 (1H, s, N*H*), 7.35 (2H, d, *J* 10.0, aromatic C*H*), 6.68 (2H, d, *J* 10.0, aromatic C*H*), 2.22 (2H, t, *J* 8.0, COCH_2), 1.57 (2H, quin, *J* 7.0, $COCH_2CH_2$), 1.26 (24H, m, remaining CH_2), 0.87 (3H, t, *J* 5.0 CH_3); δ_C(ppm, 400 MHz; MeOD) 170.9 (*C*=O), 153.5 (*C*), 121.2 and 115.4 (*C*H), 40.67, 40.6, 40.4, 40.2, 39.7, 39.6, 39.3, 36.7, 31.2, 29.5, 29.4, 29.2, 25.7 and 22.6 (CH_2) 14.5 and 14.4 (CH_3); m/z (ES) 348 (MH^+).

4.4.3 Encapsulation studies

4.4.3.1 Encapsulation of targeting group

Co-precipitate method was used for the encapsulation of the targeting group. Volumes of 10ml each for both the targeting group ($1x10^{-3}$M) and the dendrimer (1×10^{-4} M) were prepared in methanol. The solutions were combined and stirred for 1 hour. The solvent was removed in vacuo to give a complex following which, 10 mL of TRIS buffer (0.1 M, pH 7.36) was added. The complex was filtered and analysed via UV-Vis Spectroscopy.

4.4.3.2 Encapsulation of ZnTHPP

Co-precipitate method was used for the encapsulation of the metallated porphyrin. Excess ZnTHPP was dissolved in 5ml of G3.5 Carboxylate PAMAM ($1x10^{-4}$M) using methanol as the common solvent. The solution was stirred briefly followed by removal of the solvent in vacuo. 5 ml of TRIS buffer (0.01M, pH 7.4) was added to the complex. The complex solution formed

was filtered, diluted and analysed by UV-Vis Spectroscopy at a characteristic wavelength of 430.5nm to give a final concentration of $5x10^{-6}$M for encapsulated ZnTHPP.

4.4.4 Protein binding studies

4.4.4.1 Titration of Cytochrome C in the ZnTHPP-G3.5 Carboxylate PAMAM complex solution

The above prepared ZnTHPP-G3.5 Carboxylate PAMAM complex solution was diluted 43-fold to give a value close to the desired stoichiometry. A concentrated solution of Cytochrome C (400µM, 49.54mg) was prepared in 10ml of the above formed complex solution. The fluorescence excitation wavelength for the porphyrin was set at 420nm and an emission wavelength at 610nm. In a cuvette, 2ml of the complex solution was added to which 10µl of the Cytochrome C solution was added after every emission reading until the intensity became constant. The total volume of Cytochrome C added was 300µl. Change in the intensity vs concentration of Cytochrome C in the complex solution was plotted to give the binding constant, $Ka=2.08x10^{5}$.

4.5 References

1. Conte, L., Chothia, C. and Janin, J. (1999). The atomic structure of protein-protein recognition sites 1 1Edited by A. R. Fersht. *Journal of Molecular Biology*, 285(5), pp.2177-2198.

2. Huang, J. and Schreiber, S. (1997). A yeast genetic system for selecting small molecule inhibitors of protein-protein interactions in nanodroplets. *Proceedings of the National Academy of Sciences*, 94(25), pp.13396-13401.

3. Jain, R. and Hamilton, A. (2000). Protein Surface Recognition by Synthetic Receptors Based on a Tetraphenylporphyrin Scaffold. *Organic Letters*, 2(12), pp.1721-1723.

4. Mann, G., Twyman, L. and Gale, P. (2016). Controlling microenvironments and modifying anion binding selectivities using core functionalised hyperbranched polymers. *Chemical Communications*, 52(36), pp.6131-6133.

5. Chiba, F., Hu, T., Twyman, L. and Wagstaff, M. (2008). Dendrimers as size selective inhibitors to protein–protein binding. *Chemical Communications*, (36), p.4351.

6. Chiba, F. and Twyman, L. (2017). Effect of Terminal-Group Functionality on the Ability of Dendrimers to Bind Proteins. *Bioconjugate Chemistry*, 28(8), pp.2046-2050.

7. Bushnell, G., Louie, G. and Brayer, G. (1990). High-resolution three-dimensional structure of horse heart cytochrome c. *Journal of Molecular Biology*, 214(2), pp.585-595.

8. Chiba, F., Hu, T., Twyman, L. and Wagstaff, M. (2010). Dendritic Macromolecules as Inhibitors to Protein-Protein Binding. *Macromolecular Symposia*, 287(1), pp.37-41.

Chapter 5

Novel Approach for Artificial Blood-Surface Crosslinked Micelles

Table of Contents

Abbreviations

^{13}C NMR – Carbon Nuclear Magnetic Spectroscopy

^{1}H NMR – Proton Nuclear Magnetic Spectroscopy

4-DBB – 4-(dodecyloxy)benzyltripropargylammonium bromide

$CDCL_3$ – Deutrated chloroform

CMC – Critical micelle concentration

Co(II)TPPS – Tetrakis(4-sulfonatophenyl) porphinato cobalt (II)

Co(II)TPPS-TM-β-CD – Tetrakis(4-sulfonatophenyl) porphinato cobalt (II)-Heptakis-(2,3,6-tri-O-methyl)-β-cyclodextrin

$CuCl_2$ – Copper (II) chloride

ES-MS – Electron spray-Mass Spectroscopy

Fe(II)TPP – 5,10,15,20-Tetraphenyl-21H,23H-porphyrin iron (II)

Fe(II)TPPS – tetrakis(4-sulphonatophenyl)porphyrinato iron(II)

Fe(III)TPP – 5,10,15,20-Tetraphenyl-21H,23H-porphyrin iron (III)

Fe(III)TPPS – tetrakis(4-sulphonatophenyl)porphyrinato iron(III)

Fluosol-DA – a patented emulsion of two perfluorochemical compounds, perfluorodecalin and perfluorotripropylamine

FT-IR – Fourier Transformed Infrared Spectroscopy

Hb – Haemoglobin

HbA_0 – Human Haemoglobin

HBOC(s) – Haemoglobin-based Oxygen Carriers

MH^+ - Pseudo molecular ion/ Positive molecular ion

MHz – Mega hertz

$Na_2S_2O_4$ – Sodium dithionite

PEG – Poly(ethylene glycol)

PEG-*b*-P(4VP-*co*-4VPHep) – Poly(ethylene glycol)-b-poly(4-vinylpyridine-co-Nheptyl-4-vinylpyridine

PEG-b-PLys – Poly(ethylene glycol)-block-poly(L-lysine)

PFBOC(s)/ PFC(s) – Perfluorocarbon-based Oxygen Carriers

pH – Power of Hydrogen

RBC(s) – Red Blood Cells

SCBOC(s) – Stem Cell-based Oxygen Carriers

SCM(s) – Surface crosslinked micelles

TM-β-CD – Heptakis-(2,3,6-tri-O-methyl)-β-cyclodextrin

TPP – 5,10,15,20-Tetraphenyl-21H,23H-porphyrin

β-CD – β-cyclodextrin

List of Figures

List of Graphs

List of Scheme(s)

5.1 Introduction

With an ageing population on the rise globally, the availability of blood donors continues to descend leading to chronic blood donor shortage. The most affected are developing countries due to poor safety and storage standards when it comes to blood donations and transfusion. Besides, enough blood supplies during times of war, natural disasters, and epidemics remains a concern [1]. Hence, development of a perfect artificial blood substitute has become vital over the years to meet the increasing demands. Although there have been breakthroughs in this field with different types of artificial blood substitutes being discovered, there end use as a blood replacement lingers. This brief introduction will touch on types of artificial blood substitutes (Figure 5.1) that have been developed and associated obstacles while considering the prospects of new emerging artificial blood substitutes. Finally, how porphyrin encapsulated micelles can overcome routine challenges as potential artificial blood substitutes will be discussed.

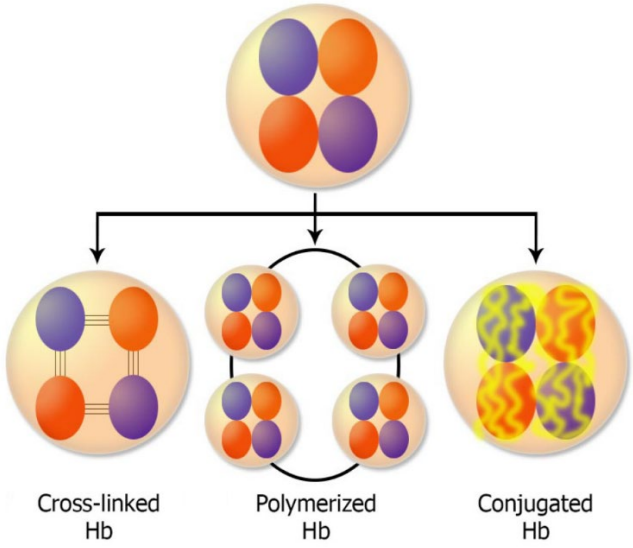

Figure 5.1. Graphical representation of types of polymeric artificial blood substitutes. **Reprinted by permission from Moradi, S., Jahanian-Najafabadi, A., & Roudkenar, M. H. (2016). Artificial Blood Substitutes: First Steps on the Long Route to Clinical Utility. *Clinical Medicine Insights: Blood Disorders*, *9*, 33–41. http://doi.org/10.4137/CMBD.S38461.**

5.1.1 Types of artificial blood substitutes

Red Blood Cells (RBCs) contain haemoglobin capable of carrying oxygen when it comes to blood transfusion for saving patients' lives [2]. Infectious and non-infectious complications make the RBC transfusion difficult [3]. Currently, three types of RBC substitutes have been developed: perfluorocarbon-based oxygen carriers (PFBOC), haemoglobin-based oxygen carriers (HBOC) (Figure 5.2) and stem cell-based oxygen carriers (SCBOCs). The first two artificial blood substitutes dominate the market.

Figure 5.2. Graphical representation of types of RBC substitutes[3]

5.1.1.1 Perfluorocarbon-based oxygen carriers

The ability to carry oxygen by PFCs was first reported in 1966 [5]. The dissolve oxygen rather than binding to it [6] with a solubility twenty times better than water [7]. This is possible due to their straight or cyclic hydrocarbon structure, although linear PFCs are known to perform better [8,9]. Besides, their fluorine-carbon bonds are so strong, the metabolizing of the substitute is prevented [9]. In addition, they are heat resistant with temperatures above 300°C and hence can be heat sterilized [10]. Clinical potential of PFCs has been studied as well in the past. For instance, in 1985, Mushlin et al reported the benefits of small sized PFCs in maintaining myocardial function by improving the oxygenation rate of occluded coronary artery [11].

Having said that, over the years, PFCs have not been able to succeed in clinical trials. PFCs are generally insoluble in water and this is rectified by using emulsifying agents. Adverse effects associated with the use of emulsifying agents were observed in the clinical trials of Fluosol-DA (a patented emulsion of two perfluorochemical compounds, perfluorodecalin and perfluoro tripropylamine) [12]. Also, the ability of Fluosol-DA to carry oxygen was found to be less than that of RBCs [13]. Another well-known PFC, Oxygent^{TM} displayed signs of mild thrombocytopenia leading to its discontinuation in clinical trials [14].

5.1.1.2 Haemoglobin based oxygen carriers (HBOCs)

Hb extracted from outdated human or bovine blood in chemically modified to give HBOCs [15]. For an increased intravascular retention, the chemical modifications are important as they stabilise Hb [16]. However, before they can be used as substitutes, their purification becomes necessary. With HbA_0 (human Hb), approximately 99% purity was reported following purification with anionic and cationic chromatography [17].

HBOCs ideally bind with oxygen and their oxygen-binding affinity is temperature, pH and oxygen tension dependant [16]. HBOCs have been developed and studied in three forms: cross-linked, polymerised, and surface-modified HBOCs. With respect to clinical trials, their performance has been undermined with emergence of adverse effects. End organ damage, myocardial infarction, neurotoxicity, renal failure, and heightened risk of mortality are few of the side effects that have brought the development of HBOCs to a halt [17].

5.1.1.3 Stem cell-based oxygen carriers (SCBOCs)

The literature on SCBOCs is inadequate making their introduction comprehensive. These types of RBC substitutes are bone marrow derived. At present, three types of SCBOCs that are being developed and researched upon are known: erythropoiesis, hematopoietic SCBOCs, and pluripotent SCBOCs. There are significant challenges that need to be overcome for SCBOCs to become the future of artificial blood substitute. To name a few, production scale up, removal of cells with tumour forming potential, shortening of expansion time, differentiation, genetic mutation, selection, and testing are the hurdles that need to be sorted for SCBOCs to progress in clinical trials [18].

5.1.2 Porphyrin encapsulated micelles as artificial blood substitutes

Polymeric micelles have been extensively studied as potential drug and gene delivery systems. They are known for their characteristically high drug loading capacity, modifiable particle size, good stability, and increased accumulation in solid tumours among many others [19]. In addition, their structural and physiochemical properties can be modified in tune with their end applications. Here, their ability to encapsulate porphyrins and subsequently be utilised as artificial blood substitutes are discussed.

Diblock copolymer poly(ethylene glycol)-b-poly(4-vinylpyridine-co-*N*heptyl-4-vinylypridine)(PEG-*b*-P(4VP-*co*-4VPHep)) were self-assembled with the host-guest inclusion β-CD/Fe(III)TPPS (β-cyclodextrin/ tetrakis(4-sulphonatophenyl)porphyrinato iron(III)) to form a core-shell complex micelle mimicking haemoglobin [20] (Figure 5.3). The inclusion of the Fe(II)TPPS (tetrakis(4-sulphonatophenyl)porphyrinato iron(II)) in the cavity of β-CD via host-guest interaction avoided the formation of a dimer. This system was encapsulated in the hydrophobic interior of the micelle while the hydrophilic PEG exterior stretched in aqueous media providing increased solubility. With increased blood circulation time, the micelle system,

a potential artificial blood substitute could possibly be used for the treatment of hypoxia in the future.

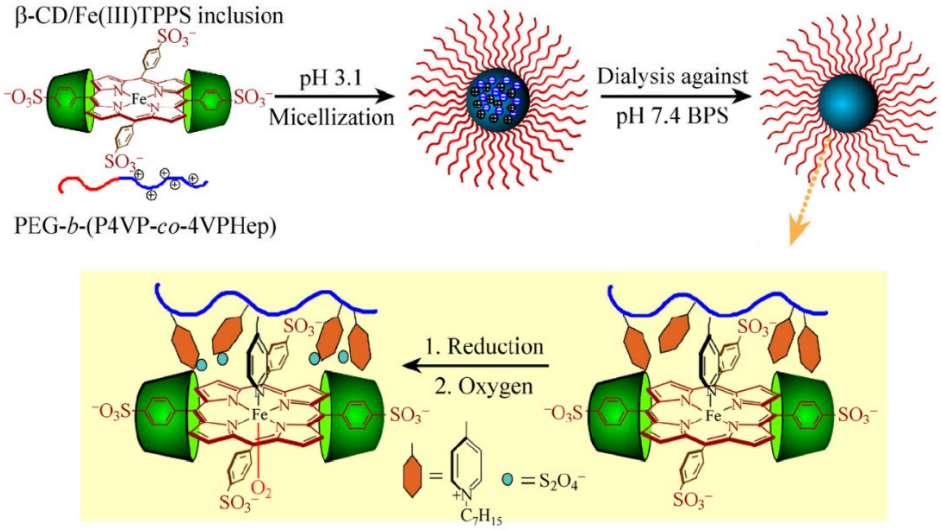

Figure 5.3. Graphical representation of complex micelles formation and subsequent oxygen binding Reprinted by permission from Springer Customer Service Centre GmbH: Springer Nature, Nano Research (Complex micelles with the bioactive function of reversible oxygen transfer, Liangliang Shen, Lizhi Zhao, Rui Qu et al), © (Jan 1, 2014) [21].

Similar hierarchical self-assembled complex micelles were synthesized and studied for their respective oxygen binding affinity. Poly(ethylene glycol)-block-poly(L-lysine) (PEG-b-PLys), tetrakis(4-sulfonatophenyl) porphinato cobalt(II) (Co(II)TPPS), a heptapeptide (Cys-His-His-His-His-His-His) and heptakis-(2,3,6-tri-O-methyl)-β-cyclodextrin (TM-β-CD) were self-assembled encapsulating Co(II)TPPS-TM-β-CD system in their hydrophobic interior. The complex micelle proved to be a potential oxygen carrier in vivo by displaying superior biocompatibility and cellular uptake [22].

After briefly focusing on different types of artificial blood substitutes, it was understood that complex polymer micelles show exceptional characteristics comparable to that of PFCs and HBOCs. This chapter also aims to study the ability of a porphyrin complex micelle as an artificial blood substitute. The following section details the aims of this study.

5.2 Aims

As the search for the perfect artificial blood substitute is in progress, the utilisation of therapeutic polymers continues to grow. Micelles are one such class of therapeutic polymers that have recently gained attention for their use as artificial blood substitutes. From the introduction, we gathered that polymer micelles were successful in showing potential as future artificial blood mimics.

This chapter focuses on the use of non-covalent approach in designing a simplified artificial blood mimic in the form of porphyrin encapsulated surface crosslinked micelles (SCMs). Surfactant molecule will be synthesised consisting of a hydrophobic tail and hydrophilic head (Figure 5.4). Upon determining their critical micelle concentration (CMC), they'll later be crosslinked to form SCMs.

These SCMs will incorporate iron(III) cored porphyrins(Fe(III)TPP) non-covalently in their hydrophobic interior preventing autoxidation in aqueous media. As the micelles will be crosslinked, their stability below CMC will be corroborated. The synthesis of the surfactant molecule is discussed in Chapter 2 Section 2.2.6.2. This chapter will discuss the micellisation and cross-linking of this surfactant molecules.

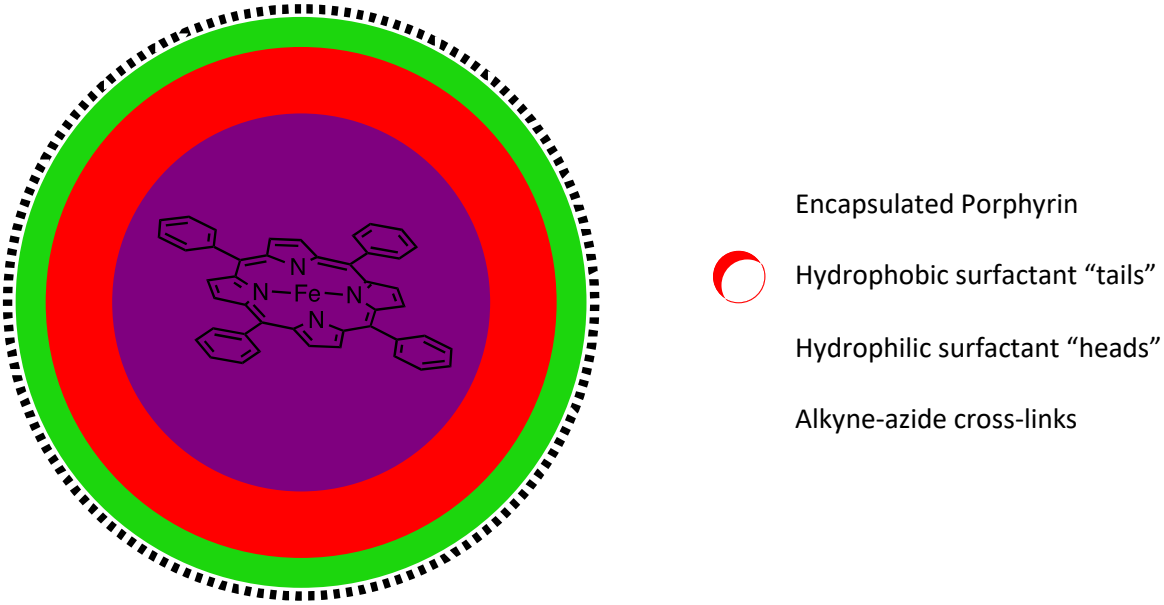

Figure 5.4. Graphical representation of SCMs encapsulated Fe (III)TPP [23].

Before crosslinking the micelles, Fe(III)TPP will be encapsulated in 1:1 ratio to avert porphyrin aggregation. To overcome the issue of porphyrin insolubility in water, the encapsulation will take place in aqueous media. The complex micelles will then be crosslinked using an azide

functionalised cross-linker via ‘click’ chemistry. The inactive Fe^{3+} core of the encapsulated porphyrin will be reduced to active Fe^{2+}. The time taken for the oxidation of the active Fe^{2+} to inactive Fe^{3+} will be monitored using UV-Vis Spectroscopy to give the half-life of the porphyrin encapsulated SCMs after studying their iron stability, respectively.

5.3 Results and discussion

Part 1 Non-crosslinked micelles

5.3.1 Micellisation of 4-(dodecyloxy)benzyltripropargylammonium bromide

The micellisation of the surfactant could be carried out only when its critical micelle concentration was known. To do this, a standard method using fluorescence spectroscopy for calculating the critical micelle concentration (CMC) was applied. Concentrations of the surfactant ranging from 0.3-10 x 10^{-5}M were prepared using pyrene. The fluorescence spectra (Figure 5.5) with respective I_1 and I_3 transitions were recorded and analysed to give the CMC of the surfactant as ~9 x 10^{-5}M (Graph 5.1). This value was close to the literature value[25] calculated to be ~1.5 x 10^{-5}M.

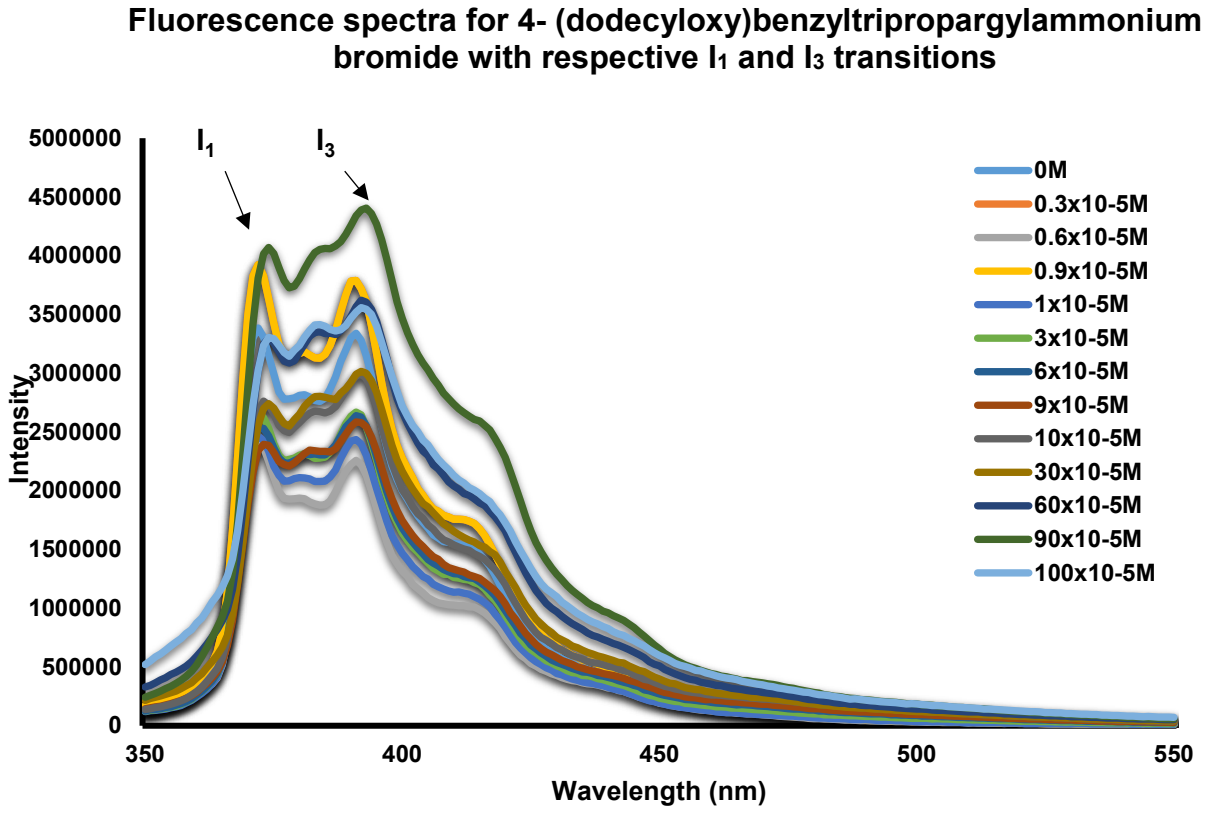

Figure 5.5. Fluorescence emission spectra of pyrene in the presence of 4-(dodecyloxy)benzyltripropargylammonium bromide in water where I_1 and I_3 are the pyrene transitions, respectively. A drop in the intensity for the surfactant is observed with dilution (concentration dependant).

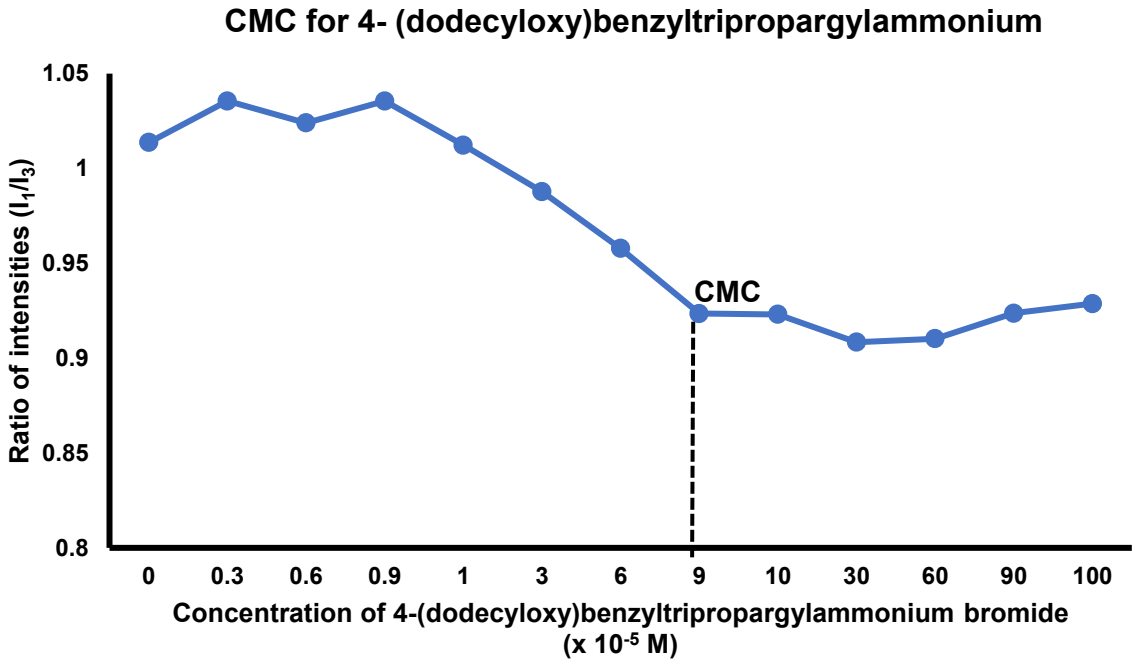

Graph 5.1. A plot between the concentrations of 4-DBD used for recording fluorescence spectra, and the ratio of the respective intensities I_1 and I_3 provides with the CMC of the surfactant. From the graph a gradual decrease in the intensity ratio is observed from 0.9-9 x 10^{-5}M indicating micelle formation before it plateaus off, suggesting the CMC of surfactant to be 9.0 x 10^{-5}M, respectively.

5.3.2 Encapsulation studies

5.3.2.1 Control experiment with metal free tetraphenyl porphyrin (TPP)

After the CMC of the surfactant was determined, the next step involved encapsulating the metal free tetraphenyl porphyrin (TPP). To do this, the surfactant was prepared at its critical micelle concentration in water. In this micelle solution, TPP dissolved in dichloromethane was added. In theory, as dichloromethane would evaporate, TPP will subsequently get incorporated within the micelle. However, this was not the case when the formed complex was analysed via UV-Vis spectroscopy. To optimise encapsulation, acetone was used as a solvent for TPP. This is because, TPP is partially soluble in acetone facilitating formation of a blend ensuring insertion of TPP within the micelle. The complex once prepared was analysed by UV-Vis spectroscopy at TPP's characteristic wavelength, 417 nm. This time the encapsulation was successful with presence of Soret band at 420 nm along with the four Q peaks visible as well. Since, this was a control experiment to test whether, TPP can be encapsulated successfully by the micelle or not, the concentration of the TPP was not calculated.

5.3.2.2 Encapsulation of model haem group, 5,10,15,20-Tetraphenyl-21H,23H-porphyrin iron (III) (Fe(III)TPP)

With the confirmation that the micelle was capable of encapsulating porphyrin, the next step was to encapsulate an iron cored porphyrin, namely 5,10,15,20-Tetraphenyl-21H,23H-porphyrin iron (III) (Fe(III)TPP). For a micelle to function as a synthetic haemoglobin mimic, a site for oxygen binding was needed. Fe(III)TPP would serve the purpose. The synthesis for this porphyrin has been described in detail in Chapter 2 Section 2.3.2.2.2.

Upon successful synthesis, encapsulation of Fe(III)TPP followed the same method as did for TPP. Controlled concentrations of both the micelle and Fe(III)TPP was used to get 1:1 ratio of micelle to Fe(III)TPP. This was necessary as a 1:1 ratio would mimic the synthetic haemoglobin model. The concentration of micelle was calculated to be 2 x 10^{-6}M (using the CMC and aggregation number mean average of 45). Hence, the concentration of FeTPP was also 2x10^{-6}M. Instead of using dichloromethane, acetone was used to ensure encapsulation. The complex formed was analysed by UV-Vis spectroscopy. The absorbance of the complex was recorded at the characteristic wavelength of 423 nm. The concentration of encapsulated Fe(III)TPP was calculated by using its molar extinction coefficient 106478$M^{-1}cm^{-1}$. It was calculated to be 1.88 x 10^{-6} M. The concentration of encapsulated Fe(III)TPP was slightly lower than expected however, this meant possible aggregation was averted.

5.3.3 Studying the Iron Stability of the Synthetic haemoglobin mimic

The iron stability study involves the activation of the iron core of the porphyrin, Fe(III)TPP as it remains encapsulated within the micelle. The shift in the inactive Fe^{3+} to active Fe^{2+} state is caused by exposure of the system to air. This phenomenon can be followed by using UV-Vis spectroscopy. This study reflects on the stability of the system to withstand degradation of the activated iron core by autoxidation. Longer degradation time means better stability of the system. With the micelles encapsulating the porphyrins, longer degradation time is expected reflecting on a well stabilised haemoglobin model. As the stoichiometry is controlled with 1:1 ratio of the micelles to Fe(III)TPP, the aggregation behaviour of porphyrins is avoided. Also, as the inner cavity of micelle is hydrophobic, a ‘safe’ environment for the porphyrin exists. This avoids the protons of the water molecules to act as catalysts; initiating autoxidation. The above-mentioned iron activation was done by using equimolar amount of reducing agent, Sodium dithionite. The quantity of the reducing agent was controlled to avoid over-reduction of iron centres.

While stirring, the porphyrin-micelle system was flushed with nitrogen atmosphere after the addition of the reducing agent. Samples of the mixture were drawn before and after the addition of the reducing agent and UV-Vis analysed using a capped nitrogen flushed cuvette. There was a soret band shift from 425 nm to 437 nm, indicating reduction of the iron centre.

Following this, the characteristic wavelength of the system was adjusted to 430 nm. Hereafter, the sample in the cuvette was exposed to air and readings every fifteen seconds for an hour were recorded. The gradual decay of Fe^{2+} to Fe^{3+} took 600 seconds giving a half-life of ~300 seconds (Graph 5.2) which was three-fold better than that of free 5,10,15,20-Tetraphenyl-21H,23H-porphyrin iron (II) (Fe(II)TPP).

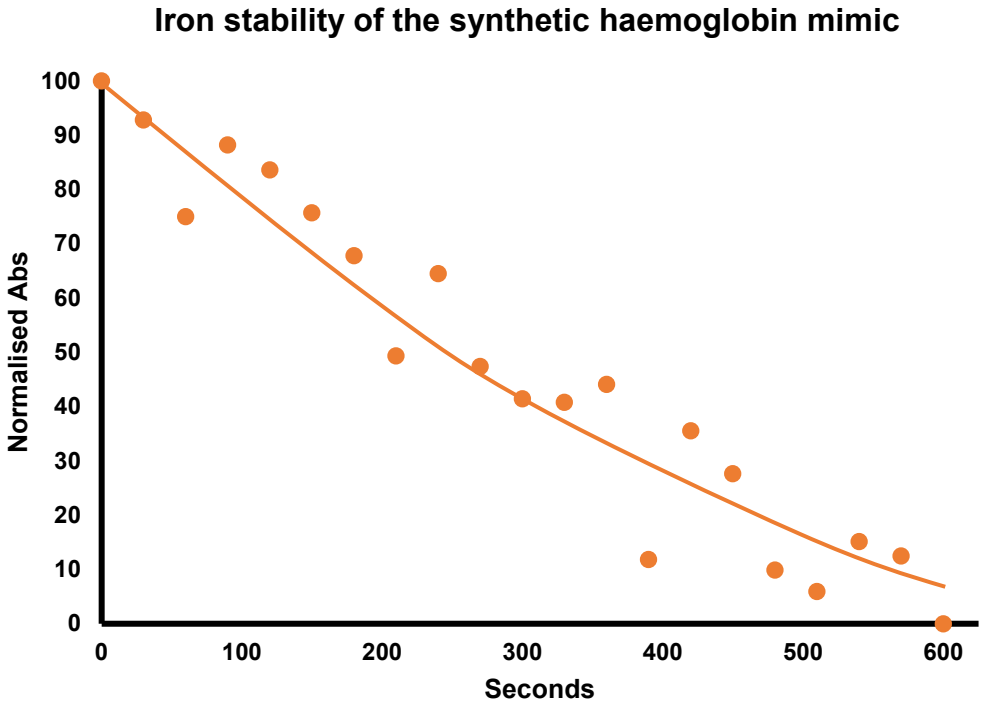

Graph 5.2. Normalised absorbance of the Fe(II)TPP complexes encapsulated in micelles at 430nm over a period of 600 seconds. Hence, the half-life of the porphyrin encapsulated micelle system was ~300 seconds, respectively.

Part 2 Surface crosslinked micelles (SCMs)

The second milestone of this research involved formation of porphyrin encapsulated SCMs and their subsequent iron stability studies. Synthesis of the crosslinker was the first step in achieving this milestone. This was followed by encapsulation of Fe(III)TPP within the micelles in a ratio 1:1. Once, the porphyrin-micelle system was ready, it underwent crosslinking to give SCMs. Hereafter, the porphyrin encapsulated SCMs were subjected to Iron stability tests just as the micelles in first part of this chapter were. To begin with, synthesis of the crosslinker is described below.

5.3.4 Synthesis of azide functionalised cross-linker

Crosslinking the micelles was important for isolating and protecting Fe(III)TPP while providing increased solubility. Therefore, the preferred azide functionalised crosslinker was synthesised (Scheme 5.1).

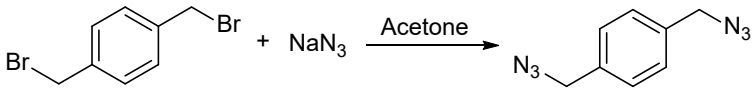

Scheme 5.1. Reaction scheme of the azide functionalised crosslinker 1,4-Bis(azidomethyl)benzene [24]

Dry acetone was used to dissolved p-xylene dibromide to which sodium azide was added [24]. The reaction mixture was refluxed for twelve hours under a nitrogen atmosphere. Upon reaction completion, the mixture was filtered and concentrated in vacuo to give a yellow oil as the crosslinker. Standard characterisation techniques were applied to verify the synthesis. FT-IR gave a peak at around ~2097 cm^{-1} corresponding confirming the presence of C-N_3. Also, ES-MS gave a molecular ion peak of 188 MH^+ corresponding to the molecular weight of the crosslinker.

5.3.5 Encapsulation of Fe(III)TPP

Before micelles were crosslinked, the encapsulation of Fe(III)TPP was necessary. Once the crosslinkers would crosslink on the surface of the micelles, a cage like sphere will be formed. The incorporation of the porphyrin after crosslinking hence, would become even more difficult. To avoid this situation, the encapsulation of the porphyrin was done first, followed by crosslinking of the micelles. The method for encapsulation was the same method used in Part 1. The stoichiometry of the porphyrin-micelle system was maintained at 1:1 ratio.

5.3.6 Surface crosslinking of micelles

After the incorporation of Fe(III)TPP in the micelles, surface crosslinking of the micelles formed the next step. Equimolar amount of the surfactant and the crosslinker were to be used. This was to ensure that for every surfactant molecule, a crosslinker was present. As the micelles were prepared in distilled water during the encapsulation of Fe(III)TPP, the concentration was maintained at $2x10^{-6}$M. To this micellar solution, copper (II) chloride (6.7mg/ml) and sodium ascorbate (99mg/ml) were added. The mixture was stirred at room temperature for 24 hours after which it was directly used for Iron stability study.

5.3.7 Iron stability study of SCMs

For conducting the iron stability study, the procedure followed in Part 1 Section 5.3.3 was repeated here. Samples before and after the addition of reducing agent, Sodium dithionite, were drawn and analysed by UV-Vis Spectroscopy in a capped, nitrogen flushed quartz cuvette. Unfortunately, a soret band shift for the Fe(II)TPP from 427 nm to ~435nm was not observed. This indicated that the reduction of iron centre from inactive Fe^{3+} to active Fe^{2+} was unsuccessful. Due to limited time, this experiment was carried out once.

5.4 Conclusions and Future work

This study comprised of five milestones. First milestone was the synthesis of surfactant molecule 4-(dodecyloxy)benzyltripropargylammonium bromide. Once it was successfully synthesized and characterised, its CMC was calculated using fluorescence spectroscopy. The CMC was determined to be $2x10^{-6}$M. This gave us the concentration at which the surfactant molecule will form micelles, $1x10^{-6}$M. This was relatively a new type of surfactant molecule and was being synthesised for the first time. Even though the synthesis (discussed in Chapter 2 Section 2.2.6.2) was straight forward, it was extensive and time consuming. Optimising the synthetic approach should be one of the future milestones for this study.

The second milestone involved the encapsulation of Fe(III)TPP non-covalently within the micelle in 1:1 ratio using aqueous media. However, before Fe(III)TPP could be encapsulated, a control experiment was conducted by encapsulating free TPP within the micelle using non-covalent approach. UV-Vis Spectroscopy was utilized to verify the encapsulation of TPP. As the control experiment was successful, encapsulation of Fe(III)TPP followed. The complex micelle was analysed via UV-Vis Spectroscopy and a soret band at 425nm confirmed the encapsulation. From the introduction, it was understood that porphyrins other than Fe(III)TPP could be used as for encapsulation within the micelles. It'll be interesting to study whether Co(II)TPP (for instance) could be incorporated within the above formed micelles and their iron stability and oxygen binding performance investigated.

Once the complex micelle was formed, the third milestone was to conduct iron stability and oxygen binding studies. To do that, the inactive Fe^{3+} core of the encapsulated porphyrin was reduced to active Fe^{2+} A shift in the soret band from 425 nm to 437 nm confirmed iron reduction. After this, the UV-Vis Spectroscopy was used to determine the time it took for oxidation of the Fe^{2+} to occur and revert to inactive Fe^{3+} state. This was calculated to be 600 seconds giving a half-life of 300 seconds. This was found to be three time better than that of free TPP.

The fourth milestone consisted of synthesising an 'azide' functionalised crosslinker and crosslinking a porphyrin encapsulated micelle to form a surface crosslinked SCM. This SCM would represent a simplified version of artificial blood mimic. The azide functionalised crosslinker was synthesised successfully following which the complex micelle was crosslinked using copper(II) chloride and sodium ascorbate. Studying the surface charge of the SCMs using zeta-potential to confirm successful crosslinking should be explored.

Finally, the fifth milestone was the iron stability and oxygen binding studies using UV-Vis Spectroscopy. An attempt to reduce the inactive iron core of the encapsulated porphyrin was carried out. Once the procedure was conducted, UV-Vis Spectroscopy was used to verify the reduction of the iron core. Unfortunately, the reduction of the inactive Fe^{3+} to active Fe^{2+} had been unsuccessful. A soret band shift from 425 nm to ~437nm was not detected. It was evident that the experiment had to be repeated however, due to time constraints, the study could not be repeated. In the presence of imidazole, a model ligand representing the distal histidine in haemoglobin, the iron stability and oxygen binding studies of the SCM-porphyrin system would be required.

The idea of designing a simplified artificial blood mimic using complex micelles was conceived and tested. Even though the SCMs could not be tested for their respective iron stability and oxygen binding studies, as failure in reducing the iron core was encountered, it wasn't the end of the research. We were able to prove that micelles can be used to encapsulate hydrophobic porphyrin molecules using non-covalent approach. The iron core of the complex micelle was reduced and tested for its stability. The longer it took for the iron to return to its inactive state, the better was the half-life. This was found to 300 seconds, better than free TPP. Overall, the conceived idea is half achieved. Attempts in studying the iron stability and oxygen binding study for the SCMs have already begun.

5.5 Experimental

5.5.1 Instrumentation

5.5.1.1 NMR

Proton NMR spectra were obtained using a Bruker AV-400 machine at 400 MHz with a 5mm BB-1H probe. Carbon NMR spectra were obtained using a Bruker AV-400 machine at 400 MHz with a 5 mm BB-1H probe. NMR data was evaluated using the Bruker software, 'TopSpin'. All NMR samples were made using deuterated chloroform.

5.5.1.2 Ultra Violet-Visible Spectroscopy

UV-Vis spectra were measured using a Perkin Elmer Lambda 35 UV-Vis Spectrometer. Solutions were made up in oven dried volumetric flasks with dichloromethane solvent and filtered into glass cuvettes. The machine was calibrated with pure dichloromethane before use. The machine scanned in the 200-800 nm region with a resolution of 1 nm.

5.5.1.3 Fourier Transform Infrared (FTIR) Spectroscopy

All FTIR samples were analysed neat on a Perkin-Elmer Paragon 1000 FT-IR spectrophotometer with integral DuraSample IR-II.

5.5.1.4 Mass Spectroscopy

Electrospray ionisation mass spectrometry (ES-MS) was carried out using a Micromass Prospec spectrometer with a mass range 2-800 Da.

5.5.1.5 Fluorescence Emission Spectrometry

All spectra were recorded using a Fluoromax-4 fluorescence spectrometer using the FluorEssence software in the s mode.

5.5.1.6 Flash Column chromatography

Flash column chromatography was carried out using Bio-Beads^{TM} S-X1 Support sourced from BIO-RAD.

5.5.1.7 Thin layer chromatography

Thin layer chromatography was performed using TLC Silica gel 60 F_{254} Aluminium sheets sourced from Merck KGaA.

5.5.2 Synthesis of Cross-Linker

Sodium azide (3.9 g, 60 mmol) was added to a solution of p-xylylene dibromide (4.0 g, 15 mmol) in dry acetone (20 mL) in a round bottom flask. The reaction mixture was heated to reflux under Nitrogen for 12 hours. The solid was removed by filtration and the filtrate was concentrated *in vacuo* to give a yellow oil.

Yield 2.33 g 83 %; IR ν_{max}/cm^{-1} 2097 (C-N_3); ^{1}H NMR ($CDCl_3$, 400 MHz,∂): 7.45 (s, 4H), 4.40 ppm (s, 4H) ^{13}C NMR ($CDCl_3$, 100 MHz) 135.9, 128.9, 55.0 ppm; m/z [MS(ESI)] 188 (MH+) (calculated for $C_8H_8N_6^+$ 188.1 $gmol^{-1}$)

5.5.3 Iron stability and oxygen binding studies of micelles-Part 1

1:1 metalloporphyrin-micelle complex (Fe(III)TPP) was prepared in water (20 ml) at a concentration of 2 x 10^{-6} M. 10ml of the solution was transferred into a rubber sealed double-neck round bottom flask before degassing and nitrogen refilling cycle was repeated 3 times. An equal molar (2 x 10^{-6} M) of aqueous sodium dithionite ($Na_2S_20_4$) solution was added to the solution. The mixture was stirred for 20 minutes. A glass syringe was used to collect 1.5ml of the sample solution which was transferred into a rubber sealed, degassed and nitrogen flushed quartz cuvette. The sample was then analysed using UV-Vis spectroscopy to ascertain successful iron reduction (at 437 nm). Then, time-scanning at fixed wavelength (430 nm) was set-up and the sample was left continuously stirring under atmospheric air. The UV-Vis reading was taken every 15 seconds for 1 hour.

5.5.3 Surface crosslinking of porphyrin encapsulated micelles

$CuCl_2$ (1ml of 6.7mg/ml aqueous solution, 5µmol), and sodium ascorbate (1ml of 99mg/ml aqueous solution, 50µmol) were added to an aqueous solution of porphyrin encapsulated micelle (10ml, 0.02mmol). The reaction mixture was stirred for 24 hours at room temperature to obtain porphyrin encapsulated SCMs.

5.5.5 Iron stability and oxygen binding studies of SCMs

About 10ml of the SCM solution was transferred into a rubber sealed double-neck round bottom flask before degassing and nitrogen refilling cycle was repeated 3 times. An equal molar (2 x 10^{-6} M) of aqueous sodium dithionite ($Na_2S_20_4$) solution was added to the solution. The mixture was stirred for 20 minutes. A glass syringe was used to collect 1.5ml of the sample solution which was transferred into a rubber sealed, degassed and nitrogen flushed quartz cuvette. The sample was then analysed using UV-Vis spectroscopy to ascertain successful iron reduction (at 437 nm) followed by time-scanning at fixed wavelength (430 nm) for every 15 seconds for 1 hour.

5.6 References

1. Tao, Z. and Ghoroghchian, P. (2014). Microparticle, nanoparticle, and stem cell-based oxygen carriers as advanced blood substitutes. *Trends in Biotechnology*, 32(9), pp.466-473.

2. Klein, H., Spahn, D. and Carson, J. (2007). Red blood cell transfusion in clinical practice. *The Lancet*, 370(9585), pp.415-426.

3. N Singh, B C Semwal, (2012) Artifical blood: a tool for survival humans. *International Research Journal of Pharmacy,* 3(5), pp.119-123.

4. Sharma, S., Sharma, P. and Tyler, L. (2017). Transfusion of Blood and Blood Products: Indications and Complications. *American Family Physician,* 83(6), pp.719-724.

5. Anilkumar, D. and Sudarshan, P. (2015). A Review of Artificial Blood. *International Journal of Pharmaceutical, Chemical and Biological Sciences*, 5(2), pp.477-480.

6. Lane, T. (1995). Perfluorochemical-based artificial oxygen carrying red cell substitutes. *Transfusion Science*, 16(1), pp.19-31.

7. Cohn, C. and Cushing, M. (2009). Oxygen Therapeutics: Perfluorocarbons and Blood Substitute Safety. *Critical Care Clinics*, 25(2), pp.399-414.

8. Shi, Q., Huang, Y., Chen, X., Wu, M., Sun, J. and Jing, X. (2009). Hemoglobin conjugated micelles based on triblock biodegradable polymers as artificial oxygen carriers. *Biomaterials*, 30(28), pp.5077-5085.

9. Lapillonne, H. and Kobari, L. (2010). Red blood cell generation from human induced pluripotent stem cells: perspectives for transfusion medicine. *Haematologica*, 95(10), pp.1651-1659.

10. Lowe, K. (1999). Perfluorinated blood substitutes and artificial oxygen carriers. *Blood Reviews*, 13(3), pp.171-184.

11. Hammerschmidt, D. and Vercellotti, G. (1988). Limitation of Complement Activation by Perfluorocarbon Emulsions:Superiority of Lecithin-Emulsified Preparations. *Biomaterials, Artificial Cells and Artificial Organs*, 16(1-3), pp.431-438.

12. Mushlin, P., Boucek, R., Parrish, M., Graham, T. and Olson, R. (1985). Beneficial effects of perfluorochemical artificial blood on cardiac function following coronary occlusion. *Life Sciences*, 36(22), pp.2093-2102.

13. Lane, T. (1995). Perfluorochemical-based artificial oxygen carrying red cell substitutes. *Transfusion Science*, 16(1), pp.19-31.

14. Nishimura, N., Nitsuno, T. and Naito, R. (1981). Clinical Studies of a Perfluorochemical, Whole Blood Substitute. *Critical Care Medicine*, 9(3), p.168.

15. Roudkenar, Moradi, S. and Jahanian-Najafabadi, A. (2016). Artificial Blood Substitutes: First Steps on the Long Route to Clinical Utility. *Clinical Medicine Insights: Blood Disorders*, p.33.

16. Cohn, C. and Cushing, M. (2009). Oxygen Therapeutics: Perfluorocarbons and Blood Substitute Safety. *Critical Care Clinics*, 25(2), pp.399-414.

17. Fox, I. and Daley, G. (2017). *Use of differentiated pluripotent stem cells in replacement therapy for treating diseases*.

18. Leytin, V., Mazer, D., Mody, M., Garvey, B. and Freedman, J. (2003). Hemolinktm, an o-raffinose cross-linked haemoglobin-based oxygen carrier, does not affect activation and function of human platelets in whole blood in vitro. *British Journal of Haematology*, 120(3), pp.535-541.

19. Alayash, A. (2010). Setbacks in Blood Substitutes Research and Development: A Biochemical Perspective. *Clinics in Laboratory Medicine*, 30(2), pp.381-389.

20. Nishiyama, N. and Kataoka, K. (2006). Current state, achievements, and future prospects of polymeric micelles as nanocarriers for drug and gene delivery. *Pharmacology & Therapeutics*, 112(3), pp.630-648.

21. Shen, L. and Zhao, L. (2014). Complex micelles with the bioactive function of reversible oxygen transfer. *Nano Research*, 8(2), pp.491-501.

22. Shen, L. and Qu, R. (2016). A biocompatible cobaltporphyrin-based complex micelle constructed via supramolecular assembly for oxygen transfer. *Biomater. Sci.*, 4(5), pp.857-862.

23. G Sowden, (2017) Surface crosslinked micelles as simplified models of artificial blood, MChem Thesis, University of Sheffield

24. Zhang, S. and Zhao, Y. (2010). Facile Synthesis of Multivalent Water-Soluble Organic Nanoparticles via “Surface Clicking” of Alkynylated Surfactant Micelles. *Macromolecules*, 43(9), pp.4020-4022.